LIGHT WAVES IN A COMPOSITE OF CYLINDRICAL NANOINCLUSIONS IN PASSIVE AND ACTIVE HOST MATRICES

By

YILAK ALEMU ABBO

SUBMITTED IN PARTIAL FULFILLMENT OF THE
REQUIREMENTS FOR THE DEGREE OF
MASTER OF SCIENCE IN PHYSICS
AT
ADDIS ABABA UNIVERSITY
ADDIS ABABA, ETHIOPIA
JUNE 2014

ADDIS ABABA UNIVERSITY
COLLEGE OF NATURAL SCIENCES
DEPARTMENT OF PHYSICS

The undersigned hereby certify that they have read and recommend to the School of Graduate Studies for acceptance a thesis entitled "**LIGHT WAVES IN A COMPOSITE OF CYLINDRICAL NANOINCLUSIONS IN PASSIVE AND ACTIVE HOST MATRICES** " by **YILAK ALEMU ABBO** in partial fulfillment of the requirements for the degree of **Master of Science in Physics**.

Dated: June 2014

Supervisor:

Prof. Vadim N. Mal'nev

Examiners:

Dr. Mulugeta Bekele
Associate Professor

Dr. Teshome Senbeta
Assistant Professor

ADDIS ABABA UNIVERSITY

Date: **June 2014**

Author: **YILAK ALEMU ABBO**

Title: **LIGHT WAVES IN A COMPOSITE OF CYLINDRICAL NANOINCLUSIONS IN PASSIVE AND ACTIVE HOST MATRICES**

Department: **Physics**

Degree: **M.Sc.** Convocation: **June** Year: **2014**

Signature of Author

To my parents, sisters, brothers and relatives

Table of Contents

Table of Contents vi

List of Figures vii

List of Symbols xiii

Abstract xv

Acknowledgements xvi

1 Introduction 1
- 1.1 Introduction . . . 1
- 1.2 Scope and Outline of the Thesis . . . 2
  - 1.2.1 Scope . . . 2
  - 1.2.2 Outline . . . 2

2 Maxwell Equations 4
- 2.1 Maxwell Equations . . . 4
- 2.2 Constitutive Relations . . . 5
- 2.3 Electromagnetic Wave Equation . . . 5

3 Models for Dielectric Permittivity $\epsilon(\omega)$ 7
- 3.1 Introduction . . . 7
- 3.2 Lorentz - Harmonic Oscillator Model . . . 8
- 3.3 The Drude Dielectric model . . . 9

4 Propagation of Narrow Light Pulse in a Dispersive Medium 11
- 4.1 Introduction . . . 11
- 4.2 Refractive Index . . . 11
- 4.3 Phase and Group Velocity . . . 13
- 4.4 Pulse Distortion . . . 16

5 Light Waves in a Composite of Nanoinclusions in Passive/Active Host Matrices 17
- 5.1 Introduction . . . 17
- 5.2 Clausius - Mossoti Relations . . . 19

5.3 Effective Medium Theory 21
5.4 Cylindrical Assemblage 23
5.4.1 Electrical Potential Distribution 23
5.4.2 Resonant Frequencies and Enhancement Factor of Local Field 26
5.4.3 Effective Polarizability 32
5.4.4 Refractive Index 34
5.4.5 Slow, Superluminal and Backward light 40
5.5 Spherical Assemblage 49
5.5.1 Electrical Potential Distribution 49
5.5.2 Resonant Frequencies and Enhancement Factor Of Local Field 50
5.5.3 Effective Polarizability 55
5.5.4 Refractive Index 56
5.5.5 Slow, Superluminal and Backward Lights 60

6 Conclusion **67**

Bibliography **68**

List of Figures

4.1 Group and phase velocity of a pulse 16

5.1 Model for Maxwell-Garnett effective medium theory 22

5.2 Model for composite with cylindrical inclusion embedded in a host matrix 24

5.3 Enhancement factor $\mid A \mid^2$ versus dimensionless frequency z of cylindrical metal inclusion with dielectric core at different metal fraction in the inclusion p; $\epsilon_\infty = 4.5, \epsilon_1 = 6, \epsilon_h = 2.25, \omega_p = 1.45 \times 10^{16}$(frequency of the silver surface plasmons), $\nu = 1.68 \times 10^{14}, \gamma = 1.15 \times 10^{-2}$. 27

5.4 Enhancement factor $|A|^2$ versus dimensionless frequency z of cylindrical metal inclusion with dielectric core at different metal fraction in the inclusion p; $\epsilon_\infty = 1, \epsilon_1 = 6, \epsilon_h = 2.25, \omega_p = 1.45 \times 10^{16}$(frequency of the silver surface plasmons), $\nu = 1.68 \times 10^{14}, \gamma = 1.15 \times 10^{-2}$. 28

5.5 Enhancement factor $|A|^2$ versus dimensionless frequency z of cylindrical dielectric inclusion with metal core at different metal fraction in the inclusion p; $\epsilon_\infty = 4.5, \epsilon_1 = 6, \epsilon_h = 2.25, \omega_p = 1.45 \times 10^{16}$(frequency of the silver surface plasmons), $\nu = 1.68 \times 10^{14}, \gamma = 1.15 \times 10^{-2}$. 29

5.6 Enhancement factor $|A|^2$ versus dimensionless frequency z of cylindrical dielectric inclusion with metal core at different metal fraction in the inclusion p; $\epsilon_\infty = 1, \epsilon_1 = 6, \epsilon_h = 2.25, \omega_p = 1.45 \times 10^{16}$(frequency of the silver surface plasmons), $\nu = 1.68 \times 10^{14}, \gamma = 1.15 \times 10^{-2}$. 29

5.7 Enhancement factor $|A|^2$ versus dimensionless frequency z of pure metal cylindrical inclusion ; $\epsilon_\infty = 4.5, \epsilon_h = 2.25, \omega_p = 1.45 \times 10^{16}$(frequency of the silver surface plasmons), $\nu = 1.68 \times 10^{14}, \gamma = 1.15 \times 10^{-2}$. 31

5.8 Enhancement factor $|A|^2$ versus dimensionless frequency z of pure metal cylindrical inclusion; $\epsilon_\infty = 1, \epsilon_h = 2.25, \omega_p = 1.45 \times 10^{16}$(frequency of the silver surface plasmons), $\nu = 1.68 \times 10^{14}, \gamma = 1.15 \times 10^{-2}$. 31

5.9 Passive composite with tuned cylindrical nanoinclusions ($\epsilon_h^{''} = 0$). a)Real part of refractive index n' versus dimensionless frequency z; b) Imaginary part of refractive index n'' versus z. Numerical values of composite parameters; $\epsilon_1 = 9, \epsilon_h^{'} = 2.25$, metal fraction in the inclusion $p = 0.4, 0.6, 0.7, 0.85, 0.9, \epsilon_\infty = 4.5, \omega_p = 1.6 \times 10^{16}(silver), \gamma = 1.15 \times 10^{-2}$, fraction of inclusion in the composite $f = 0.001$ 36

5.10 Passive composite with pure metal cylindrical nanoinclusions ($\epsilon_h^{''} = 0$) .a)Real part of refractive index n' versus dimensionless frequency z; b) Imaginary part of refractive index n'' versus z. Numerical values of composite parameters; $\epsilon_1 = 9, \epsilon_h^{'} = 2.25, \epsilon_\infty = 4.5, \omega_p = 1.6 \times 10^{16}(silver), \gamma = 1.15 \times 10^{-2}$, fraction of the inclusion in the composite $f = 0.001, 0.002, 0.003$ 36

5.11 Active composite with tuned cylindrical nanoinclusions ($\epsilon_h^{''} = -0.13866$). a)Real part of refractive index n' versus dimensionless frequency z; b) Imaginary part of refractive index n'' versus z. Numerical values of composite parameters; $\epsilon_1 = 9, \epsilon_h^{'} = 2.25$, metal fraction in the inclusion $p = 0.85, 0.9, 0.85, \epsilon_\infty = 4.5, \omega_p = 1.6 \times 10^{16}(silver), \gamma = 1.15 \times 10^{-2}$, fraction of the inclusion in the composite $f = 0.001$ 39

5.12 Active composite with pure metal cylindrical nanoinclusions ($\epsilon_h^{''} = -0.1159113$). a)Real part of refractive index n' versus dimensionless frequency z; b) Imaginary part of refractive index n'' versus z. Numerical values of composite parameters; $\epsilon_1 = 9, \epsilon_h^{'} = 2.25$, metal fraction in the inclusion $p = 1, \epsilon_\infty = 4.5, \omega_p = 1.6 \times 10^{16}(silver), \gamma = 1.15 \times 10^{-2}$, fraction of the inclusion in the composite $f = 0.0001, 0.0002, 0.0006, 0.0007$ 39

5.13 Passive composite with tuned cylindrical nanoinclusions ($\epsilon_h^{''} = 0$) . a) is group index n_g versus dimensionless frequency z. $a1$) is enlarged left tip of n_g. $a2$) is enlarged right tip of n_g. b) is normalized group velocity $\mathbf{v}_g/c$ versus z. $b1$) is enlarged left tip of $\mathbf{v}_g/c$. $b2$) is enlarged right tip of $\mathbf{v}_g/c$. Numerical values of composite parameters; $\epsilon_1 = 9, \epsilon_h^{'} = 2.25$, metal fraction in the inclusion $p = 0.9, \epsilon_\infty = 4.5, \omega_p = 1.6 \times 10^{16}(silver), \gamma = 1.15 \times 10^{-2}$, fraction of inclusion in the composite $f = 0.001$ 42

5.14 Passive composite with tuned cylindrical nanoinclusions ($\epsilon_h^{''} = 0$) . a) is group index n_g versus dimensionless frequency z. $a1$) is enlarged left tip of n_g. $a2$) is enlarged right tip of n_g. b) is normalized group velocity $\mathbf{v}_g/c$ versus z. $b1$) is enlarged left tip of $\mathbf{v}_g/c$. $b2$) is enlarged right tip of $\mathbf{v}_g/c$. Numerical values of composite parameters; $\epsilon_1 = 9, \epsilon_h^{'} = 2.25$, metal fraction in the inclusion $p = 0.7, \epsilon_\infty = 4.5, \omega_p = 1.6 \times 10^{16}(silver), \gamma = 1.15 \times 10^{-2}$, fraction of inclusion in the composite $f = 0.001$ 43

5.15 Passive composite with tuned cylindrical nanoinclusions ($\epsilon_h^{''} = 0$) . a) is group index n_g versus dimensionless frequency z. $a1$) is enlarged left tip of n_g. $a2$) is enlarged right tip of $n_g.b$) is normalized group velocity $\mathbf{v}_g/c$ versus z. $b1$) is enlarged left tip of $\mathbf{v}_g/c$. $b2$) is enlarged right tip of $\mathbf{v}_g/c$. Numerical values of composite parameters; $\epsilon_1 = 9, \epsilon_h^{'} = 2.25$, metal fraction in the inclusion $p = 0.4, \epsilon_\infty = 4.5, \omega_p = 1.6 \times 10^{16}(silver), \gamma = 1.15 \times 10^{-2}$, fraction of inclusion in the composite $f = 0.001$ 44

5.16 Passive composite with pure metal inclusions ($\epsilon_h^{''} = 0$) . a) is group index n_g versus dimensionless frequency z. b) is normalized group velocity $\mathbf{v}_g/c$ versus z. Numerical values of composite parameters; $\epsilon_1 = 9, \epsilon_h^{'} = 2.25, \epsilon_\infty = 4.5, \omega_p = 1.6 \times 10^{16}(silver), \gamma = 1.15 \times 10^{-2}$, fraction of the inclusion in the composite $f = 0.001$ 45

5.17 Passive composite with pure metal inclusions ($\epsilon_h^{''} = 0$) . a) is group index n_g versus dimensionless frequency z. b) is normalized group velocity v_g/c versus z. Numerical values of composite parameters; $\epsilon_1 = 9, \epsilon_h^{'} = 2.25$, fraction of the inclusion in the composite $f = 0.003$ 45

5.18 Activee composite with tuned cylindrical nanoinclusions ($\epsilon_h^{''} = -0.13866$) . a) is group index n_g versus dimensionless frequency z. $a1$) is enlarged left tip of n_g. $a2$) is enlarged right tip of n_g. b) is normalized group velocity $\mathbf{v}_g/c$ versus z. $b1$) is enlarged left tip of $\mathbf{v}_g/c$. $b2$) is enlarged right tip of $\mathbf{v}_g/c$. Numerical values of composite parameters; $\epsilon_1 = 9, \epsilon_h^{'} = 2.25$, metal fraction in the inclusion $p = 0.9, \epsilon_\infty = 4.5, \omega_p = 1.6 \times 10^{16}(silver), \gamma = 1.15 \times 10^{-2}$, fraction of inclusion in the composite $f = 0.001$ 47

5.19 Active composite with cylindrical pure metal inclusions ($\epsilon_h^{''} = -0.115911$) . a) is group index n_g versus dimensionless frequency z. b) is normalized group velocity $\mathbf{v}_g/c$ versus z. Numerical values of composite parameters; $\epsilon_1 = 9, \epsilon_h^{'} = 2.25, \epsilon_\infty = 4.5, \omega_p = 1.6 \times 10^{16}(silver), \gamma = 1.15 \times 10^{-2}$, fraction of the inclusion in the composite $f = 0.0001$ 48

5.20 Active composite with cylindrical pure metal inclusions ($\epsilon_h^{''} = -0.115911$) . a) is group index n_g versus dimensionless frequency z. b) is normalized group velocity v_g/c versus z. Numerical values of composite parameters; $\epsilon_1 = 9, \epsilon_h^{'} = 2.25, p = 1, \epsilon_\infty = 4.5, \omega_p = 1.6 \times 10^{16}(silver), \gamma = 1.15 \times 10^{-2}$, fraction of the inclusion in the composite $f = 0.0007$ 48

5.21 Enhancement factor $|A|^2$ versus dimensionless frequency z of spherical metal inclusion with a dielectric core at different metal fraction in the inclusion p; $\epsilon_\infty = 4.5, \epsilon_1 = 6, \epsilon_h = 2.25, \omega_p = 1.45 \times 10^{16}$(frequency of the silver surface plasmons), $\upsilon = 1.68 \times 10^{14}, \gamma = 1.15 \times 10^{-2}$. 51

5.22 Enhancement factor $|A|^2$ versus dimensionless frequency z of spherical metal inclusion with a dielectric core at different metal fraction in the inclusion p; $\epsilon_\infty = 1, \epsilon_1 = 6, \epsilon_h = 2.25, \omega_p = 1.45 \times 10^{16}$(frequency of the silver surface plasmons), $\upsilon = 1.68 \times 10^{14}, \gamma = 1.15 \times 10^{-2}$. 51

5.23 Enhancement factor $|A|^2$ versus dimensionless frequency z of spherical metal inclusion covered by dielectric at different metal fraction in the inclusion p; $\epsilon_\infty = 4.5, \epsilon_1 = 6.\epsilon_h = 2.25, \omega_p = 1.45 \times 10^{16}$(frequency of the silver surface plasmons), $\upsilon = 1.68 \times 10^{14}, \gamma = 1.15 \times 10^{-2}$. 52

5.24 Enhancement factor $|A|^2$ versus dimensionless frequency z of spherical metal inclusion covered by dielectric at different metal fraction in the inclusion p; $\epsilon_\infty = 1, \epsilon_1 = 6, \epsilon_h = 2.25, \omega_p = 1.45 \times 10^{16}$(frequency of the silver surface plasmons), $\upsilon = 1.68 \times 10^{14}, \gamma = 1.15 \times 10^{-2}$. 52

5.25 Enhancement factor $|A|^2$ versus dimensionless frequency z of pure metal cylindrical inclusion ; $\epsilon_\infty = 4.5, \epsilon_h = 2.25, \omega_p = 1.45 \times 10^{16}$(frequency of the silver surface plasmons), $\upsilon = 1.68 \times 10^{14}, \gamma = 1.15 \times 10^{-2}$. 54

5.26 Enhancement factor $|A|^2$ versus dimensionless frequency z of pure metal cylindrical inclusion;$\epsilon_\infty = 1, \epsilon_h = 2.25, \omega_p = 1.45 \times 10^{16}$(frequency of the silver surface plasmons), $\upsilon = 1.68 \times 10^{14}, \gamma = 1.15 \times 10^{-2}$. 54

5.27 Passive composite with tuned spherical nanoinclusions ($\epsilon_h^{''} = 0$) .a)Real part of refractive index n' versus dimensionless frequency z; b) Imaginary part of refractive index n'' versus z. Numerical values of composite parameters; $\epsilon_1 = 9, \epsilon_h^{'} = 2.25$, metal fraction in the inclusion $p = 0.4, 0.7, 0.9, \epsilon_\infty = 4.5, \omega_p = 1.6 \times 10^{16}(silver), \gamma = 1.15 \times 10^{-2}$, fraction of inclusion in the inclusion $f = 0.001$ 57

5.28 Passive composite with pure metal spherical nanoinclusions ($\epsilon_h^{''} = 0$) .*a*)Real part of refractive index n' versus dimensionless frequency z. *b*) Imaginary part of refractive index n'' versus z. Numerical values of composite parameters; $\epsilon_1 = 9, \epsilon_h^{'} = 2.25, \epsilon_\infty = 4.5, \omega_p = 1.6 \times 10^{16}(silver), \gamma = 1.15 \times 10^{-2}$, fraction of the inclusion in the composite $f = 0.001, 0.002, 0.003$ 58

5.29 Active composite with tuned spherical nanoinclusions ($\epsilon_h^{''} = -0.13866$). *a*)Real part of refractive index n' versus dimensionless frequency z. *b*) Imaginary part of refractive index n'' versus z. Numerical values of composite parameters; $\epsilon_1 = 9, \epsilon_h^{'} = 2.25$, metal fraction in the inclusion $p = 0.99, 0.9, 0.8, \epsilon_\infty = 4.5, \omega_p = 1.6 \times 10^{16}(silver), \gamma = 1.15 \times 10^{-2}$, fraction of the inclusion in the composite $f = 0.001$ 59

5.30 Active composite with pure metal spherical nanoinclusions ($\epsilon_h^{''} = -0.115911$). *a*)Real part of refractive index n' versus dimensionless frequency z. *b*) Imaginary part of refractive index n'' versus z. Numerical values of composite parameters; $\epsilon_1 = 9, \epsilon_h^{'} = 2.25, \epsilon_\infty = 4.5, \omega_p = 1.6 \times 10^{16}(silver), \gamma = 1.15 \times 10^{-2}$, fraction of the inclusion in the composite $f = 0.0001, 0.0002, 0.0003$ 59

5.31 Passive composite with tuned spherical nanoinclusions ($\epsilon_h^{''} = 0$) . *a*) is group index n_g versus dimensionless frequency z. *a*1) is enlarged left tip of n_g. *a*2) is enlarged right tip of n_g. *b*) is normalized group velocity $\mathbf{v}_g/c$ versus dimensionless frequency z. *b*1) is enlarged left tip of v_g/c . *b*2) is enlarged right tip of $\mathbf{v}_g/c$. Numerical values of composite parameters; $\epsilon_1 = 9, \epsilon_h^{'} = 2.25$, metal fraction in the inclusion $p = 0.9, \epsilon_\infty = 4.5, \omega_p = 1.6 \times 10^{16}(silver), \gamma = 1.15 \times 10^{-2}$, fraction of inclusion in the composite $f = 0.001$ 61

5.32 Passive composite with tuned spherical nanoinclusions ($\epsilon_h^{''} = 0$) . *a*) is group index n_g versus dimensionless frequency z. *a*1) is enlarged left tip of n_g. *a*2) is enlarged right tip of n_g. *b*) is normalized group velocity $\mathbf{v}_g/c$ versus z. *b*1) is enlarged left tip of $\mathbf{v}_g/c$. *b*2) is enlarged right tip of v_g/c. Numerical values of composite parameters; $\epsilon_1 = 9, \epsilon_h^{'} = 2.25$, metal fraction in the inclusion $p = 0.4, \epsilon_\infty = 4.5, \omega_p = 1.6 \times 10^{16}(silver), \gamma = 1.15 \times 10^{-2}$, fraction of the inclusion in the composite $f = 0.001$ 62

5.33 Passive composite with spherical pure metal inclusions ($\epsilon_h^{''} = 0$) . *a*) is group index n_g versus dimensionless frequency z. *b*) is normalized group velocity $\mathbf{v}_g/c$ versus z. Numerical values of composite parameters; $\epsilon_1 = 9, \epsilon_h^{'} = 2.25, \epsilon_\infty = 4.5, \omega_p = 1.6 \times 10^{16}(silver), \gamma = 1.15 \times 10^{-2}$, fraction of the inclusion in the composite $f = 0.001$ 63

5.34 Passive composite with spherical pure metal inclusions ($\epsilon_h^{''} = 0$) . a) is group index n_g versus dimensionless frequency z. b) is normalized group velocity $\mathbf{v}_g/c$ versus z. Numerical values of composite parameters; $\epsilon_1 = 9, \epsilon_h^{'} = 2.25, \epsilon_\infty = 4.5, \omega_p = 1.6 \times 10^{16}(silver), \gamma = 1.15 \times 10^{-2}$, fraction of the inclusion in the composite $f = 0.003$ 63

5.35 Active composite with tuned spherical nanoinclusions ($\epsilon_h^{''} = -0.13866$). a) is group index n_g versus dimensionless frequency z. $a1$) is enlarged left tip of n_g. $a2$) is enlarged right tip of n_g. b) is normalized group velocity $\mathbf{v}_g/c$ versus z . $b1$) is enlarged left tip of v_g/c. $b2$) is enlarged right tip of $\mathbf{v}_g/c$. Numerical values of composite parameters; $\epsilon_1 = 9, \epsilon_h^{'} = 2.25$, metal fraction in the inclusion $p = 0.99, \epsilon_\infty = 4.5, \omega_p = 1.6 \times 10^{16}(silver), \gamma = 1.15 \times 10^{-2}$, fraction of the inclusion in the composite $f = 0.001$ 64

5.36 Active composite with tuned spherical nanoinclusions ($\epsilon_h^{''} = -0.13866$) . a) is group index n_g versus dimensionless frequency z. $a1$) is enlarged left tip of n_g. $a2$) is enlarged right tip of n_g.b) is normalized group velocity $\mathbf{v}_g/c$ versus z . $b1$) is enlarged left tip of $\mathbf{v}_g/c$. $b2$) is enlarged right tip of v_g/c. Numerical values of composite parameters; $\epsilon_1 = 9, \epsilon_h^{'} = 2.25$, metal fraction in the inclusion $p = 0.8, \epsilon_\infty = 4.5, \omega_p = 1.6 \times 10^{16}(silver), \gamma = 1.15 \times 10^{-2}$, fraction of the inclusion in the composite $f = 0.001$ 65

5.37 Active composite with spherical pure metal inclusions ($\epsilon_h^{''} = -0.115911$) . a) is group index n_g versus dimensionless frequency z. b) is normalized group velocity $\mathbf{v}_g/c$ versus z. Numerical values of composite parameters; $\epsilon_1 = 9, \epsilon_h^{'} = 2.25, \epsilon_\infty = 4.5, \omega_p = 1.6 \times 10^{16}(silver), \gamma = 1.15 \times 10^{-2}$, fraction of the inclusion in the composite $f = 0.0001$ 66

5.38 Active composite with spherical pure metal inclusions ($\epsilon_h^{''} = -0.115911$) . a) is group index n_g versus dimensionless frequency z. b) is normalized group velocity $\mathbf{v}_g/c$ versus z. Numerical values of composite parameters; $\epsilon_1 = 9, \epsilon_h^{'} = 2.25, p = 1, \epsilon_\infty = 4.5, \omega_p = 1.6 \times 10^{16}(silver), \gamma = 1.15 \times 10^{-2}$, fraction of the inclusion in the composite $f = 0.0003$ 66

List of Symbols

B - Magnetic field, or magnetic induction

c - Speed of light in vacuum

D - Electric displacement, or electric induction

D - Effective polarizability of inclusion

E - Electric field strength

$\mathbf{E}_{at}$ - characteristic atomic electric field strength

$\mathbf{E}_{loc}$ - Local electric field

f - Fraction of inclusions in the composite

H - Magnetic field strength, or magnetic intensity

J - Total current density

k - Wave number

k_{spring} - Force spring constant

L - Depolarization factor

m -Mass of an electron

M - Magnetization

n - Refractive index

n_g -Group index

P- Polarization

$\mathbf{P}^L$ - Linear polarization

$\mathbf{P}^{NL}$ - Nonlinear polarization

$\boldsymbol{p}$ - Dipole moment

p - Metal fraction in the inclusion

σ - Conductivity

-e - Charge of electron

$\mathbf{v}_p$ - Phase velocity

$\mathbf{v}_g$ - Group velocity

a_0 - Bohr radius of hydrogen atom

ϵ_0 - Free space permitivity

ϵ - Dielectric constant(permitivity) of a medium

ϵ_{rel} - Relative permitivity(dielectric constant) of a medium

ϵ_{eff} - Effective petmitivity(dielectric constant) of a composite

ϵ_h - Dielectric constant (permitivity) of host matrix

ϵ_i - Dielectric constant (permitivity)of the i^{th} inclusion

μ_0 - Free space permeability

μ - Permeability of a medium

μ_{rel} - Relative permeability

ρ - Charge density

χ_e - Electric susceptibility

χ_m - Magnetic susceptibility

χ - Nonlinear kerr coefficient (nonlinear susceptibility)

ω - Angular frequency of an electromagnetic wave

ω_0 - Natural frequency of an electron in an atom

ω_p - Plasma frequency

ϕ - Phase of an electromagnetic wave

ν - Damping constant

α - Polarizability

α_c - Polarizability of a cylinder

α_s - Polarizability of a sphere

α_{abso} - Absorption coefficient

l - Typical length of light propagation in a medium

$|A|^2$ - Local field enhancement factor for a composite

Abstract

In this thesis work, we have studied the optical properties of a composite with metal coated dielectric cylindrical nanoinclusions / pure metal cylindrical nanoinclusions in passive and active dielectric host matrices. In order to compare results, we have also briefly discussed optical properties of a composite with spherical nanoinclusions in passive and active dielectric host matrices.

One of the optical properties of the composite we have investigated by this work is the local field enhancement factor at the core of the inclusions. The obtained result shows that for a composite of metal covered dielectric inclusions in passive host matrix there are two maximum values of the local field enhancement factor at two different resonant frequencies. For composite with dielectric covered metal inclusions only one peak of local field enhancement factor determined. We have also found that for a composite with pure metal cylindrical inclusion there is only one maxima of the local field enhancement factor.

In this work, the second main target of study interest was to determine the group velocity of narrow light wave packet that propagate in the overstated composites. We have determined that wave can travel with group velocity much slower than the speed of light in vacuum and faster than the speed of light in vacuum. Furthermore, we have found light waves that propagates with negative group velocity through the composite. In passive host matrix the light pulse seen absorbed within a very small distance when compared to the distance it travels in active host matrix. Hence the problem of absorption considerably reduced by using active host matrix.

Acknowledgements

Above all the greatest of my gratitude goes to "**God**" for everything he has done to me.

My parents, sisters, brothers and relatives also greatly acknowledged for their financial support, from the beginning to the end of this thesis work and in my stay as a graduate student at Addis Ababa University. Moreover, their effort on keeping my psychological strength in a very well manner stays with me forever !!!

At last but not at least, it is my deepest pleasure to express my thanks to my advisor and instructor Professor Vadim N. Mal'nev for his support, advice, warm encouragement, guidance and friendly approach. Prof. Mal'nev also made our stay with him comfortable and enjoyable.

Chapter 1

Introduction

1.1 Introduction

In classical physics, light is described as a type of an electromagnetic wave. The classical behaviors of the electromagnetic field is described by Maxwell's equations. In modern quantum physics, the electromagnetic field is described by the theory of quantum electrodynamics (QED). In this theory, light is described by the fundamental excitation (or quanta) of the electromagnetic field, called photons. In QED, photons are massless particles [1, 2, 3, 4].

Before the 17th century scientists believed that there was no such thing as the " speed of light ". They thought that light could travel any distance in no time at all. Later, several attempts were made to measure that speed. Ole Romer first demonstrated in 1676 that light traveled with a finite speed by studying the apparent motion of Jupiter's moon Io. In 1865, James Clerk Maxwell proposed that light is an electromagnetic wave and traveled at the speed c with which all electromagnetic waves propagates through the vacuum and c is related to the electric constant ϵ_0 and the magnetic constant μ_0 by the equation $c = 1/\sqrt{\epsilon_0 \mu_0}$ [1, 2, 5].

In 1905, Albert Einstein postulated that the speed of light with respect to any inertial frame is independent of the motion of the light source. According to Einstein special theory of relativity the speed of light in vacuum c is the maximum speed at which all energy, matter and information in the universe can travel. It is the speed at which all massless particles and associated fields (including electromagnetic fields such as light) travel in vacuum. After centuries of increasing precise measurements, in 1975 the speed of light was known to be 299,792,458 m/s with a measurement uncertainty of 4 parts/billion.[1]

In a medium, light doesn't travel at speed c; further, different type of light waves travels at different speeds. The speed at which the individual crest and trough of a plane wave propagates is called the phase velocity. An actual physical signal with a finite extent (a pulse of light)

travels at a speed different from phase velocity. The largest part of the pulse travels at the group velocity [1, 2, 5].

The concept of slow, superluminal and backward light related with the value of the group velocity in comparison to the speed of light in vacuum. And recent investigations showed that a light pulse can propagate in a dispersive optical medium with a group velocity very much slower and faster than the speed of light in vacuum. In early times, the concept of superluminal group velocity was in conflict with the notion of special theory of relativity and then it was solved by Sommerfield and Brillouin. According to Sommerfield and Brillouin signal velocity can't exceed c in the region of anomalous dispersion [3, 6].

Early investigations on slow and superluminal light have been conducted in atomic media with a cryogenic temperature. Hau et al [7, 8] showed slow light in ultra-cold sodium vapor. This report was followed by that of Kash et al [7, 9], who showed that ultra slow light speed in a hot atomic vapor of rubidium. Akulashin et at [7, 10] and Kim et al [7, 11] observed fast light using a method electromagnetically induced absorption and Wang et at [7, 12] also demonstrate fast light using gain assisted superluminal light propagation which was first introduced by Steinberg and Chiao [10, 13].

Recently, the study of slow and superluminal light focuses on solid state materials at room temperature. Bigelow et al [7] studied ultra-slow and superluminal light propagation in solid states at room temperature. V.N Mal'nev and Sisay [14] theoretically investigate slow, superluminal and backward light in a composite of spherical metal covered dielectric/pure metal nanoinclusions in active/passive host matrix.

1.2 Scope and Outline of the Thesis

1.2.1 Scope

The scope of this thesis work is to investigate the optical properties of a composite with metal covered dielectric cylindrical nanoinclusions and pure metal cylindrical nanoinclusions embedded in passive/active host matrices. Specially, the study focus on two targets : finding the local field enhancement factor of an electric field at the core of the inclusion and determining the speed of a light pulse that propagates within the composite.

1.2.2 Outline

Chapter 1 introduces the historical progress and findings towards slow and fast light. Early thought about speed of light to recent results of speed of light in solid state optical materials

briefly presented.

Chapter 2 provide us the four fundamental laws of classical electrodynamics which are known as Maxwell equations. Using Maxwell's equations, wave equation is derived and its solution is presented as equation of monochromatic plane wave.

Chapter 3 focus on the two dielectric models namely Lorentz Harmonic oscillator model and Drude dielectric model for dielectric and metal respectively. These two models allow one to derive the refractive index of a resonant systems.

Chapter 4 address the fundamental concepts of normal dispersion, anomalous dispersion and resonant absorption in a dispersive medium. The concept of phase velocity, group velocity, and also pulse distortion discussed.

Chapter 5 is the main part of our study. In this chapter the numerical results of our study presented. Local field enhancement factor of the composite, extreme values of group velocity of a light pulse in the composite discussed and outcomes of the study presented graphically.

Chapter 2

Maxwell Equations

The basis of electromagnetic theory is Maxwell's equations. They allow the derivation of the properties of electromagnetic waves. According to electromagnetic theory light is an electromagnetic phenomena described by the same theoretical principles that governs all forms of electromagnetic radiations. Optical frequencies occupy a band of the electromagnetic spectrum that extends from the infrared through the visible to the ultraviolet [4].

2.1 Maxwell Equations

The Maxwell equations are the set of four fundamental equations governing electromagnetism (i.e. the behavior of electric and magnetic fields). They were first written down in complete form by physicist James Clerk Maxwell, who added the so-called displacement current term to the final equation, although steady-state forms were known earlier [15].

$$\vec{\nabla} \cdot \mathbf{E} = \frac{\rho}{\epsilon_0} \tag{2.1.1}$$

$$\vec{\nabla} \times \mathbf{E} = -\frac{\partial \mathbf{B}}{\partial t} \tag{2.1.2}$$

$$\vec{\nabla} \cdot \mathbf{B} = 0 \tag{2.1.3}$$

$$\vec{\nabla} \times \mathbf{B} = \mu_0 \mathbf{J} + \mu_0 \epsilon_0 \frac{\partial\ \mathbf{E}}{\partial t} \tag{2.1.4}$$

where $\mathbf{E}$ is electric field strength, $\mathbf{B}$ is induced magnetic field, ρ is charge density, $\mathbf{J}$ is current density, $\epsilon_0 = 8.85 \times 10^{-1} \frac{F}{m}$ is free space permittivity and $\mu_0 = 4\pi \times 10^{-7} \frac{H}{m}$ is free space permeability.

The above four equations respectively known as Gauss's law for electricity, Gauss's law for magnetism, Faraday's law and Amper - Maxwell equation.

The term that Maxwell added to Amper's law [i.e. $\epsilon_0 \frac{\partial \mathbf{E}}{\partial t}$] is known as the displacement current. Its presence means a changing electric field causes a magnetic field even with out a current. It's the converse of Faraday's Law [2, 5].

2.2 Constitutive Relations

Electric displacement ($\mathbf{D}$) and magnetic induction ($\mathbf{B}$) related to the field intensities $\mathbf{E}$ and $\mathbf{H}$ via the so called constitutive relations. In vacuum they take their simple form

$$\mathbf{D} = \epsilon_0 \mathbf{E} \tag{2.2.1}$$

$$\mathbf{B} = \mu_0 \mathbf{H} \tag{2.2.2}$$

For simple homogeneous, isotropic dielectric materials:

$$\mathbf{D} = \epsilon_0 \mathbf{E} + \mathbf{P} = \epsilon_0 \mathbf{E} + \epsilon_0 \chi_e \mathbf{E} = \epsilon_0 (1 + \chi_e) \mathbf{E} = \epsilon_0 \epsilon_{rel} \mathbf{E} = \epsilon \mathbf{E} \tag{2.2.3}$$

where $\mathbf{P}$ is polarization, χ_e electrical susceptibility, $\epsilon_{rel} = \frac{\epsilon}{\epsilon_0} = 1 + \chi_e$ relative permitivity or dielectric constant

In magnetic material

$$\mathbf{B} = \mu_0 \mathbf{H} + \mathbf{M} = \mu_0 \mathbf{H} + \mu_0 \chi_m \mathbf{H} = \mu_0 (1 + \chi_m) \mathbf{H} = \mu_0 \mu_{rel} = \mu \mathbf{H} \tag{2.2.4}$$

where $\mathbf{M}$ is magnetization, χ_m magnetic susceptibility and $\mu_{rel} = \frac{\mu}{\mu_0} = 1 + \chi_m$ relative permeability

2.3 Electromagnetic Wave Equation

The electromagnetic wave equation is the second order partial differential equation that describes the propagation of electromagnetic wave through a vacuum or a medium. These wave equations follow immediately from maxwell equation. For a uniform and source free (i.e. $\rho = 0$ and $\mathbf{J} = 0$) space maxwell equations looks [1, 2, 3, 4, 5].

$$\vec{\nabla} \cdot \mathbf{E} = 0 \tag{2.3.1}$$

$$\vec{\nabla} \cdot \mathbf{B} = 0 \tag{2.3.2}$$

$$\vec{\nabla} \times \mathbf{E} = \frac{-\partial \mathbf{B}}{\partial t} \tag{2.3.3}$$

$$\vec{\nabla} \times \mathbf{B} = \mu_0 \epsilon_0 \frac{\partial \mathbf{E}}{\partial t} \tag{2.3.4}$$

Taking the curl of Faraday's law gives :

$$\vec{\nabla} \times (\vec{\nabla} \times \mathbf{E}) = -\frac{\partial}{\partial t}(\vec{\nabla} \times \mathbf{B}) \tag{2.3.5}$$

Using the vector identity $\vec{\nabla} \times \vec{\nabla} \times V = \vec{\nabla}(\vec{\nabla}.V) - \vec{\nabla}^2 V$ Eq.(2.3.5) can be written as

$$\vec{\nabla}(\vec{\nabla} \cdot \mathbf{E}) - \vec{\nabla}^2 \mathbf{E} = -\mu_0 \epsilon_0 \frac{\partial^2 \mathbf{E}}{\partial t^2} \tag{2.3.6}$$

And again the curl of Ampere - Maxwell equation can be written as :

$$\vec{\nabla}(\vec{\nabla} \cdot \mathbf{B}) - \vec{\nabla}^2 \mathbf{B} = -\mu_0 \epsilon_0 \frac{\partial^2 \mathbf{B}}{\partial t^2} \tag{2.3.7}$$

Since $\nabla \cdot \mathbf{E} = 0$ and $\nabla \cdot \mathbf{B} = 0$ the first term on the left side of the Eq.(2.2.6) and Eq.(2.2.7) vanishes and we obtain the wave equations also known as Helmholtz wave equation:

$$\vec{\nabla}^2 \mathbf{E} - \frac{1}{c^2} \frac{\partial^2 \mathbf{E}}{\partial t^2} = 0 \tag{2.3.8}$$

$$\vec{\nabla}^2 \mathbf{B} - \frac{1}{c^2} \frac{\partial^2 \mathbf{B}}{\partial t^2} = 0 \tag{2.3.9}$$

Where $c = 1/\sqrt{\mu_0 \epsilon_0}$ is the speed of light in vacuum

Eq.(2.3.8) and Eq.(2.3.9) can be written in general form of wave equation in one dimension as:

$$\vec{\nabla}^2 U(x,t) - \frac{1}{c^2} \frac{\partial^2 U(x,t)}{\partial t^2} = 0 \tag{2.3.10}$$

The solution of Eq.(2.3.10) is equation of plane wave and it represent a monochromatic plane wave :

$$U(x,t) = Ae^{i(kx-\omega t)} + Be^{-i(kx+\omega t)} \tag{2.3.11}$$

The first term of the general solution represents wave in positive direction of the $x - axis$ and the second term represents wave in opposite direction.

Chapter 3

Models for Dielectric Permittivity

$\epsilon(\omega)$

3.1 Introduction

When an electromagnetic wave interacts with matter it exerts a force by both electric **E** and magnetic **B** fields on the electrons in the matter. At high frequencies (optical frequencies) electric field **E** can displace the electrons in the atom. As a result each atoms becomes an electric dipole with dipole moment $\boldsymbol{p}$. And the total number of dipole moment per unit volume is known as polarization. The connection between macroscopic net polarization **P** and the applied electric field **E** described by [4, 5, 16, 17, 18, 19]:

$$\mathbf{P} = \epsilon_0 \chi_e \mathbf{E} \tag{3.1.1}$$

At high light intensities the resonance of matter on electric field **E** becomes dependent on higher power of the fields such phenomena is known as optical nonlinearity [17, 18]. Nonlinearity occurs typically only at very high intensities, that is value of the electric field is comparable to the characteristic atomic electric field strength $\mathbf{E}_{at} = \frac{e}{4\pi\epsilon_0 a_0^2}$ [17, 18], where -e is charge of an electron and $a_0 = 0.529A^0$ is the Bohr radius of the hydrogen atom. Numerically, $\mathbf{E}_{at} = 5.14 \times 10^{11}$ v/m.

In nonlinear optics, the optical response can often described by generalizing Eq.(3.1.1) by expressing polarization at a power series in the field strength **E** as :

$$\mathbf{P} = \epsilon_0(\chi_e^{(1)}\mathbf{E} + \chi_e^{(2)}\mathbf{E}^2 + \chi_e^{(3)}\mathbf{E}^3 + ...) \tag{3.1.2}$$

where $\chi_e^{(n)}$ are the n^{th} order susceptibility of the medium and the presence of such term is generally referred to us an n^{th} order nonlinearity.

The above expansion can be written as the sum of two terms

$$\mathbf{P} = \mathbf{P}^L + \mathbf{P}^{NL} \tag{3.1.3}$$

where
$\mathbf{P}^L = \epsilon_0 \chi_e^{(1)} \mathbf{E}$ is linear polarization
$\mathbf{P}^{NL} = \epsilon_0 \chi_e^{(2)} \mathbf{E}^2 + \epsilon_0 \chi_e^{(3)} \mathbf{E}^3 + ...$ is nonlinear polarization

3.2 Lorentz - Harmonic Oscillator Model

In a nonconducting isotropic medium electrons are permanently bound to the atoms comprising of the medium. Applying sufficiently small electric field can cause the electron to displace a distance $\mathbf{r}$ from its equilibrium position. But an attracting force from nucleus also act on the electron. In consequence an electron of charge $-e$ with mass m executed forced oscillations in a time - periodic electric field. The model is known as harmonic oscillatory model. From the force balance the equation of motion for an electron bounded by a harmonic force and acting on by an electric field is [20]

$$F_{inertia} + F_{damping} + F_{repulsive} = F_{electrical} \tag{3.2.1}$$

$$m\frac{\partial^2 \mathbf{r}}{\partial t^2} + m\nu\frac{\partial \mathbf{r}}{\partial t} + m\omega_0^2 \mathbf{r} = -e\mathbf{E} \tag{3.2.2}$$

where ν damping constant, $\omega_0 = \sqrt{k_{spring}/m}$ is resonance frequency of the bound electron(natural frequency) and k_{spring} is the spring constant.

Suppose that the applied electric field varies harmonically with time according to the factor $e^{-i\omega t}$ $(i.e. \mathbf{E} = \mathbf{E}_0 e^{-i\omega t})$. And assuming that the motion of the electron has the same time dependence [i.e. $\mathbf{r} = \mathbf{r}_0 e^{-i\omega t}$] we can find that

$$(-\omega^2 - i\nu\omega + \omega_0^2)\mathbf{r}_0 = \frac{-e\mathbf{E}_0}{m} \tag{3.2.3}$$

$$\mathbf{r}_0 = \frac{-e\mathbf{E}_0}{m}\frac{1}{(\omega_0^2 - \omega^2 - i\nu\omega)} \tag{3.2.4}$$

The dipole moment contribution of one electron is

$$\boldsymbol{p} = -e\mathbf{r} = \frac{e^2\mathbf{E}}{m}\frac{1}{(\omega_0^2 - \omega^2 - i\nu\omega)} \tag{3.2.5}$$

And the dipole moment per unit volume which is known as polarization becomes

$$\mathbf{P} = N\boldsymbol{p} = \frac{-Ne^2\mathbf{E}}{m}\frac{1}{(\omega_0^2 - \omega^2 - i\nu\omega)} \tag{3.2.6}$$

If there are N molecules per unit volume with f_j electrons per molecule with binding frequency ω_j and damping constant ν_j, polarization given by Eq.(3.2.6) becomes:

$$\mathbf{P} = \frac{Ne^2\mathbf{E}}{m}\sum_j f_j(\omega_j^2 - \omega^2 - i\omega\nu_j)^{-1} \tag{3.2.7}$$

Then equating Eq.(3.1.1) and Eq.(3.2.7) can give us electric susceptibility and dielectric constant respectively as follow :

$$\chi_e = \frac{Ne^2}{\epsilon_0 m}\sum_j f_j(\omega_j^2 - \omega^2 - i\omega\nu_j)^{-1} \tag{3.2.8}$$

$$\frac{\epsilon(\omega)}{\epsilon_0} = 1 + \chi_e = 1 + \frac{Ne^2}{\epsilon_0 m}\sum_j f_j(\omega_j^2 - \omega^2 - i\omega\nu_j)^{-1} \tag{3.2.9}$$

$$\frac{\epsilon(\omega)}{\epsilon_0} = 1 + \sum_j \frac{f_j\omega_p^2}{(\omega_j^2 - \omega^2 - i\omega\nu_j)} \tag{3.2.10}$$

where, $\omega_p = \sqrt{\frac{Ne^2}{\epsilon_0 m}}$ is the plasma frequency. Eq.(3.2.9) is known as Lorentz harmonic oscillator model.

3.3 The Drude Dielectric model

This model deals about electrons not bound to a particular nucleus. Since these conduction electrons are not bound there is no elastic restoring force so $k_{spring} = 0$ and $\omega_0 = 0$. Hence, the differential equation of motion has the form

$$m\frac{\partial^2\mathbf{r}}{\partial t^2} + m\nu\frac{\partial\mathbf{r}}{\partial t} = -e\mathbf{E} \tag{3.3.1}$$

Assuming that $\mathbf{r}$ and $\mathbf{E}$ are harmonically time dependent and has the form $\mathbf{r} = \mathbf{r}_0 e^{-i\omega t}$ and $\mathbf{E} = \mathbf{E}_0 e^{-i\omega t}$ respectively, then the above equation of motion can be written as

$$(-\omega^2 - i\omega\nu)\mathbf{r}_0 = \frac{-e\mathbf{E}_0}{m} \tag{3.3.2}$$

$$\mathbf{r}_0 = \frac{e\mathbf{E}_0}{m(\omega^2 + i\omega\nu)} \tag{3.3.3}$$

Therefore, dipole moment contribution by an electrons becomes

$$\boldsymbol{p} = -e\mathbf{r} = \frac{-e^2\mathbf{E}}{m(\omega^2 + i\omega\nu)} \tag{3.3.4}$$

And polarization $\mathbf{P}$ will be

$$\mathbf{P} = N\boldsymbol{p} = \frac{-Ne^2\mathbf{E}}{m(\omega^2 + i\omega\nu)} \tag{3.3.5}$$

Eq.(3.1.1) and Eq.(3.3.5) gives us electrical susceptibility as

$$\chi_e = \frac{-Ne^2}{\epsilon_0 m(\omega^2 + i\omega\nu)} = \frac{-\omega_p^2}{\omega^2 + i\omega\nu} \tag{3.3.6}$$

And the relative dielectric constant becomes

$$\frac{\epsilon(\omega)}{\epsilon_0} = 1 + \chi_e = 1 - \frac{\omega_p^2}{\omega^2 + i\omega\nu} \tag{3.3.7}$$

Equation (3.3.7) is well known as the Drude dielectrics model. But since all electrons in a metal are not free the Drude model has to be modified by accounting bound electrons in a metal. The contribution from bound electrons to the dielectric function $\epsilon(\omega)$ is quite similar to the corresponding resonance in dielectric materials, and these can be written in Lorentz form as [20]

$$\epsilon_{ib} = 1 + \sum_j \frac{f_j\omega_p^2}{(\omega_j^2 - \omega^2 - i\omega\nu_j)} \tag{3.3.8}$$

The overall dielectric function of the metal therefore contains both the Drude term for free electrons and ϵ_{ib} for bound ones.

$$\begin{aligned}
\epsilon(\omega)_{rel} &= \epsilon_{ib} + 1 - \frac{\omega_p^2}{\omega^2 + i\omega\nu} && (3.3.9)\\
&= \epsilon_\infty - \frac{\omega_p^2}{\omega^2 + i\omega\nu} && (3.3.10)\\
&= \epsilon_\infty - \frac{\omega_p^2}{\omega^2 + \nu^2} + i\frac{\nu\omega_p^2}{\omega(\omega^2 + \nu^2)} && (3.3.11)\\
&= \epsilon^{'}(\omega) + i\epsilon^{''}(\omega) && (3.3.12)
\end{aligned}$$

where $\epsilon^{'}(\omega)$ and $\epsilon^{''}(\omega)$ are the real part and the imaginary part of the dielectric constant $\epsilon(\omega)$ of a metal, respectively.

Chapter 4

Propagation of Narrow Light Pulse in a Dispersive Medium

4.1 Introduction

In vacuum, regardless the difference in their frequencies, light waves of different frequency travel with the same speed $c = 3 \times 10^8$ m/s. But in a dispersive medium (i.e. medium in which the refractive index of the medium depends on the frequency of the propagating light wave) light waves of different frequencies can travel with different speeds.

4.2 Refractive Index

In optics the refractive index or index of refraction n of a substance (optical medium) is a dimensionless number that describes how light, or any other radiation, propagates through that medium. It is defined as the ratio of the speed of light in vacuum to the speed of light in the medium. In vacuum refractive index is not a function of the angular frequency of the incident light, but the refractive index of a dispersive medium depends on the angular frequency of the light that propagates through it. In general the refractive index n of a medium is a complex quantity, and its real part related with propagation of the electromagnetic field in the medium. The imaginary part of the refractive index related with the absorption of the incident light. Positive imaginary part refers to absorption of an electromagnetic wave, but when it is negative it shows amplification of an electromagnetic wave that propagates through a medium. To see how the polarization of a medium affects the propagation of light, consider the following procedures.

Take the curl of Faraday law

$$\vec{\nabla} \times (\vec{\nabla} \times \mathbf{E}) = -\frac{\partial}{\partial t}(\vec{\nabla} \times \mathbf{B}) \tag{4.2.1}$$

Now substitute Ampere - Maxwell equation in the place of $\vec{\nabla} \times \mathbf{B}$

$$\vec{\nabla} \times (\vec{\nabla} \times \mathbf{E}) = -\mu_0(\frac{\partial}{\partial t}\mathbf{J} + \frac{\partial^2}{\partial t^2}\epsilon_0\mathbf{E} + \frac{\partial^2}{\partial t^2}\mathbf{P}) \tag{4.2.2}$$

From vector identity we have

$$\vec{\nabla} \times \vec{\nabla} \times \mathbf{E} = \vec{\nabla} \cdot (\vec{\nabla} \cdot \mathbf{E}) - \vec{\nabla}^2 \cdot \mathbf{E} \tag{4.2.3}$$

Since $\vec{\nabla} \cdot \mathbf{E} = 0$ equating Eq.(4.2.2) and Eq. (4.2.3) can give as the expression below.

$$\vec{\nabla}^2\mathbf{E} = \mu_0\frac{\partial}{\partial t}\mathbf{J} + \mu_0\epsilon_0\frac{\partial^2}{\partial t^2}\mathbf{E} + \mu_0\frac{\partial^2}{\partial t^2}\mathbf{P} \tag{4.2.4}$$

For dielectric there is no conduction term ($i.e. \sigma = 0, \mathbf{J} = \sigma\mathbf{E} = 0$), so Eq.(4.2.4) reduced to the form

$$\vec{\nabla}^2\mathbf{E} = \frac{1}{c^2}\frac{\partial^2}{\partial t^2}\mathbf{E} + \mu_0\frac{\partial^2}{\partial t^2}\mathbf{P} \tag{4.2.5}$$

Substitute polarization $\mathbf{P}$ from Eq.(3.2.7) in to Eq.(4.2.5), then we get

$$\vec{\nabla}^2\mathbf{E} = \frac{1}{c^2}\frac{\partial^2}{\partial t^2}\mathbf{E} + \frac{\mu_0 Ne^2}{m}\sum_j f_j(\omega_j^2 - \omega^2 - i\omega\gamma_j)^{-1}\frac{\partial^2}{\partial t^2}\mathbf{E} \tag{4.2.6}$$

$$= \frac{1}{c^2}(1 + \frac{Ne^2}{\epsilon_0 m}\sum_j f_j(\omega_j^2 - \omega^2 - i\omega\nu_j)^{-1})\frac{\partial^2}{\partial t^2}\mathbf{E} \tag{4.2.7}$$

Seek the solution to the above equation in the form of equation of homogeneous plane harmonic wave (i.e $\mathbf{E} = \mathbf{E}_0 e^{i(kx-\omega t)}$)and direct substitution to Eq.(4.2.7) gives

$$\vec{\nabla}^2\mathbf{E}_0 e^{i(kx-\omega t)} = \frac{1}{c^2}(1 + \frac{Ne^2}{\epsilon_0 m}\sum_j f_j(\omega_j^2 - \omega^2 - i\omega\nu_j)^{-1})\frac{\partial^2}{\partial t^2}\mathbf{E}_0 e^{i(kx-\omega t)} \tag{4.2.8}$$

$$i^2k^2\mathbf{E} = \frac{1}{c^2}(1 + \frac{Ne^2}{\epsilon_0 m}\sum_j f_j(\omega_j^2 - \omega^2 - i\omega\nu_j)^{-1})i^2\omega^2\mathbf{E} \tag{4.2.9}$$

$$k^2 = \frac{\omega^2}{c^2}(1 + \frac{Ne^2}{\epsilon_0 m}\sum_j f_i(\omega_j^2 - \omega^2 - i\omega\nu_j)^{-1}) \tag{4.2.10}$$

The presence of the imaginary part in the denominator implies wave vector k must be complex and $k = k(\omega)^{'} + k(\omega)^{''}$. Complex wave number k and refractive index n related by the expression below.

$$k(\omega) = \frac{\omega}{c}n(\omega) \tag{4.2.11}$$

where $n(\omega)$ is complex refractive index and $n(\omega) = n(\omega)^{'} + n(\omega)^{''}$.

So relating Eq.(4.2.10) and Eq.(4.2.11) gives us the expression for frequency dependent complex refractive index

$$n(\omega)^2 = (1 + \frac{Ne^2}{\epsilon_0 m} \sum_j f_i(\omega_j^2 - \omega^2 - i\omega\nu_j)^{-1}) \tag{4.2.12}$$

In order to find the real and the imaginary parts of the refractive index take the square root

$$\begin{aligned} n(\omega)^2 &= (n(\omega)^{'} + in(\omega)^{''})^2 & (4.2.13)\\ &= 1 + \frac{Ne^2}{\epsilon_0 m} \sum_j f_i(\omega_j^2 - \omega^2 - i\omega\nu_j)^{-1} & (4.2.14) \end{aligned}$$

Then equating real and imaginary parts yields

$$\begin{aligned} (n(\omega)^{'})^2 - (n(\omega)^{''})^2 &= 1 + \frac{Ne^2}{\epsilon_0 m} \sum_j f_j(\frac{\omega_j^2 - \omega^2}{(\omega_j^2 - \omega^2)^2 + \nu^2\omega^2}) & (4.2.15)\\ 2n(\omega)^{'} n(\omega)^{''} &= \frac{Ne^2}{\epsilon_0 m} \sum_j f_j(\frac{\nu\omega}{(\omega_j^2 - \omega^2)^2 + \nu^2\omega^2}) & (4.2.16) \end{aligned}$$

In a dispersive medium the case in which the real part of the refractive index increase as the angular frequency of the incident light increases is known as *normal dispersion*. And in the reverse, the decrease in the real part of the refractive index as the angular frequency of the incident wave increase called *anomalous dispersion*. Normal dispersion is seen to occur everywhere except in the neighborhood of the resonant frequency. Since a positive imaginary part of $n(\omega)$ represents dissipation of energy from the electromagnetic wave into the medium, the regions where imaginary part of $n(\omega)$ is large are called *region of resonant absorption* [5].

4.3 Phase and Group Velocity

The phase velocity of a monochromatic wave in a dispersive medium is defined as the velocity of points of constant phase. For a given complex electric field **E**:

$$\mathbf{E}(x,t) = \mathbf{E}_0 e^{i(kx-\omega t)} = \mathbf{E}_0 e^{ik(x-\frac{\omega}{k}t)} \tag{4.3.1}$$

where k is wave number, n is refractive index, ω is angular frequency of the wave and c is the

speed of light in vacuum.

The phase of this wave is $\phi = kx - \omega t$. And point of constant phase moves a distance Δx in a time Δt is

$$\mathbf{v} = \frac{\Delta x}{\Delta t} = \frac{\omega}{k} \tag{4.3.2}$$

Thus, phase velocity $\mathbf{v}_p$ well be

$$\mathbf{v}_p = \frac{\Delta x}{\Delta t} = \frac{\omega}{k} = \frac{c}{n} \tag{4.3.3}$$

For a dispersive medium n is a function of ω, so the phase velocity also becomes frequency dependent and the above expression can be modified as

$$\mathbf{v}_p = \frac{c}{n(\omega)} \tag{4.3.4}$$

where $n(\omega)$ is phase index.

The concept of group velocity was first introduced by William Rowan Hamilton in 1839. John Scott Russel in his paper reporting the first observation of soliton water wave in 1844 may also have been the first to observe and identify the group velocity of a wave. Lord Rayleigh in 1881 distinguished between phase velocity and group velocity in an article "On The Velocity Of Light"[3].

The notion of group velocity related with a wave packet(pulse), and it can be defined as the velocity with which the overall shape of the wave's amplitude known as the modulation or envelope of the wave propagates through space.

According to Fourier theory a pulse is necessarily composed of a range of frequencies. In a sense a pulse can be thought of resulting from constructive and destructive interference among varies Fourier (frequencies) components, will tend to add up in phase while interfering destructively in temporal wings of the pulse. A pulse can be constructed upon the theory of the Fourier integral by choosing the amplitude of the component harmonic waves as an appropriate function of the frequency or wave number and integrating [21].

$$U(x,t) = \int_{-\infty}^{\infty} A(k) e^{i(kx-\omega t)} dk \tag{4.3.5}$$

The concept of group velocity applies only to such Fourier representation are confined to a narrow band of the spectrum. If the amplitude function A(k) is of negligible magnitude outside the

region:

$$k_0 - \delta k \leq k \leq k_0 + \delta k \tag{4.3.6}$$

we may replace Eq.(4.3.5) by

$$U(x,t) = \int_{k_0-\delta k}^{k_0+\delta k} A(k) e^{i(kx-\omega t)} dk \tag{4.3.7}$$

Equation (4.3.7) represents narrow wave packet. If the distribution $A(k)$ is fairly sharp peaked around some value k_0, then the frequency $\omega(k)$ can be expand around that value of k using Taylor series as ;

$$\omega(k) = \omega_0 + \frac{d\omega}{dk} \mid_{k_0} (k - k_0) + \frac{1}{2} \frac{d^2\omega}{dk^2} \mid_{k_0} (k - k_0)^2 + ... \tag{4.3.8}$$

Consider only the first two terms in the derivation of group velocity for a narrow wave packet. Now narrow wave packet can be represented by

$$U(x,t) = e^{i(k_0 x - \omega_0 t)} \int_{k_0-\delta k}^{k_0+\delta k} A(k) e^{i(x - \frac{d\omega}{dk}|_{k_0} t)(k-k_0)} dk \tag{4.3.9}$$

This shows that the pulse travels undistorted in shape with a velocity called group velocity given by :

$$\mathbf{v}_g = \frac{d\omega}{dk}|_{k_0} \tag{4.3.10}$$

If this pulse is to propagate without distortion its component must be in phase for all value of the propagation distance x and requires that there be no change in ϕ to the first order in ω, that is $\frac{d\phi}{d\omega} = 0$. The group velocity which is expressed as $\mathbf{v}_g = \frac{d\omega}{dk}$ can be expressed in terms of group refractive index as

$$\mathbf{v}_g = \frac{c}{n(\omega) + \omega \frac{dn}{d\omega}} = \frac{c}{n_g} \tag{4.3.11}$$

where $n_g = n(\omega) + \omega \frac{dn}{d\omega}$ - is group refractive index.

In vacuum all frequency components of a light wave packet travel at the same speed that is the speed of light in vacuum c hence phase velocity and group velocity are equal. In general group velocity will be different from the phase velocity if a wave packet interacts with the material at any frequency and the material becomes dispersive at all frequencies. Due to dispersion group velocity and phase velocity are different in a dispersive medium.

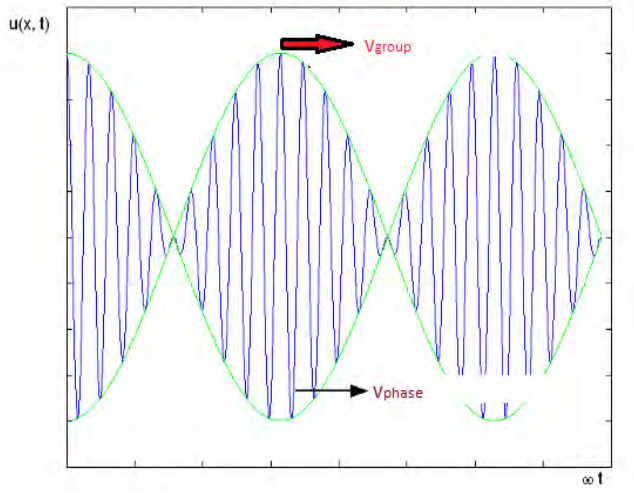

Figure 4.1: Group and phase velocity of a pulse

4.4 Pulse Distortion

The derivation of the group velocity in the previous section is by assuming

$$\omega(k) \approx \omega_0 + \frac{d\omega}{dk}(k - k_0) \tag{4.4.1}$$

If the wave packet has a relatively large frequency spread or if the wave packet travels over very long distance, this assumption is not valid and the higher order terms should be taken in to consideration.

As a result, the envelop of the wave packet distorts. Loosely speaking, different frequency component of the wave packet travels at different speeds, with the faster components moving towards the front of the wave packet and the slower moving towards the back. Eventual, the wave packet gets stretched out.

Chapter 5

Light Waves in a Composite of Nanoinclusions in Passive/Active Host Matrices

5.1 Introduction

According to the number of their constituent, materials can be classified into *monolithic* or *composite* material [22]. A monolithic material has a single constituent, while Composite materials (also called composition materials or shortened to composites) are materials made from two or more constituent materials with significantly different physical or chemical properties, that when combined, produce a material with characteristics different from the individual components. In composite material one of the constituent is continuous matrix which is called host matrix and the others dispersed in the host matrix are called inclusions or fillers. The new material may be preferred for many reasons: common examples include materials which are stronger and lighter when compared to traditional materials [23].

Composites are prevalent in both nature and among engineered materials. Natural composites exist in both animals and plants. Wood is a composite it is made from long cellulose fibers (a polymer) held together by a much weaker substance called lignin. Bone is also a composite. It is made from a hard but brittle material called hydroxyapatite (which is mainly calcium phosphate) and a soft and flexible material called collagen (which is a protein). Some rocks, such as sandstone, are aggregates of grains; other rocks, such as granite, are aggregates of crystals. In porous rocks the pores are often filled with a fluid such as salt water or oil. Cloud, fog, mist, and

rain are composites of air and water. High-altitude clouds are composite of air and ice crystals [24].

Typical engineered composite materials include: Fiberglass - a composite of glass and plastic matrices. Composite building materials such as cements, concrete and Ceramic Composites (composite of ceramic and metal matrices). Composite materials are generally used for buildings, bridges and structures such as boat hulls, swimming pool panels, race car bodies, shower stalls, bathtubs, storage tanks.

The properties of a composite material are related to the properties and fractions of the constituents, so the electromagnetic properties of composites can be tailored by varying the properties and fractions of the constituents [23].

A nanocomposite is a composite with nano sized dispersed particles in the matrix where the dimension of the particles are in the scale of nanometer at least in one direction.

Composite material, consisting of small, nonlinear metallic particles (existing in the shape of sphere or cylinder) are preferred for their complex responses to incident light field. Composites are of particular interests because their nonlinearities may be strongly enhanced relative to bulk sample of the same materials [25]. Amusing nonlinear phenomena, for example, optical bistability have been predicted theoretically [26] and observed experimentally [27]. Their promising applications include optical switches and transistors, pulse shaper, as well as memory elements [26, 28].

The composite model which we deal in our study is metal covered dielectric and pure metal cylindrical nanoinclusions embedded in a dielectric host matrix. Our model can be imagined as Figure(5.2). The dielectric constants of the dielectric core, the metal shell and the dielectric host matrix are ϵ_1, ϵ_2 and ϵ_h respectively. The radii of the core and the coating shell are r_1 and r_2 ($r_1 < r_2$). The shape of the inclusion can be spherical or cylindrical with the shell being concentric with the core. Usually, the shape of the inclusion can be identified by introducing the dimensionality factor d ($d = 3$ sphere, $d = 2$ cylinder) in the solution of Laplace equation [29].

5.2 Clausius - Mossoti Relations

The electric field that appears in Maxwell equation is known as the macroscopic or Maxwell field. This field is obtained by performing a spatial averaging of the actual (i.e. microscopic) electric field over a region of space whose linear dimensions are of the order of at least several atomic diameter [18]. However, the local field is the field resulting from all external sources and from all molecules within the sample except the one under consideration. This field can be calculated through use of a procedure described by Lorentz (1952).

If an electric field is applied to a medium made up of large number of atoms/molecules, the charge bound in each molecule will respond to the applied field and will execute perturbed motion. The molecular charge density will be distorted. The multipole moments are all zero, at least when averaged over many molecules. The dominant molecular multipole with the applied field is the dipole. There is thus produced in the medium an electric polarization $\mathbf{P}$ [5, 16].

In a rarefied media where molecular separations are large there is little difference between the macroscopic field and that acting on any molecule/group of molecules, but in dense media with closely packed molecules the polarization of neighboring molecules gives rise to an internal field at any given molecule in addition to the average macroscopic field $\mathbf{E}$ [16]. Therefor in condensed matter (liquid or solid) polarization due to neighboring has to be taken into account. After Lorentz work the effective local field is the sum of the macroscopic filed and the depolarization filed. The Lorentz local field effect can be expressed as [16]

$$\mathbf{E}_{loc} = \mathbf{E} + L\frac{\mathbf{P}}{\epsilon_0} \tag{5.2.1}$$

where L is the depolarization factor and it depends on shape. $L = \frac{1}{3}$ for sphere and $L = \frac{1}{2}$ for cylinder [19].

Consider lossless and dispersionless medium. The dipole moment induced in a typical molecule is

$$\boldsymbol{p} = \epsilon_0 \alpha \ \mathbf{E}_{loc} \tag{5.2.2}$$

where α linear polarizability, $\mathbf{E}_{loc}$ Lorentz local field, ϵ_0 free space permettivity and $\boldsymbol{p}$ dipole moment.

By definition the polarization of a material is given by

$$\mathbf{P} = N \ \boldsymbol{p} \tag{5.2.3}$$

where N is density number of molecules and **P** polarization.

Assume that the response of the system to an applied field **E** is linear and suppose that the medium is isotropic. Combining Eq.(5.2.1), Eq.(5.2.2) and Eq.(5.2.3) gives us the following relationship between the electric field applied to the system and polarization of the medium.

$$\mathbf{P} = N\epsilon_0\alpha\mathbf{E}_{loc} = \frac{N\epsilon_0\alpha}{1 - LN\alpha}\mathbf{E} \tag{5.2.4}$$

Combining Eq.(3.1.1) and Eq.(5.2.4) allows us to get linear susceptibility as below

$$\chi_e = \frac{N\alpha}{1 - LN\alpha} \tag{5.2.5}$$

From classical electrodynamics we know that the relative dielectric constant and linear susceptibility related as

$$\epsilon_{rel} = 1 + \chi_e \tag{5.2.6}$$

Dielectric properties of a homogeneous condensed material in terms of the microscopic property (the molecular polarizability α) and the macroscopic property (permittivity ϵ) was derived by Clausius and Mossoti. After some simple algebra we can get the following expression which is known as *The Clausius - Mossoti relation.*

$$\frac{\epsilon - \epsilon_0}{\epsilon + \epsilon_0(1/L - 1)} = LN\alpha \tag{5.2.7}$$

Since L depends on the shape of the dielectric, Clausius-Mossoti equation for spherical and cylindrical dielectrics becomes respectively as:

$$\frac{\epsilon_- \epsilon_0}{\epsilon + 2\epsilon_0} = \frac{N\alpha_s}{3} \tag{5.2.8}$$

$$\frac{\epsilon_- \epsilon_0}{\epsilon + \epsilon_0} = \frac{N\alpha_c}{2} \tag{5.2.9}$$

where ϵ electrical permittivity of a medium, ϵ_0 permittivity of free space, N density number of atoms/molecules, α_s polarizability of a sphere and α_c polarizability of a cylinder.

The Clausius-Mossoti relation can be expressed in terms of refractive index and it is known as Lorentz - Lorenz relation

$$\frac{n^2 - 1}{n^2 + (1/L - 1)} = LN\alpha \tag{5.2.10}$$

5.3 Effective Medium Theory

For the study of the optical properties of a composite system with an inhomogeneity scale much smaller than the wavelength of interest, electrodynamic quantities of each constituent particles is overshadowed by the average response of the whole system. Therefore, the optical properties of a microscopically heterogeneous composite can be investigated by evaluating the effective dielectric function in terms of the permittivities of the individual components as well as their respective volume fractions, this is known as *effective medium theory* [30].

Two of the most widely used effective medium approaches are Maxwell-Garnett Theory (MGT)and Bruggman Effective Medium Theory. Each of these two methods is based up on slightly different assumptions regarding the composite topology and the material properties of each constituent in the mixture.

The simplest approach to an effective medium that explicitly considers also the shape of the particles stems from J. C. Maxwell and Garnett in 1904 for spherical inclusions [30]. Fig.(5.1) shows a model in which we can apply the Maxwell - Garnett effective medium formula. The Rayleigh mixing formula for spherical inclusion is given as [30, 31]

$$\frac{\epsilon_{eff} - \epsilon_h}{\epsilon_{eff} + 2\epsilon_h} = f\frac{\epsilon_i - \epsilon_h}{\epsilon_i + 2\epsilon_h} \tag{5.3.1}$$

where $f = NV$ is the volume fraction of the spherical inclusion in the composite and ϵ_i dielectric constant for the i^{th} inclusion.

Rayleigh rule can be written explicitly below, and it is known as the Maxwell- Garnett formula for spherical inclusions embedded in a host matrix.

$$\epsilon_{eff} = \epsilon_h(1 + \frac{3f(\epsilon_i - \epsilon_h)}{(\epsilon_i + 2\epsilon_h) - f(\epsilon_i - \epsilon_h)}) \tag{5.3.2}$$

$$\epsilon_{eff} = \epsilon_h(1 + \frac{3f\beta}{1 - f\beta}) \tag{5.3.3}$$

where the term $\beta = \frac{\epsilon_i - \epsilon_h}{\epsilon_i + 2\epsilon_h}$ for spherical inclusion.

For the cylindrical inclusion the Rayleigh mixing formula is given as [31]

$$\frac{\epsilon_{eff} - \epsilon_h}{\epsilon_{eff} + \epsilon_h} = f\frac{\epsilon_i - \epsilon_h}{\epsilon_i + \epsilon_h} \tag{5.3.4}$$

where $f = NV$ - is the volume fraction of the cylindrical inclusion in the composite and ϵ_i-dielectric constant for the i^{th} inclusion.

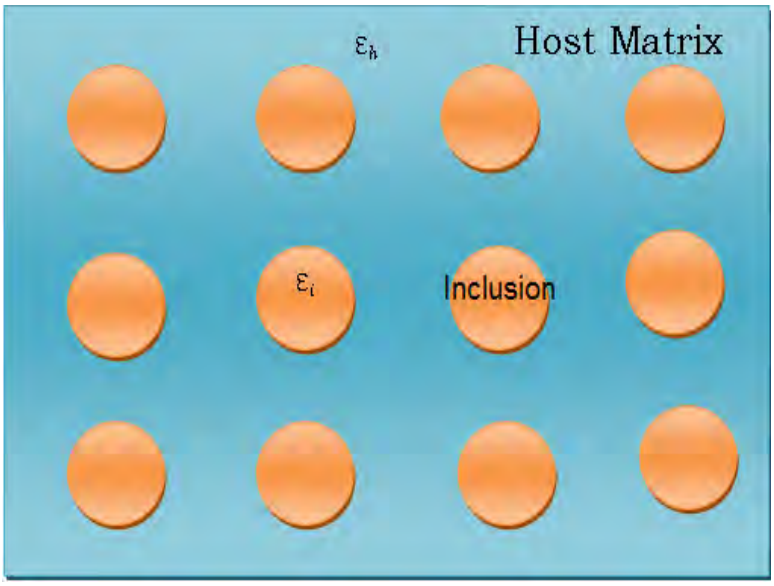

Figure 5.1: Model for Maxwell-Garnett effective medium theory

Like for the spherical case Rayleigh rule can be written explicitly below, and it is known as the Maxwell- Garnett formula.

$$\epsilon_{eff} = \epsilon_h(1 + \frac{2f(\epsilon_i - \epsilon_h)}{(\epsilon_i + \epsilon_h) - f(\epsilon_i - \epsilon_h)}) \tag{5.3.5}$$

$$\epsilon_{eff} = \epsilon_h(1 + \frac{2f\beta}{1 - f\beta}) \tag{5.3.6}$$

where the term $\beta = \frac{\epsilon_i - \epsilon_h}{\epsilon_i + \epsilon_h}$ for cylindrical inclusion.

5.4 Cylindrical Assemblage

In this section we deal with the optical properties of a composite of cylindrical nanoinclusions in passive and active host matrices. Here the cylindrical inclusion investigated in two formation: metal covered dielectric cylindrical assemblage and pure metal cylindrical assemblage. The graphical representation of our composite model is given by Fig.(5.2).

5.4.1 Electrical Potential Distribution

The potential distribution in a coated cylindrical and spherical inclusions in terms of the dimensionality factor (i.e. $d = 3$ for sphere and $d = 2$ for cylinder) is given by [29]

$$\Phi_1 = -\mathbf{E}_h A r \cos\theta, r \leq r_1 \tag{5.4.1}$$

$$\Phi_2 = -\mathbf{E}_h (Br - \frac{C}{r^{d-1}}) \cos\theta, r_1 \leq r \leq r_2 \tag{5.4.2}$$

$$\Phi_h = -\mathbf{E}_h (r - \frac{D}{r^{d-1}}) \cos\theta, r \geq r_2 \tag{5.4.3}$$

where Φ_1, Φ_2, and Φ_h are potentials in the dielectric core, metallic shell and the dielectric host matrix respectively, $\mathbf{E}_h$ electric field in the host, r_1 and r_2 are radii of the dielectric core and the metal shell respectively and, A, B, C and D are unknown coefficients which can be obtained from electrostatics boundary conditions.

The above three equations holds true for varying fields provided that the radius of the inclusion much less than the wave length of the incident radiation (i.e. $r_2 << \lambda$) [32].

In cylindrical coordinate system Laplace equation (i.e $\nabla^2\Phi = 0$) has the form

$$\frac{\partial^2\Phi}{\partial r^2} + \frac{1}{r}\frac{\partial\Phi}{\partial r} + \frac{1}{r^2}\frac{\partial^2\Phi}{\partial\theta^2} + \frac{\partial^2\Phi}{\partial z^2} = 0 \tag{5.4.4}$$

Since potential is not the function of z-axis Eq.(5.4.4) can be reduced to the form below

$$\frac{\partial^2\Phi}{\partial r^2} + \frac{1}{r}\frac{\partial\Phi}{\partial r} + \frac{1}{r^2}\frac{\partial^2\Phi}{\partial\theta^2} = 0 \tag{5.4.5}$$

Therefore, using Eq.(5.4.1), Eq.(5.4.2), and Eq.(5.4.3) we get the following potentials which satisfy the Laplace equation given by Eq.(5.4.5)

$$\Phi_1 = -\mathbf{E}_h A r \cos\theta, r \leq r_1 \tag{5.4.6}$$

$$\Phi_2 = -\mathbf{E}_h (Br - \frac{C}{r}) \cos\theta, r_1 \leq r \leq r_2 \tag{5.4.7}$$

$$\Phi_h = -\mathbf{E}_h (r - \frac{D}{r}) \cos\theta, r \geq r_2 \tag{5.4.8}$$

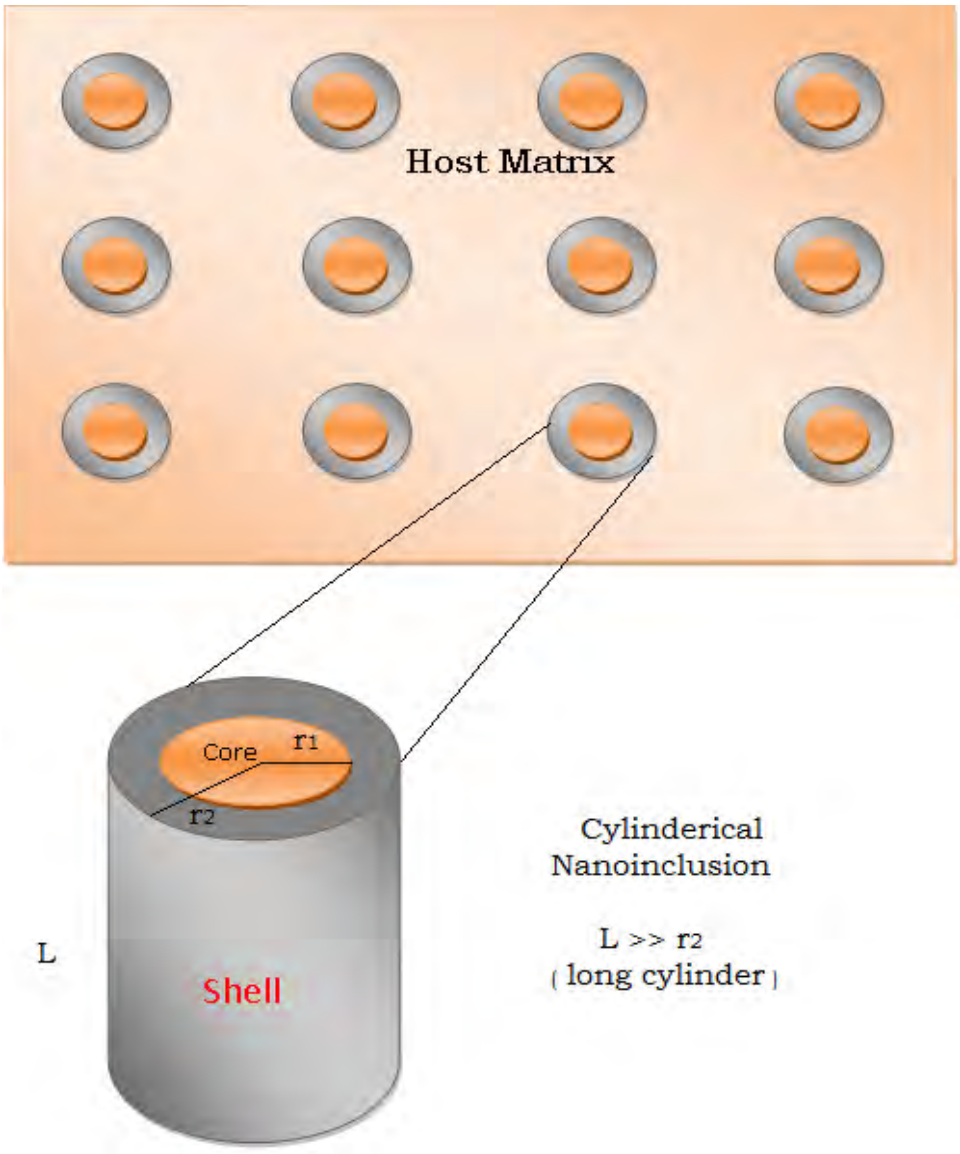

Figure 5.2: Model for composite with cylindrical inclusion embedded in a host matrix

Under the long wave approximation, the case in which the wave length of the incident electromagnetic wave grater than the size of the particle we can apply the following electrostatics boundary conditions in order to get the value of the coefficients A, B, C, and D.

1. Potential is continuous at the interface therefor ,
   at $r = r_1$, $\Phi_1 = \Phi_2$ and we get
   $$A = B - \frac{C}{r_1^2} \tag{5.4.9}$$
   at $r = r_2$, $\Phi_2 = \Phi_h$ and we get
   $$D = -Br_2^2 + C + r_2^2 \tag{5.4.10}$$

2. Displacement vector is continuous at the interface

   at $r = r_1$, $\epsilon_1 \frac{\partial \Phi_1}{\partial r} = \epsilon_2 \frac{\partial \Phi_2}{\partial r}$ and we get
   $$A = \frac{\epsilon_1}{\epsilon_2}(B - \frac{C}{r_1^2}) \tag{5.4.11}$$

   at $r = r_2$, $\epsilon_2 \frac{\partial \Phi_2}{\partial r} = \epsilon_h \frac{\partial \Phi_h}{\partial r}$ and we get
   $$D = \frac{\epsilon_2}{\epsilon_h} r_2^2 B + \frac{\epsilon_2}{\epsilon_h} C - r_2^2 \tag{5.4.12}$$

Solving Eq.(5.4.9), Eq.(5.4.10), Eq.(5.4.11) and Eq.(5.4.12) simultaneously can give us the value of the unknown coefficients as listed below

$$A = \frac{4\epsilon_2\epsilon_h}{p\Delta} \tag{5.4.13}$$
$$B = \frac{2\epsilon_h(\epsilon_1 + \epsilon_2)}{p\Delta} \tag{5.4.14}$$
$$C = \frac{2\epsilon_h(\epsilon_1 - \epsilon_2)r_1^2}{p\Delta} \tag{5.4.15}$$
$$D = [1 - 2\epsilon_h \frac{[\epsilon_2(2-p) + \epsilon_1 p]}{p\Delta}] r_2^2 \tag{5.4.16}$$

where,
$p = 1 - (\frac{r_1}{r_2})^2$ is the metal volume fraction in the cylindrical inclusion
$\Delta = \epsilon_2^2 + q\epsilon_2 + \epsilon_1\epsilon_h$
$q = (\frac{2}{p} - 1)\epsilon_1 + (\frac{2}{p} - 1)\epsilon_h$

5.4.2 Resonant Frequencies and Enhancement Factor of Local Field

The local field in the core is constant and it can be determined from the gradient of the electrical potential in the core [33].

$$\mathbf{E}_{loc} = -\nabla\Phi_1 = A.\mathbf{E}_h \tag{5.4.17}$$

Since A is a complex quantity it is appropriate to take the square of its module, which is a real quantity.

$$\mid A \mid^2 = \frac{16\epsilon_h^2}{p^2} \frac{\epsilon_2'^2 + \epsilon_2''^2}{(\epsilon_2'^2 - \epsilon_2''^2 + q\epsilon_2' + \epsilon_1\epsilon_h)^2 + \epsilon_2''^2(q + 2\epsilon_2')^2} \tag{5.4.18}$$

where,
$|A|^2$ is local field enhancement factor
$q = (\frac{2}{p} - 1)\epsilon_1 + (\frac{2}{p} - 1)\epsilon_h$

In general the dielectric constant of the host is complex, but for simplicity we take it real. The dielectric function of the metal in the inclusion is chosen to be in the Drude form

$$\epsilon_2 = \epsilon_\infty - \frac{1}{z(z + i\gamma)} \tag{5.4.19}$$

with,

$$\epsilon_2^{'} = \epsilon_\infty - \frac{1}{z^2 + \gamma^2} \tag{5.4.20}$$

$$\epsilon_2^{''} = \frac{\gamma}{z(z^2 + \gamma^2)} \tag{5.4.21}$$

where $\epsilon_2^{'}$ and $\epsilon_2^{''}$ are the real and imaginary parts of ϵ_2 respectively, $z = \frac{\omega}{\omega p}$ dimensionless frequency, ω frequency of the incident radiation, ω_p plasma frequency of the inclusion metal part, υ the electron collision frequency and $\gamma = \frac{\nu}{\omega_p}$.

The dielectric function of the dielectric core is given by

$$\epsilon_1 = \epsilon_{10} + \chi|\mathbf{E}|^2 \tag{5.4.22}$$

where ϵ_{10} is the linear part of ϵ_1, χ is known as nonlinear Kerr coefficient(nonlinear susceptibility) and for weak field $\chi|E|^2 << \epsilon_{10}$. At intense incident electromagnetic fields (laser radiation), it is necessary to consider the nonlinear part of the dielectric.

The figures below, $|A|^2$ versus z, shows that the local field enhancement factor varies with

z. For metal coated dielectric inclusion, Fig.(5.3) and Fig.(5.4) depicts that $|A|^2$ has two peaks at two different resonant frequencies and its magnitude increases as the metal fraction in the inclusion (i.e. p) increases. Furthermore, increasing the metal fraction in the inclusion cause the two maximum value of the enhancement factor to become more closer to each other.

The second factor that determine the magnitude of the local field enhancement factor is ϵ_∞. Fig.(5.3) is plotted for $\epsilon_\infty = 4.5$ and it prevails that the magnitude of the first maxima is greater than the second one for the same p. For $\epsilon_\infty = 1$, $|A|^2$ greater than its magnitude at the same p for $\epsilon_\infty = 4.5$ but the second maxima is greater than the first and its width becomes narrow.

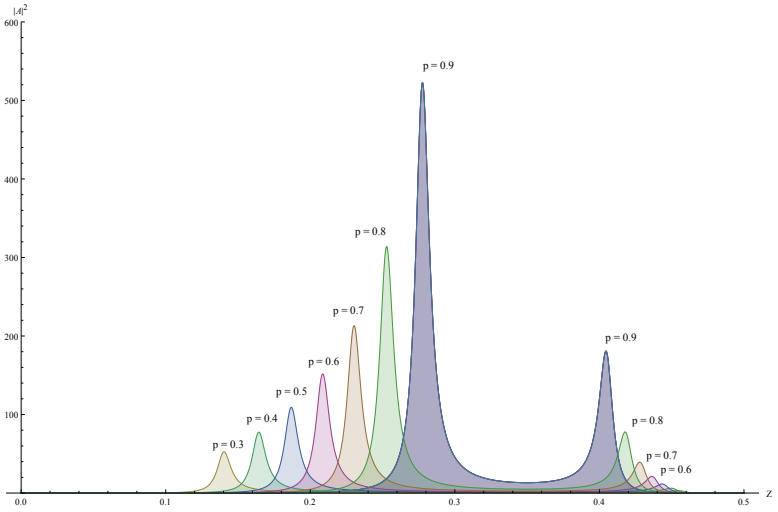

Figure 5.3: Enhancement factor $\mid A \mid^2$ versus dimensionless frequency z of cylindrical metal inclusion with dielectric core at different metal fraction in the inclusion p; $\epsilon_\infty = 4.5, \epsilon_1 = 6, \epsilon_h = 2.25, \omega_p = 1.45 \times 10^{16}$(frequency of the silver surface plasmons), $\nu = 1.68 \times 10^{14}, \gamma = 1.15 \times 10^{-2}$.

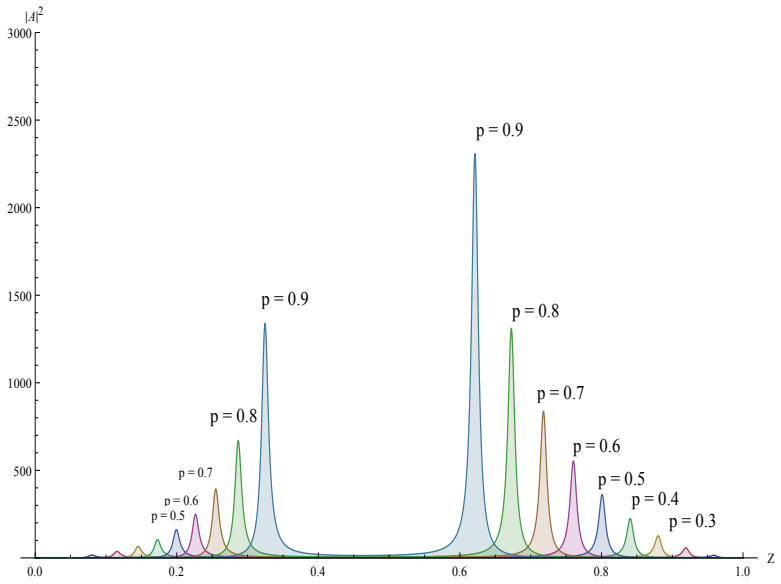

Figure 5.4: Enhancement factor $|A|^2$ versus dimensionless frequency z of cylindrical metal inclusion with dielectric core at different metal fraction in the inclusion p; $\epsilon_\infty = 1, \epsilon_1 = 6, \epsilon_h = 2.25, \omega_p = 1.45 \times 10^{16}$(frequency of the silver surface plasmons), $\nu = 1.68 \times 10^{14}, \gamma = 1.15 \times 10^{-2}$.

In the case of dielectric coated metal cylindrical nanoinclusion the expression for the local field enhancement can be determined from Eq.(5.4.13) by changing ϵ_1 to ϵ_2 and ϵ_2 to ϵ_1.

$$|A|^2 = \frac{16\epsilon_1^2\epsilon_h^2}{p^2} \frac{1}{(\epsilon_1^2 + q^*\epsilon_1 + \epsilon_2'\epsilon_h)^2 + \epsilon_2''^2((\frac{2}{p} - 1)\epsilon_1 + \epsilon_h)^2} \tag{5.4.23}$$

where $q^* = (\frac{2}{p} - 1)\epsilon_2' + (\frac{2}{p} - 1)\epsilon_h$.

Fig.(5.5) and Fig.(5.6) shows that for a composite with dielectric covered metal cylindrical nanoinclusion there is only one resonant frequency and one maximum of the enhancement factor. For this type of composite varying the thickness of the metal plays a role on obtaining higher value of the enhancement factor. We can easily observe from the results on Fig.(5.5) and Fig.(5.6), as we decrease the volume fraction of the metal core the magnitude of the local field enhancement factor rise. Here again ϵ_∞ determine the magnitude of the enhancement factor and is higher for $\epsilon_\infty = 1$ than for $\epsilon_\infty = 4.5$.

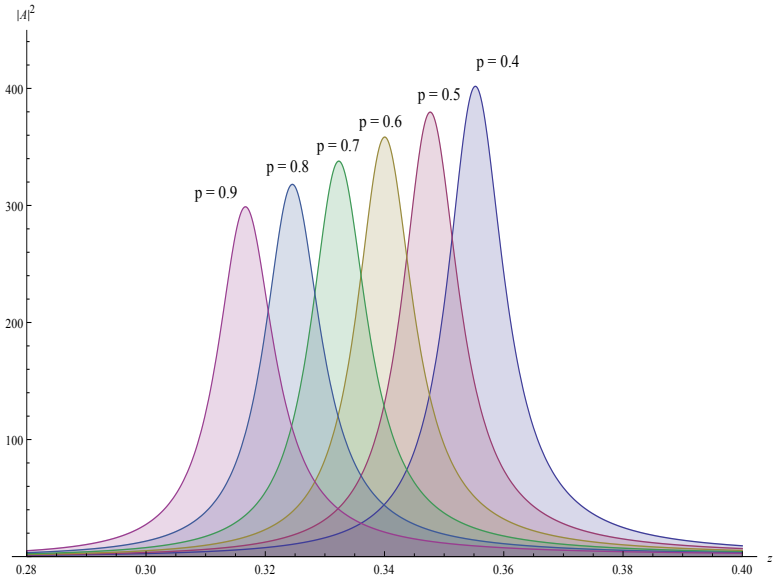

Figure 5.5: Enhancement factor $|A|^2$ versus dimensionless frequency z of cylindrical dielectric inclusion with metal core at different metal fraction in the inclusion p; $\epsilon_\infty = 4.5, \epsilon_1 = 6, \epsilon_h = 2.25, \omega_p = 1.45 \times 10^{16}$(frequency of the silver surface plasmons), $\nu = 1.68 \times 10^{14}, \gamma = 1.15 \times 10^{-2}$.

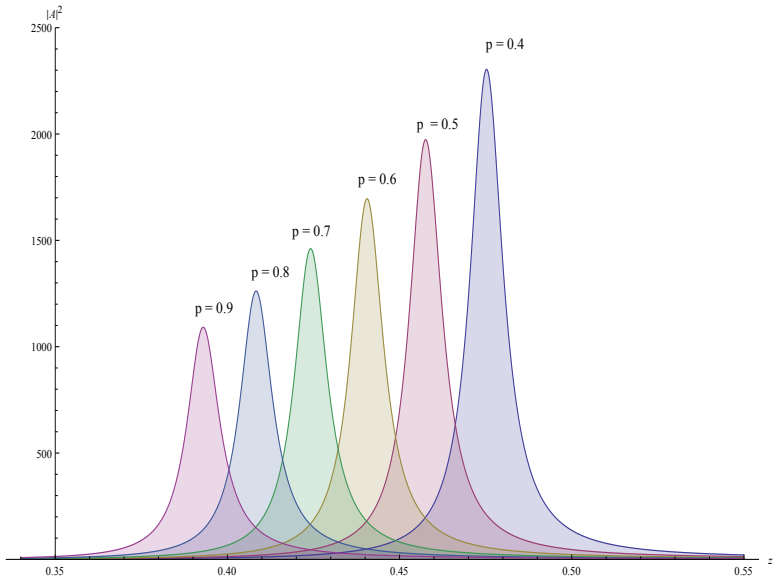

Figure 5.6: Enhancement factor $|A|^2$ versus dimensionless frequency z of cylindrical dielectric inclusion with metal core at different metal fraction in the inclusion p; $\epsilon_\infty = 1, \epsilon_1 = 6, \epsilon_h = 2.25, \omega_p = 1.45 \times 10^{16}$(frequency of the silver surface plasmons), $\nu = 1.68 \times 10^{14}, \gamma = 1.15 \times 10^{-2}$.

The potential distribution for a pure metal cylindrical inclusion with radius r_2 in a dielectric host matrix is [34]

$$\Phi_{in} = -\mathbf{E}_h A r cos\theta, r < r_2 \quad (5.4.24)$$

$$\Phi_{out} = -\mathbf{E}_h (r + \frac{B}{r}) cos\theta, r > r_2 \quad (5.4.25)$$

Where Φ_{in} and Φ_{out} are potentials inside the cylinder and out side the cylinder respectively, A and B are unknown coefficients which can be obtained form electrostatics boundary conditions

By applying electrostatics boundary conditions give by the section (5.4.1) we get

$$A = \frac{2\epsilon_h}{\epsilon_2 + \epsilon_h} \quad (5.4.26)$$

$$B = \frac{\epsilon_2 - \epsilon_h}{\epsilon_2 + \epsilon_h} r_2^2 \quad (5.4.27)$$

Therefore the local field enhancement factor for pure metal cylindrical inclusion becomes :

$$\mid A \mid^2 = \frac{4\epsilon_h^2}{[(\epsilon_2' + \epsilon_h)^2 + \epsilon_2''^2]} \quad (5.4.28)$$

Fig.(5.7) and Fig.(5.8) are plots for $\mid A \mid^2$ versus z for pure metal cylindrical inclusion with $\epsilon_\infty = 4.5$ and $\epsilon_\infty = 1$ respectively. These graphs shows that there is one maximum value of $\epsilon_\infty = 1$ at one resonant frequency. The magnitude of the enhancement factor significantly increase as we decrease the value of ϵ_∞.

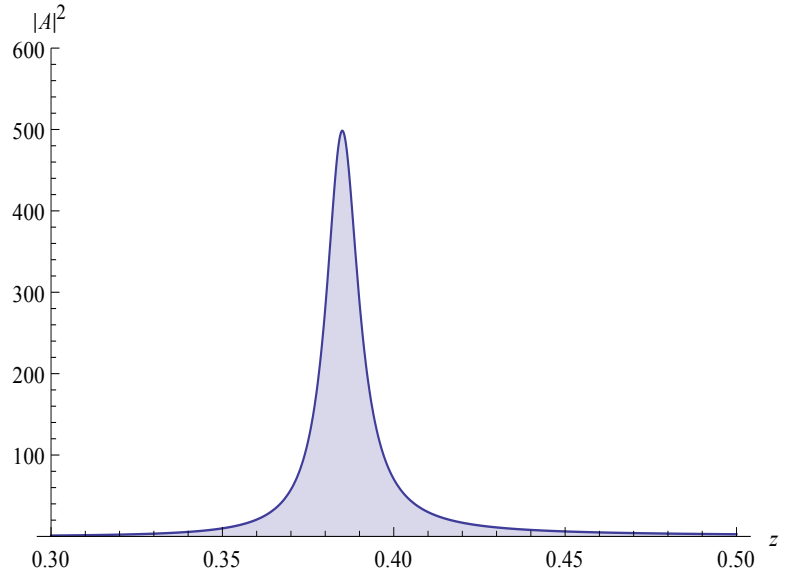

Figure 5.7: Enhancement factor $|A|^2$ versus dimensionless frequency z of pure metal cylindrical inclusion ; $\epsilon_\infty = 4.5, \epsilon_h = 2.25, \omega_p = 1.45 \times 10^{16}$(frequency of the silver surface plasmons), $\nu = 1.68 \times 10^{14}, \gamma = 1.15 \times 10^{-2}$.

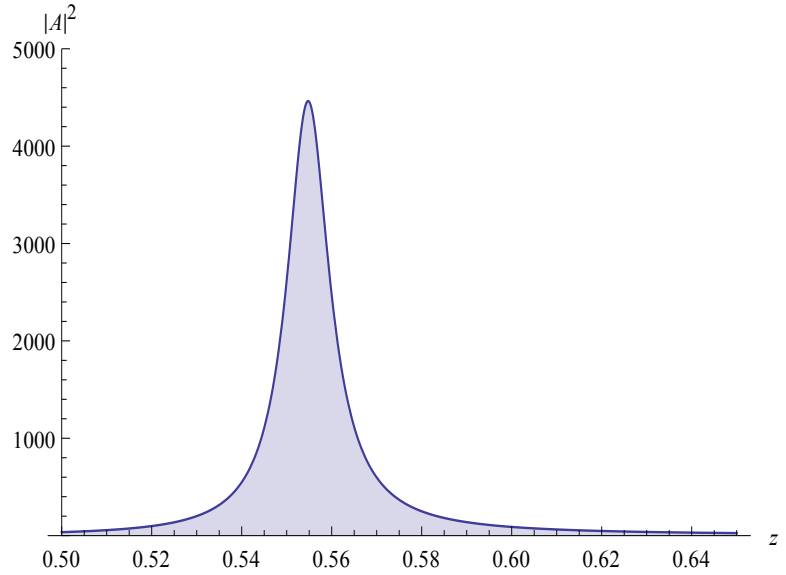

Figure 5.8: Enhancement factor $|A|^2$ versus dimensionless frequency z of pure metal cylindrical inclusion; $\epsilon_\infty = 1, \epsilon_h = 2.25, \omega_p = 1.45 \times 10^{16}$(frequency of the silver surface plasmons), $\nu = 1.68 \times 10^{14}, \gamma = 1.15 \times 10^{-2}$.

5.4.3 Effective Polarizability

The effective polarizability of an individual metal covered dielectric cylindrical nanoinclusion embedded in a dielectric host matrix can be presented by referring Eq.(5.4.8) and Eq.(5.4.16) as:

$$D = \beta r_2^2 \tag{5.4.29}$$

where,

$$\begin{aligned}
\beta &= 1 - 2\frac{\delta}{\Delta} && (5.4.30)\\
\delta &= \epsilon_h[\epsilon_2(\frac{2}{p} - 1) + \epsilon_1] && (5.4.31)\\
\Delta &= \epsilon_2^2 + q\epsilon_2 + \epsilon_1\epsilon_h && (5.4.32)\\
p &= 1 - (\frac{r_1}{r_2})^2 && (5.4.33)\\
q &= (\frac{2}{p} - 1)\epsilon_1 + (\frac{2}{p} - 1)\epsilon_h && (5.4.34)
\end{aligned}$$

The dielectric function of the core ϵ_1 is chosen to be real and frequency independent. The dielectric function of metal cover ϵ_2 is chosen to have the Drude form, its real $\epsilon_2^{'}$ and imaginary $\epsilon_2^{''}$ parts are given by Eq.(5.4.20) and Eq.(5.4.21). Since ϵ_2 and ϵ_h are complex, terms such as q, δ, Δ and β are also complex.

$$\begin{aligned}
\Delta &= \epsilon_2^2 + q\epsilon_2 + \epsilon_1\epsilon_h && (5.4.35)\\
&= (\epsilon^{'2}_2 - \epsilon^{''2}_2 + q^{'}\epsilon_2^{'} - q^{''}\epsilon_2^{''} + \epsilon_1\epsilon_h^{'}) + i(2\epsilon_1^{'}\epsilon_2^{''} + q^{'}\epsilon_2^{''} + q^{''}\epsilon_2^{'} + \epsilon_1\epsilon_h^{''}) && (5.4.36)\\
&= \Delta^{'} + i\Delta^{''} && (5.4.37)
\end{aligned}$$

where,
$q = q^{'} + iq^{''}$
$q^{'} = (\frac{2}{p} - 1)\epsilon_1 + (\frac{2}{p} - 1)\epsilon_h^{'}$
$q^{''} = (\frac{2}{p} - 1)\epsilon_h^{''}$
$\Delta^{'} = (\epsilon^{'2}_2 - \epsilon^{''2}_2 + q^{'}\epsilon_2^{'} - q^{''}\epsilon_2^{''} + \epsilon_1\epsilon_h^{'})$
$\Delta^{''} = (2\epsilon_2^{'}\epsilon_2^{''} + q^{'}\epsilon_2^{''} + q^{''}\epsilon_2^{'} + \epsilon_1\epsilon_h^{''})$

$$\begin{aligned}
\delta &= \epsilon_h[(\frac{2}{p} - 1)\epsilon_2 + \epsilon_1] && (5.4.38)\\
&= [(\frac{2}{p} - 1)(\epsilon_2^{'}\epsilon_h^{'} - \epsilon_2^{''}\epsilon_h^{''}) + \epsilon_1\epsilon_h^{'}] + i[(\frac{2}{p} - 1)(\epsilon_2^{'}\epsilon_h^{''} + \epsilon_2^{''}\epsilon_h^{'}) + \epsilon_1\epsilon_h^{''}] && (5.4.39)
\end{aligned}$$

Therefor, the real and imaginary parts of δ can be presented in a condensed form as below:

$$\delta = \delta^{'} + i\delta^{''} \tag{5.4.40}$$

where,
$\delta^{'} = (\frac{2}{p} - 1)[\epsilon_2^{'}\epsilon_h^{'} - \epsilon_2^{''}\epsilon_h^{''}] + \epsilon_1\epsilon_h^{'}$
$\delta^{''} = (\frac{2}{p} - 1)[\epsilon_2^{'}\epsilon_h^{''} + \epsilon_2^{''}\epsilon_h^{'}] + \epsilon_1\epsilon_h^{''}$

The term β is also a complex quantity and it can be written as:

$$\beta = 1 - 2\frac{\delta^{'} + i\delta^{''}}{\Delta^{'} + i\Delta^{''}} \tag{5.4.41}$$

$$= 1 - 2\frac{\delta^{'}\Delta^{'} + \delta^{''}\Delta^{''}}{\Delta^{'2} + \Delta^{''2}} + i2\frac{\delta^{'}\Delta^{''} - \delta^{''}\Delta^{'}}{\Delta^{'2} + \Delta^{''2}} \tag{5.4.42}$$

$$= \beta^{'} + i\beta^{''} \tag{5.4.43}$$

where,
$\beta^{'} = 1 - 2\frac{\delta^{'}\Delta^{'} + \delta^{''}\Delta^{''}}{\Delta^{'2} + \Delta^{''2}}$
$\beta^{''} = 2\frac{\delta^{'}\Delta^{''} - \delta^{''}\Delta^{'}}{\Delta^{'2} + \Delta^{''2}}$
For composite with pure metal cylindrical inclusion the corresponding quantities for $\beta^{'}$ and $\beta^{''}$ of Eq. (5.4.43) are respectively given by

$$\beta_m' = \frac{(\epsilon_2' - \epsilon_h')\Delta_m' + (\epsilon_2'' - \epsilon_h'')\Delta_m''}{|\Delta_m|^2} \tag{5.4.44}$$

$$\beta_m'' = \frac{(\epsilon_2'' - \epsilon_h'')\Delta_m' + (\epsilon_2' - \epsilon_h')\Delta_m''}{|\Delta_m|^2} \tag{5.4.45}$$

where,
$|\Delta_m|^2 = {\Delta_m'}^2 + {\Delta_m''}^2$
$\Delta_m' = \epsilon_2' + \epsilon_h'$
$\Delta_m'' = \epsilon_2'' + \epsilon_h''$

5.4.4 Refractive Index

By taking consideration of the effective medium theory and Eq.(5.2.10), Clausius - Mossoti equation for a composite with cylindrical inclusion has the form

$$\frac{\epsilon_{eff} - \epsilon_h}{\epsilon_{eff} + \epsilon_h} = \frac{ND}{2} \tag{5.4.46}$$

where ϵ_{eff} is the effective permittivity of the composite, ϵ_h is the permittivity of the host, N is density number of the inclusion and D effective polarizability of the inclusion.

By referring Eq.(5.3.4), Maxwell - Garnett mixing formula for the composite of our study interest can be written as:

$$\epsilon_{eff} = \epsilon_h(1 + \frac{2f\beta}{1 - f\beta}) \tag{5.4.47}$$

where β is given by Eq.(5.4.25).

For non magnetic medium $\mu = \mu_0$, hence index of refraction n can be expressed in terms of the effective dielectric constant as $n^2 = \epsilon_{eff}$. Therefore, it is possible to determine the refractive index of the composite from the above formula as

$$n^2 = \epsilon_h(1 + \frac{2f\beta}{1 - f\beta}) \tag{5.4.48}$$

Quantities such as ϵ_h and β are complex, so that its important to express n^2 in terms of its real and imaginary parts.

$$\begin{aligned}
n^2 &= (\epsilon_h^{'} + i\epsilon_h^{''})[1 + 2f\frac{(\beta^{'} + i\beta^{''})}{(1 - f\beta^{'}) - if\beta^{''}}] && (5.4.49)\\
&= (\epsilon_h^{'} + i\epsilon_h^{''})[1 + \frac{2f\beta^{'} - 2f^2(\beta^{'2} + \beta^{''2}) + i2f\beta^{''}}{\Delta_f}] && (5.4.50)\\
&= (\epsilon_h^{'} + i\epsilon_h^{''})[1 + \frac{2f\beta^{'} - 2f^2|\beta|^2 + i2f\beta^{''}}{\Delta_f}] && (5.4.51)\\
&= (\epsilon_h^{'} + 2f[\frac{(\beta^{'} - f|\beta|^2)\epsilon_h^{'} - \beta^{''}\epsilon_h^{''}}{\Delta_f}]) + i(\epsilon_h^{''} + 2f[\frac{(\beta^{'} - f|\beta|^2)\epsilon_h^{''} + \beta^{''}\epsilon_h^{'}}{\Delta_f}]) && (5.4.52)\\
&= b_1 + ib_2 && (5.4.53)
\end{aligned}$$

where,
$b_1 = (\epsilon_h^{'} + 2f[\frac{(\beta^{'} - f|\beta|^2)\epsilon_h^{'} - \beta^{''}\epsilon_h^{''}}{\Delta_f}])$
$b_2 = (\epsilon_h^{''} + 2f[\frac{(\beta^{'} - f|\beta|^2)\epsilon_h^{''} + \beta^{''}\epsilon_h^{'}}{\Delta_f}])$

$\Delta_f = 1 - f\beta^{'} + f^2|\beta|^2$

Equating the real and the imaginary parts $n = n' + in''$ with Eq.(5.4.49) can give us the expressions

$$n^{'2} - n^{''2} = b_1 \tag{5.4.54}$$

$$2n^{'}n^{''} = b_2 \tag{5.4.55}$$

The real and imaginary parts of the refractive index can be written in a condensed form by using b_1 and b_2 as

$$n^{'2} = \frac{1}{2}(\sqrt{b_1^2 + b_2^2} + b_1) \tag{5.4.56}$$

$$n^{''2} = \frac{1}{2}(\sqrt{b_1^2 + b_2^2} - b_1) \tag{5.4.57}$$

The numerical calculation of n' and n'' have been done by using Eq.(5.4.56) and Eq.(5.4.57). All the parameters used for passive composite (i.e. $\epsilon_h^{''} = 0$) and in active composite (i.e. $\epsilon_h^{''} < 0$) in this work taken from Ref.[14, 33]. The value of the parameters used are : $\epsilon_h^{'} = 2.25$, $\epsilon_\infty = 4.5$, $\omega_p = 1.6 \times 10^{16}(silver)$, $\gamma = 1.15 \times 10^{-2}$, for the composite with tuned inclusion $\epsilon_1 = 4\epsilon_h$ and for pure metal cylindrical inclusion only ϵ_2 and ϵ_h used.

Fig.(5.9a) shows n' versus z and Fig.(5.9b) shows n'' versus z near and at resonant frequencies of a composite of metal covered dielectric cylindrical inclusions in passive host matrix for different metal fraction p. However, their is a change in the magnitude of the maximum value n' for different p, there are two peak values of n' and n'' at two different resonant frequencies. The left peak is smaller in magnitude than the one on the right side for both n' and n''. The large positive value of the imaginary part n'' of the refractive index implies that at the two resonant frequencies there is strong absorption of an electromagnetic wave that propagate through the composite.

Unlike the coated inclusion case, on Fig.(5.10a) and Fig.(5.10b), we can observe that for pure metal cylindrical inclusion there is only one peak value of n' and n''. From the plots we can see, varying the fraction of the inclusion f in the composite shows change in the magnitude of the peak value. Again here in a composite with pure metal cylindrical inclusion in passive host matrix there is strong absorption of an incident electromagnetic wave at the region of anomalous dispersion.

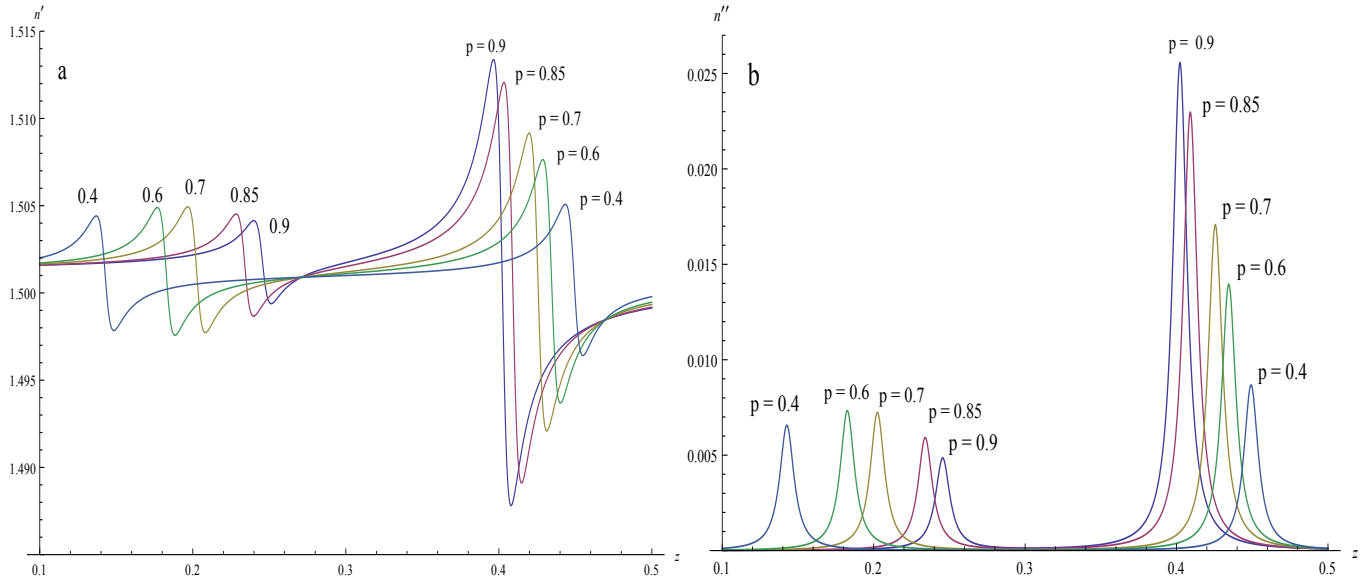

Figure 5.9: Passive composite with tuned cylindrical nanoinclusions ($\epsilon_h^{''} = 0$). *a*)Real part of refractive index n' versus dimensionless frequency z; *b*) Imaginary part of refractive index n'' versus z. Numerical values of composite parameters; $\epsilon_1 = 9, \epsilon_h^{'} = 2.25$, metal fraction in the inclusion $p = 0.4, 0.6, 0.7, 0.85, 0.9, \epsilon_\infty = 4.5, \omega_p = 1.6 \times 10^{16}(silver), \gamma = 1.15 \times 10^{-2}$, fraction of inclusion in the composite $f = 0.001$

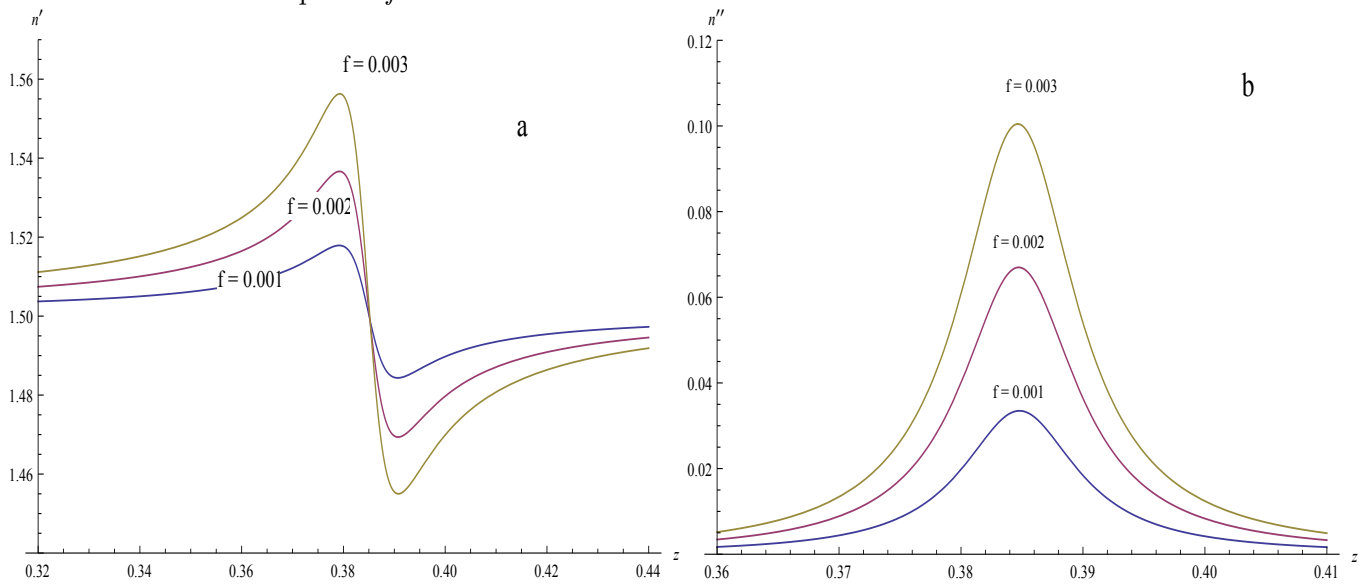

Figure 5.10: Passive composite with pure metal cylindrical nanoinclusions ($\epsilon_h^{''} = 0$) .*a*)Real part of refractive index n' versus dimensionless frequency z; *b*) Imaginary part of refractive index n'' versus z. Numerical values of composite parameters; $\epsilon_1 = 9, \epsilon_h^{'} = 2.25, \epsilon_\infty = 4.5, \omega_p = 1.6 \times 10^{16}(silver), \gamma = 1.15 \times 10^{-2}$, fraction of the inclusion in the composite $f = 0.001, 0.002, 0.003$

In order to study the absorption coefficient and the typical length of propagation, we can start out derivation from the solution of wave equation. The wave equation given by Eq.(2.3.8) admit us a solution of plane wave $\mathbf{E} = \mathbf{E}_0 e^{i(kx-\omega t)}$.

The wave number $k = n\omega/c$ is a complex quantity and has the form $k = k' + ik''$. So we can write the above equation as:

$$\mathbf{E} = \mathbf{E}_0 e^{i(k'x-\omega t)} e^{-k''x} \tag{5.4.58}$$

The presence of the term $e^{-k''x}$ implies that the wave decay as it propagates. The intensity of an electromagnetic wave is proportional to the square of the electric field ($i.e. I \sim \mathbf{E}^2$). And from Beer's law we have the relation

$$I = I_0 e^{-\alpha_{abso} x} \tag{5.4.59}$$

where α_{abso} is known as the absorption coefficient. Therefore, we can write the absorption coefficient as :

$$\alpha_{abso} = 2k'' = 2n''\omega/c \tag{5.4.60}$$

According to the obtained results in passive host matrix their is strong absorption. The absorption coefficient of the composites can be evaluated with the help of Eqn.(5.4.61).

$$\alpha_{abso} = 2n'' z_r \omega_p/c \tag{5.4.61}$$

For a composite of tuned inclusions with metal fraction $p = 0.9$ in passive host matrix, $n'' = 0.025$ at the resonant frequency $z_r = 0.4$ and by using $\omega_p = 1.6 \times 10^{16}$ we get that $\alpha_{abso} = 1 \times 10^4 cm^{-1}$. The typical length of light propagation in the media can be found by the help of $l \sim 1/\alpha_{abso}$ [33, 34]. So in our case $l \approx 9.4 \times 10^{-5} cm$.

For a composite of pure metal inclusion in passive host matrix, we got that $n'' = 0.033$ at the resonant frequency $z_r = 0.385$ and by using $\omega_p = 1.6 \times 10^{16}$ we get that $\alpha_{abso} = 1.4 \times 10^4 cm^{-1}$. The typical length of light propagation in the media can be found by the help of $l \sim 1/\alpha_{abso}$. So in our case $l \approx 7.4 \times 10^{-5} cm$.

In order to create condition for considerably propagating light waves, it is necessary to decrease n''. This can be done by introducing a negative part into the dielectric function of the host matrix [5]. The host matrix with negative ϵ_h ($i.e. \epsilon_h^{''} < 0$) amplify the incident electromagnetic wave rather than absorbing, such a medium is know as active host matrix.

Fig.(5.11a) and Fig.(5.11b) respectively shows the real and the imaginary parts of a composite of tuned inclusion in active host matrix for different metal fraction p. From the results we have found and presented on the Fig.(5.11a), we can see two maximum values of the real part of the refractive index at two different resonant frequencies. The first peak of the real part of the refractive index, on the left side, is comparatively very small to the second peak value on the right. On Fig.(5.11 b), for $p = 0.85$ the imaginary part of the refractive index has two minimum values at two different resonant frequencies. For metal thickness $p = 0.9$ and $p = 0.95$, the imaginary part of the refractive index has a fork like structure at the second resonant frequency on the right side.

For a composite of tuned inclusion with metal fraction $p = 0.9$ in active host matrix (i.e. $\epsilon_h = -0.13866$), $n'' = 0.0001361$ at the resonant frequency $z_r = 0.4$ and by using $\omega_p = 1.6 \times 10^{16}$ we get that $\alpha_{abso} = 48.4736cm^{-1}$. The typical length of light propagation in the media can be found by the help of $l \sim 1/\alpha_{abso}$ [5]. So in our case $l \approx 0.02cm$.

The real and the imaginary parts of the refractive index for a composite of pure metal inclusion in active host matrix for different fraction of the inclusion (i.e. f) in the host matrix presented on Fig.(5.12 a) and Fig.(5.12 b) respectively. There is only one maxima of n', and its magnitude can be increased by increasing f, Fig.(5.12 a). The imaginary part n'' for $f = 0.0001$ and $f = 0.0002$ has only one minima. When we increase the fraction of the inclusion to $f = 0.0006$ and $f = 0.0007$, we got that the minimum value has a fork like structure. And the minimum value of n'' goes more lower as we increase f.

For a pure metal inclusion in active host matrices we have found that the value of n'' significantly reduced and it becomes $n'' = 5.9 \times 10^{-5}$. The typical length of light propagating in a composite of pure metal cylindrical inclusion, thus becomes $l \approx 0.04cm$.

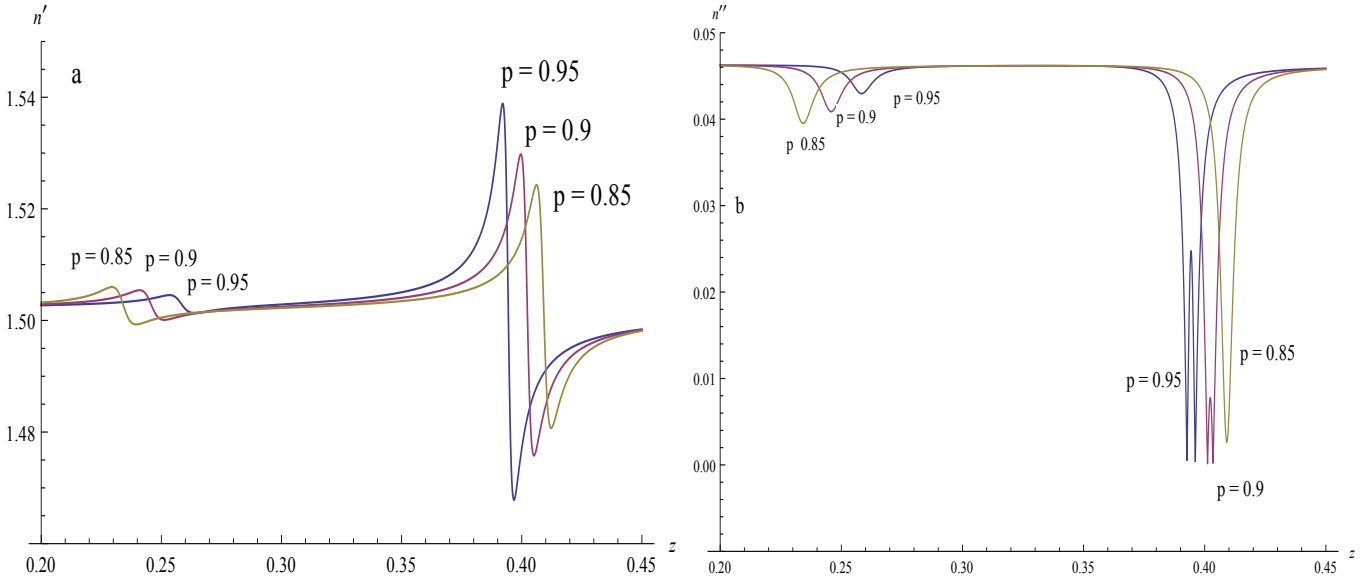

Figure 5.11: Active composite with tuned cylindrical nanoinclusions ($\epsilon_h^{''} = -0.13866$). *a*)Real part of refractive index n' versus dimensionless frequency z; *b*) Imaginary part of refractive index n'' versus z. Numerical values of composite parameters; $\epsilon_1 = 9, \epsilon_h^{'} = 2.25$, metal fraction in the inclusion $p = 0.85, 0.9, 0.85, \epsilon_\infty = 4.5, \omega_p = 1.6 \times 10^{16}(silver), \gamma = 1.15 \times 10^{-2}$, fraction of the inclusion in the composite $f = 0.001$

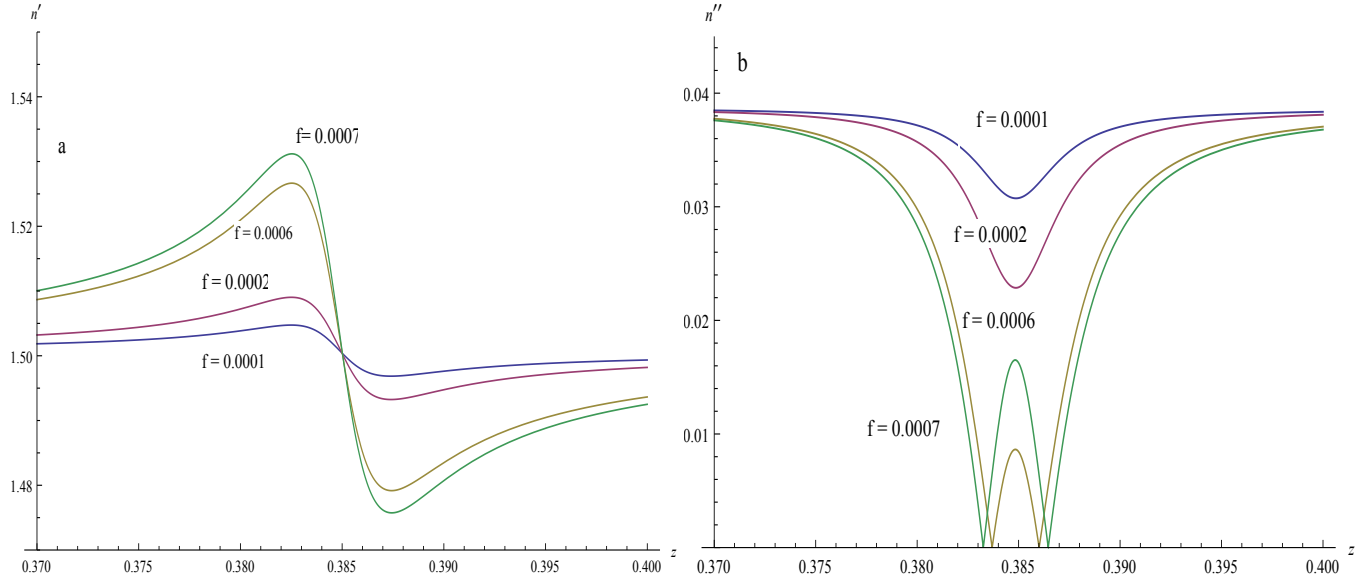

Figure 5.12: Active composite with pure metal cylindrical nanoinclusions ($\epsilon_h^{''} = -0.1159113$). *a*)Real part of refractive index n' versus dimensionless frequency z; *b*) Imaginary part of refractive index n'' versus z. Numerical values of composite parameters; $\epsilon_1 = 9, \epsilon_h^{'} = 2.25$, metal fraction in the inclusion $p = 1, \epsilon_\infty = 4.5, \omega_p = 1.6 \times 10^{16}(silver), \gamma = 1.15 \times 10^{-2}$, fraction of the inclusion in the composite $f = 0.0001, 0.0002, 0.0006, 0.0007$

5.4.5 Slow, Superluminal and Backward light

Recent researches has established that it is possible to control the velocity of propagation of light pulse through a material. Both, extremely slow propagation (much slower than c) and fast propagation (exceeding the velocity of light in vacuum c) have been observed. To understand these new results, it is crucial to recall the distinction between phase velocity and group velocity of a light field (refer section 4.3). Group velocity gives the velocity with which a pulse of light propagates though a material system [5]. One thus speaks of slow or fast light on the value of the group velocity of light in comparison to the velocity of light c in vacuum.

In order to discuss the concepts of slow, fast and negative group velocity of light we use the expression for group velocity in terms of group refractive index given by Eq.(4.3.11).

$$\mathbf{v}_g = \frac{c}{n'(\omega) + \omega\frac{dn'(\omega)}{d\omega}} = \frac{c}{n_g} \tag{5.4.62}$$

where $n'(\omega) + \omega\frac{dn'(\omega)}{d\omega}$ is the group index. We can see that the second term (i.e $\omega\frac{dn}{d\omega}$) plays a great role in obtaining extreme values of group velocity . Slow light refers to the situation in which $\mathbf{v}_g \ll c$. For normal dispersion $\frac{dn}{d\omega} > 0$, and $n > 1$; then the group velocity is less than the phase velocity [5].

Fast light refers to the light traveling faster than the speed of light in vacuum. This circumstance can occurs either when $\mathbf{v}_g > c$ or when group velocity is negative and large. In a region of anomalous dispersion, $\frac{dn}{d\omega}$ can become large and negative. Then the group velocity differs greatly from phase velocity, often becoming larger than c or even negative [5].

According to special theory of relativity nothing can travel with speed faster than the speed of light. The concept of superluminal group velocity doesn't violate special theory of relativity because at the region of anomalous dispersion group velocity doesn't have physical meaning. Large $\frac{dn}{d\omega}$ implies existence of significant absorption and a rapid variation of ω with k, consequently the approximation made on driving group velocity are no longer valid. Usually a pulse with its dominant frequency components in the neighborhood of a strong absorption line is absorbed and distorted as it travels [5].

Garret and McCumber [3,35] showed that there are circumstances in which superluminal group velocity can still have meaning, even with anomalous dispersion. S.Chu and S.Wong [36] subsequently verified experimentally what Garret and McCumber showed theoretically : namely, if absorbers are not too thick and for narrow band light pulse [3, 36].

A negative group velocity corresponds to the case when the peak of the pulse transmitted through an optical material emerges before the peak of the incident light field enters the medium. One might fear that the existence of negative group velocity would lead to a violation of the notion of causality. But physically, what occurs is pulse reshaping. Any physical pulse will have leading and trailing wings, the leading wing contains informations about the entire pulse shape, and this information traveling at normal velocities such as the speed of light in vacuum will allow the out put pulse to be fully reconstructed long before the peak of the input pulse enters the medium [5].

One of the main targets of this thesis is to study the speed of a light wave in a composite of metal covered dielectric and pure metal cylindrical nanoinclusions embedded in passive and active host matrices. The numerical values of group velocity near and at resonant frequency can be determined by using Eq. (5.4.64) with the real part of the refractive index as a function of dimensionless frequency z. All the value of the parameters used to find group velocity are the same to parameters used in finding real and imaginary part of the refractive index.

$$\mathbf{v}_g = \frac{c}{n'(z) + z\frac{dn'(z)}{dz}} = \frac{c}{n_g(z)} \tag{5.4.63}$$

In our study we have got that it is possible to control the speed of light in the composites by varying the fraction of the metal in the tuned inclusion, as well by varying the fraction of the the pure metal inclusions in the composite. All the numerical results we have obtained in our study are presented a plot of $\mathbf{v}_g/c$ versus the dimensionless frequency z .

Fig.(5.13), Fig.(5.14), and Fig.(5.15) shows the group refractive index and group velocity for tuned cylindrical inclusions in passive host matrix with $p = 0.9$, $p = 0.7$ and $p = 0.4$ respectively. From the obtained numerical results we can see that the normalized group velocity $\mathbf{v}_g/c$ for $p = 0.9$ (Fig.(5.13 b)), at the region of the first resonant frequency, the left peak show slow light of $\mathbf{v}_g = 0.77c$. In the region of the second resonant frequency there are two singularity points and when the frequency approach from the left to the first asymptote line as well the frequency approaches to the second asymptote line from the right $\mathbf{v}_g/c \to +\infty$. Between the two asymptote line on the right side, we got a negative superluminal light of group velocity $\mathbf{v}_g = -3.5c$. Reducing the thickness of metal in the inclusion shows significant change in the result and we found two maxima of the normalized group velocity. For $p = 7$ and $p = 0.4$ the plot for $\mathbf{v}_g/c$ versus z on Fig.(5.14 b) and Fig.(5.15 b) respectively depicts identical type of curve. For both $p = 0.7$and $p = 0.4$ the first peak on the left side show slow light with group velocity $\mathbf{v}_g = 0.8c$ and $\mathbf{v}_g = 0.75c$ respectively. Unlike the left peak, the right peak gives superluminal light with $\mathbf{v}_g = 4c$ and $\mathbf{v}_g = 1.2c$ for $p = 0.7$ and $p = 0.4$ respectively.

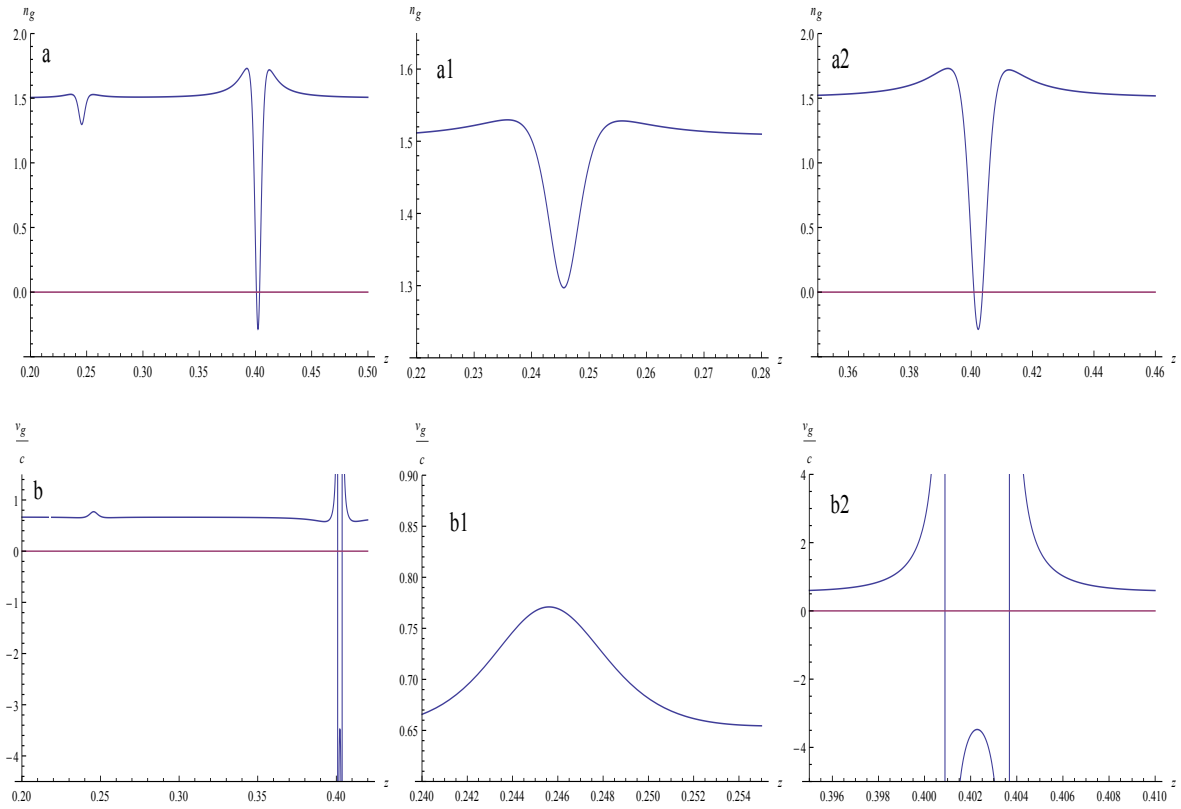

Figure 5.13: Passive composite with tuned cylindrical nanoinclusions ($\epsilon_h^{''} = 0$) . a) is group index n_g versus dimensionless frequency z. $a1$) is enlarged left tip of n_g. $a2$) is enlarged right tip of n_g. b) is normalized group velocity $\mathbf{v}_g/c$ versus z. $b1$) is enlarged left tip of $\mathbf{v}_g/c$. $b2$) is enlarged right tip of $\mathbf{v}_g/c$. Numerical values of composite parameters; $\epsilon_1 = 9, \epsilon_h^{'} = 2.25$, metal fraction in the inclusion $p = 0.9, \epsilon_\infty = 4.5, \omega_p = 1.6 \times 10^{16}(silver), \gamma = 1.15 \times 10^{-2}$, fraction of inclusion in the composite $f = 0.001$

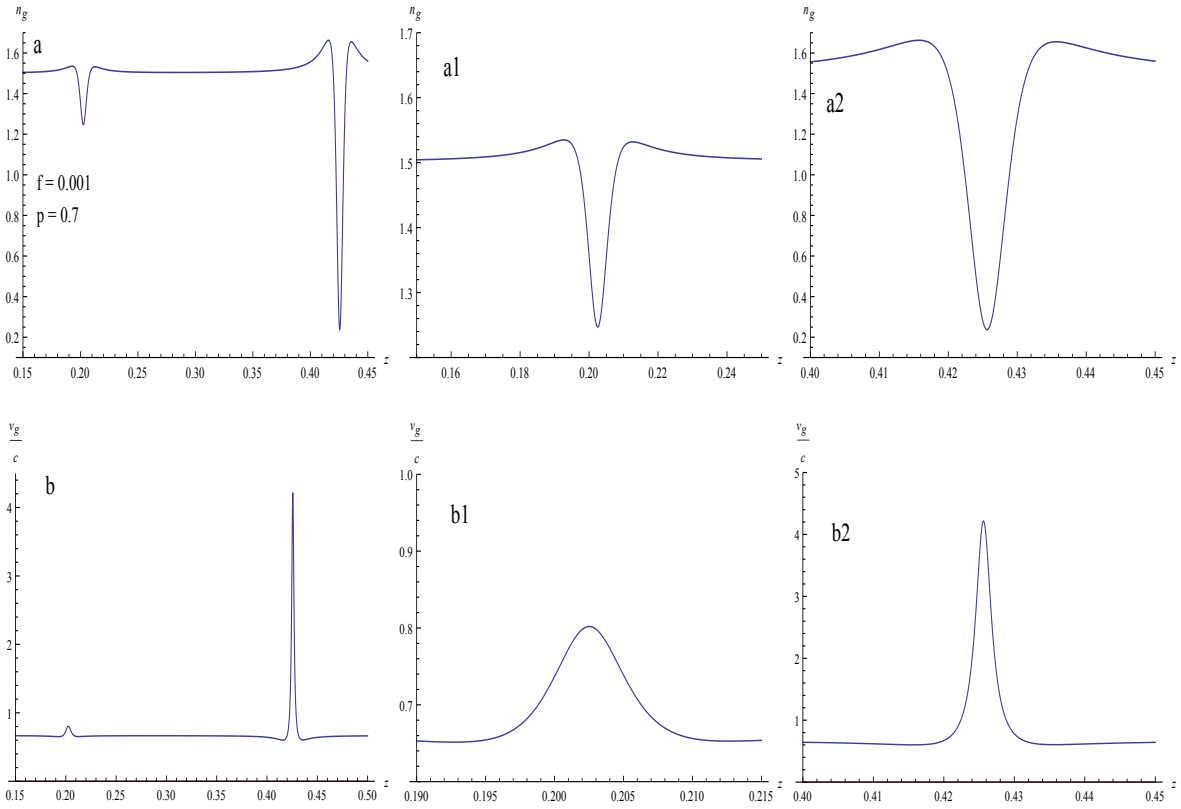

Figure 5.14: Passive composite with tuned cylindrical nanoinclusions ($\epsilon_h^{''} = 0$) . a) is group index n_g versus dimensionless frequency z. $a1$) is enlarged left tip of n_g. $a2$) is enlarged right tip of n_g. b) is normalized group velocity $\mathbf{v}_g/c$ versus z. $b1$) is enlarged left tip of $\mathbf{v}_g/c$. $b2$) is enlarged right tip of $\mathbf{v}_g/c$. Numerical values of composite parameters; $\epsilon_1 = 9, \epsilon_h^{'} = 2.25$, metal fraction in the inclusion $p = 0.7, \epsilon_\infty = 4.5, \omega_p = 1.6 \times 10^{16}(silver), \gamma = 1.15 \times 10^{-2}$, fraction of inclusion in the composite $f = 0.001$

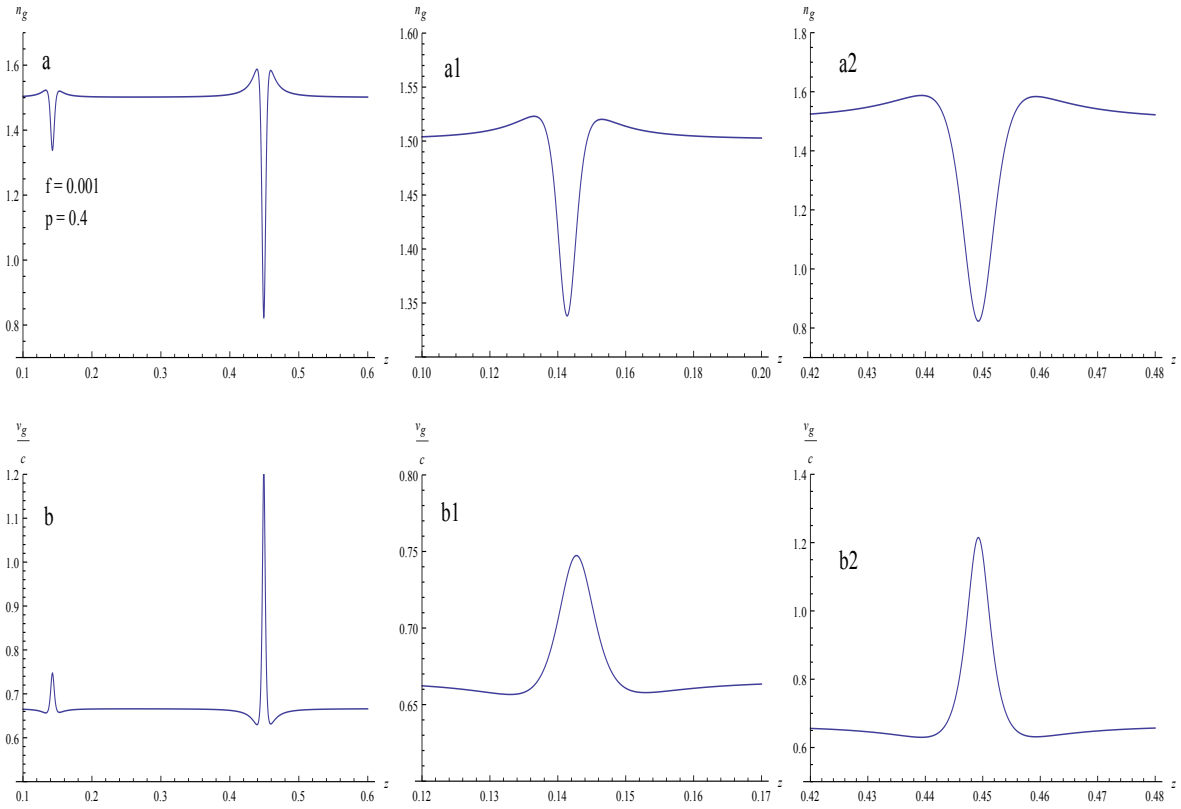

Figure 5.15: Passive composite with tuned cylindrical nanoinclusions ($\epsilon_h^{''} = 0$) . a) is group index n_g versus dimensionless frequency z. $a1$) is enlarged left tip of n_g. $a2$) is enlarged right tip of n_g.b) is normalized group velocity $\mathbf{v}_g/c$ versus z. $b1$) is enlarged left tip of $\mathbf{v}_g/c$. $b2$) is enlarged right tip of $\mathbf{v}_g/c$. Numerical values of composite parameters; $\epsilon_1 = 9, \epsilon_h^{'} = 2.25$, metal fraction in the inclusion $p = 0.4, \epsilon_\infty = 4.5, \omega_p = 1.6 \times 10^{16}(silver), \gamma = 1.15 \times 10^{-2}$, fraction of inclusion in the composite $f = 0.001$

For pure metal cylindrical inclusion embedded in passive host matrix. Numerical results for group index and group velocity presented on Fig.(5.16) and Fig.(5.17) for $f = 0.001$ and $f = 0.003$ respectively. The curves for $\mathbf{v}_g/c$ shows that as the dimensionless frequency z tends to the first asymptote from the left and to the second asymptote from the right $\mathbf{v}_g/c \to +\infty$, but between the two singularity points slow backward light is obtained. As the metal fraction in tuned inclusion $(i.e.p)$ determine variation in magnitude of peak values, here variation in the fraction of pure metal inclusion $(i.e.f)$ affects the magnitude of the peak value to go to very small. The value $\mathbf{V}_g/c = -1.5$ for $f = 0.001$ goes deeper to $\mathbf{v}_g/c = -0.25$ for $f = 0.003$.

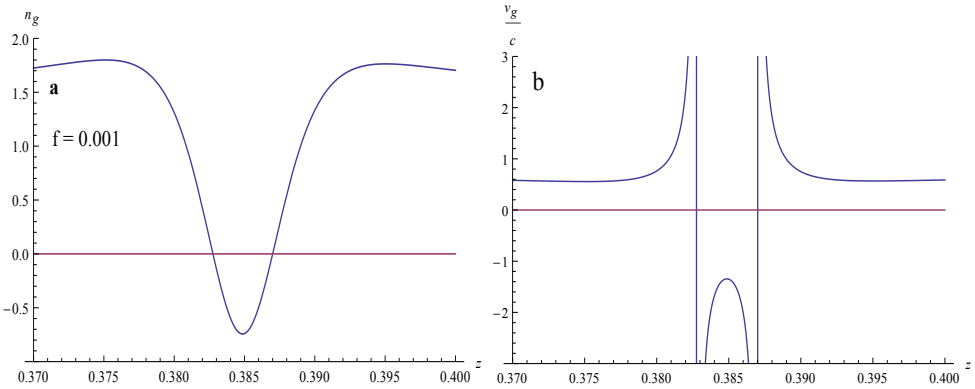

Figure 5.16: Passive composite with pure metal inclusions ($\epsilon_h^{''} = 0$) . a) is group index n_g versus dimensionless frequency z. b) is normalized group velocity $\mathbf{v}_g/c$ versus z. Numerical values of composite parameters; $\epsilon_1 = 9, \epsilon_h^{'} = 2.25, \epsilon_\infty = 4.5, \omega_p = 1.6 \times 10^{16}(silver), \gamma = 1.15 \times 10^{-2}$, fraction of the inclusion in the composite $f = 0.001$

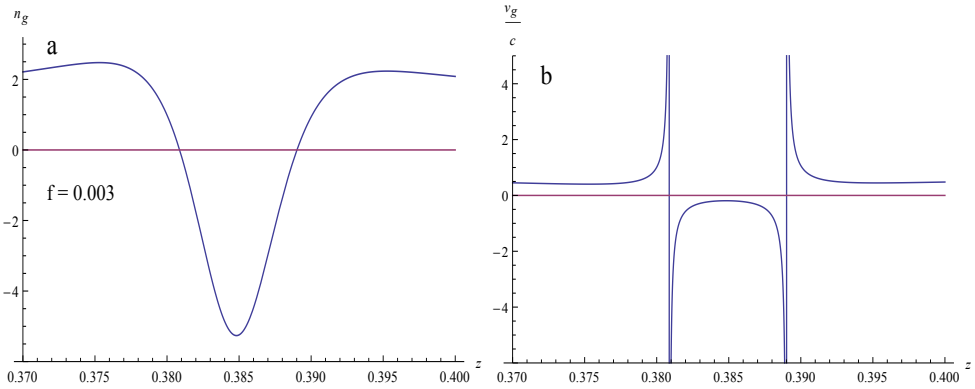

Figure 5.17: Passive composite with pure metal inclusions ($\epsilon_h^{''} = 0$) . a) is group index n_g versus dimensionless frequency z. b) is normalized group velocity v_g/c versus z. Numerical values of composite parameters; $\epsilon_1 = 9, \epsilon_h^{'} = 2.25$, fraction of the inclusion in the composite $f = 0.003$

The numerical results for the group index and group velocity of a tuned inclusion in active host ($i.e.\epsilon_h'' = -0.13866$) matrix presented on $Fig.(5.18)$ for $p = 0.9$ with $f = 0.001$. At the region of first resonant frequency slow light of magnitude $\mathbf{v}_g = 0.8c$ is obtained. Around the second resonant frequency (Fig.5.18b) $\mathbf{v}_g/c$ has three branches. As z goes to the first asymptote line from the left and z tends to the second asymptote from the right $\mathbf{v}_g/c \to +\infty$, and in between negative slow light of $\mathbf{v}_g = -0.2c$ is found.

Fig.(5.19) and Fig.(5.20) are the results for group index and group velocity for fraction of inclusion $f = 0.0001$ and $f = 0.0007$ respectively. For all fraction of inclusion investigated, the group refractive index n_g has single minimum value and it becomes negative as we increase f. For $f = 0.0001$ we have got a superluminal group velocity of $\mathbf{v}_g = 4c$ Fig.(5.19 b). When we increase the value of f to $f = 0.0007$ the obtained curve completely change its nature and we got three branches of the normalized group velocity. Far from the left from the first asymptote line and far from the right asymptotic line the group velocity is slow and estimated $\mathbf{v}_g = 0.4c$. As the frequency approaches to the first asymptotic line from the left and to the second asymptotic line from the right $\mathbf{v}_g \to \infty$. In between the two singularity points negative slow group velocity of the light pulse is obtained.

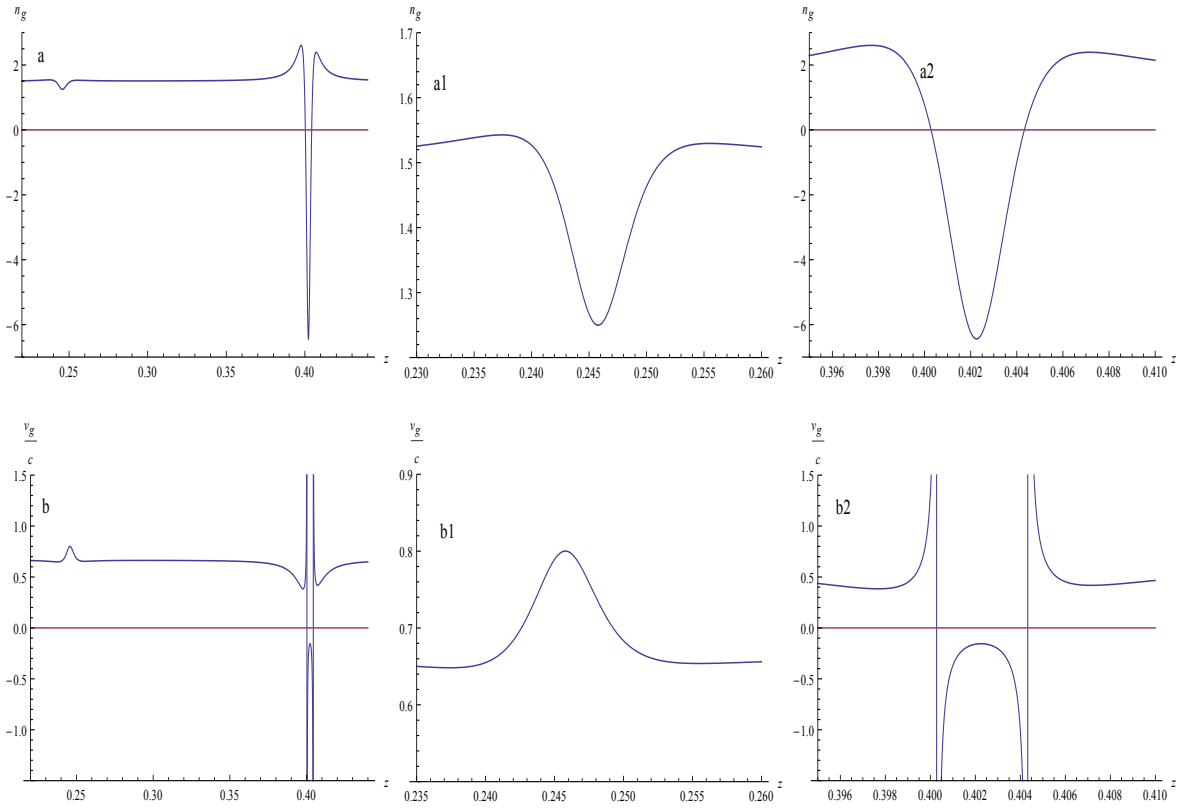

Figure 5.18: Activee composite with tuned cylindrical nanoinclusions ($\epsilon_h^{''} = -0.13866$) . *a*) is group index n_g versus dimensionless frequency z. *a*1) is enlarged left tip of n_g. *a*2) is enlarged right tip of n_g. *b*) is normalized group velocity $\mathbf{v}_g/c$ versus z. *b*1) is enlarged left tip of $\mathbf{v}_g/c$. *b*2) is enlarged right tip of $\mathbf{v}_g/c$. Numerical values of composite parameters; $\epsilon_1 = 9, \epsilon_h^{'} = 2.25$, metal fraction in the inclusion $p = 0.9, \epsilon_\infty = 4.5, \omega_p = 1.6 \times 10^{16}(silver), \gamma = 1.15 \times 10^{-2}$, fraction of inclusion in the composite $f = 0.001$

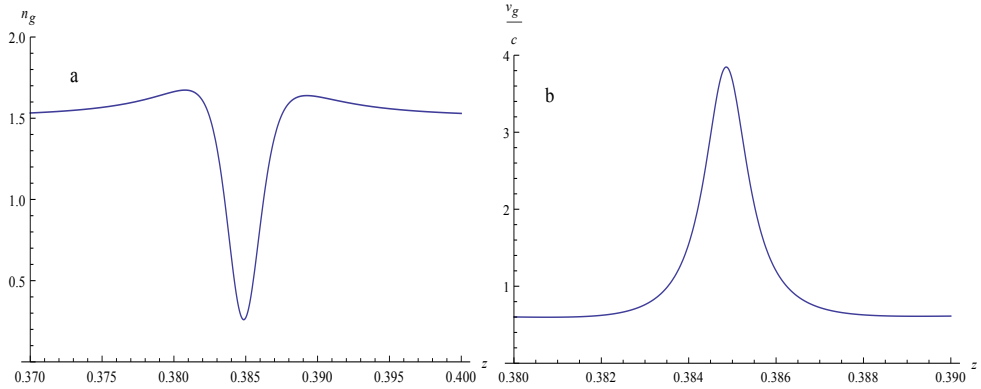

Figure 5.19: Active composite with cylindrical pure metal inclusions ($\epsilon_h^{''} = -0.115911$) . *a*) is group index n_g versus dimensionless frequency z. *b*) is normalized group velocity $\mathbf{v}_g/c$ versus z. Numerical values of composite parameters; $\epsilon_1 = 9, \epsilon_h^{'} = 2.25, \epsilon_\infty = 4.5, \omega_p = 1.6 \times 10^{16}(silver), \gamma = 1.15 \times 10^{-2}$, fraction of the inclusion in the composite $f = 0.0001$

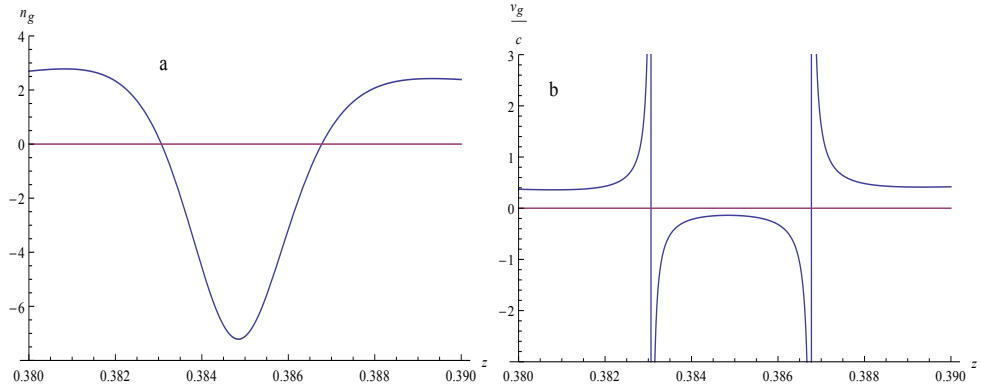

Figure 5.20: Active composite with cylindrical pure metal inclusions ($\epsilon_h^{''} = -0.115911$) . *a*) is group index n_g versus dimensionless frequency z. *b*) is normalized group velocity v_g/c versus z. Numerical values of composite parameters; $\epsilon_1 = 9, \epsilon_h^{'} = 2.25, p = 1, \epsilon_\infty = 4.5, \omega_p = 1.6 \times 10^{16}(silver), \gamma = 1.15 \times 10^{-2}$, fraction of the inclusion in the composite $f = 0.0007$

5.5 Spherical Assemblage

In this section we briefly discuses the optical properties of composite with spherical inclusions. This section is purposely introduced in order to compare effect of shape on the magnitude of the local field enhancement factor and on the value of group velocity from what we have obtained for cylindrical inclusion on section (5.4.2) and (5.4.5). And we advise an interested reader to refer, for detail and more explanation, the works of Man'lev and Sisay [14, 33] regarding optical properties of composite with spherical inclusion.

5.5.1 Electrical Potential Distribution

The potential distribution at different regions of the composite can be determined from the general solution given by Eq.(5.4.1), Eq.(5.4.2), and Eq.(5.4.3) by placing the dimensionality factor for sphere $d = 3$. Therefore, the potential at the core , shell and host respectively becomes

$$\Phi_1 = -\mathbf{E}_h A r\cos\theta, r \le r_1 \tag{5.5.1}$$

$$\Phi_2 = -\mathbf{E}_h (Br - \frac{C}{r^2})\cos\theta, r_1 \le r \le r_2 \tag{5.5.2}$$

$$\Phi_h = -\mathbf{E}_h (r - \frac{D}{r^2})\cos\theta, r \ge r_2 \tag{5.5.3}$$

Thus Laplace equation in the spherical coordinate system has the form below:

$$\frac{\partial^2\Phi}{\partial r^2} + \frac{2}{r}\frac{\partial\Phi}{\partial r} + \frac{1}{r^2\sin\theta}\frac{\partial}{\partial\theta}(\sin\theta\frac{\partial\Phi}{\partial\theta}) - \frac{1}{r^2\sin\theta^2}\frac{\partial^2\Phi}{\partial\phi^2} = 0 \tag{5.5.4}$$

Potential is not function of ϕ, so Eq.(5.5.4) reduced to the form

$$\frac{\partial^2\Phi}{\partial r^2} + \frac{2}{r}\frac{\partial\Phi}{\partial r} + \frac{1}{r^2\sin\theta}\frac{\partial}{\partial\theta}(\sin\theta\frac{\partial\Phi}{\partial\theta}) = 0 \tag{5.5.5}$$

The potentials listed above satisfy Laplace equation in spherical coordinate system given by Eq.(5.5.5) and we can obtain the value of the unknown coefficients A, B, C, and D by applying the two electrostatic boundary condition given at section (5.4.1). Therefore, the expression for the coefficients looks

$$A = \frac{9\epsilon_2\epsilon_h}{2p\Delta} \tag{5.5.6}$$

$$B = \frac{3\epsilon_h(\epsilon_1+\epsilon_2)}{2p\Delta} \tag{5.5.7}$$

$$C = \frac{3\epsilon_h(\epsilon_1-\epsilon_2)r_1^3}{2p\Delta} \tag{5.5.8}$$

$$D = [1 - 3\epsilon_h\frac{[\epsilon_2(3-p)+\epsilon_1 p]}{2p\Delta}]r_2^3 \tag{5.5.9}$$

where,
$p = 1 - (\frac{r_1}{r_2})^3$ is the metal fraction in the spherical inclusion
$\Delta = \epsilon_2^2 + q\epsilon_2 + \epsilon_1\epsilon_h$
$q = (\frac{3}{2p} - 1)\epsilon_1 + (\frac{3}{2p} - 1)\epsilon_h$

5.5.2 Resonant Frequencies and Enhancement Factor Of Local Field

By applying the same procedure we did for cylindrical assemblage, we can determine the expression for the local field enhancement factor for metal covered dielectric spherical inclusion. So the local field enhancement factor at the core of a metal covered dielectric spherical inclusion becomes

$$| A |^2 = \frac{81\epsilon_h^2}{4p^2} \frac{\epsilon_2'^2 + \epsilon_2"^2}{(\epsilon_2'^2 - \epsilon_2"^2 + q\epsilon_2' + \epsilon_1\epsilon_h)^2 + \epsilon_2"^2(q + 2\epsilon_2')^2} \quad (5.5.10)$$

where $|A|^2$ is local field enhancement factor

Fig.(5.21) and Fig.(5.22) shows that like the cylindrical metal coated dielectric nanoinclusion, metal fraction of the inclusion p and ϵ_∞ affect the magnitude of $|A|^2$ and there are two peaks of local filed enhancement factor at two different resonant frequencies. Like the cylindrical case the second peak value of the enhancement factor is important as we increase the thickness of the metal cover. From the two graphs, we can infer, there is a shift in position of the maximum value of the enhancement factor while the value of $\epsilon_\infty = 4.5$ changed to $\epsilon_\infty = 1$

For a dielectric covered metal spherical inclusion, the local field enhancement factor has the following mathematical expression:

$$|A|^2 = \frac{81\epsilon_1^2\epsilon_h^2}{4p^2} \frac{1}{(\epsilon_1^2 + q^*\epsilon_1 + \epsilon_2'\epsilon_h)^2 + \epsilon_2''^2(\epsilon_1(\frac{3}{2p} - 1) + \epsilon_h)^2} \quad (5.5.11)$$

where $q^* = \epsilon_2'(\frac{3}{2p} - 1) + \epsilon_h(\frac{3}{p} - 1)$

The local field enhancement factor in the core of a dielectric coated metal spherical nanoinclusion plotted for different p and different ϵ_∞ as a function of resonant frequency. Referring Fig.(5.23) and Fig.(5.24) provide us, spherical dielectric coated metal inclusion has only one peak value. In this case making the dielectric cover thicker increases the magnitude of the enhancement factor.

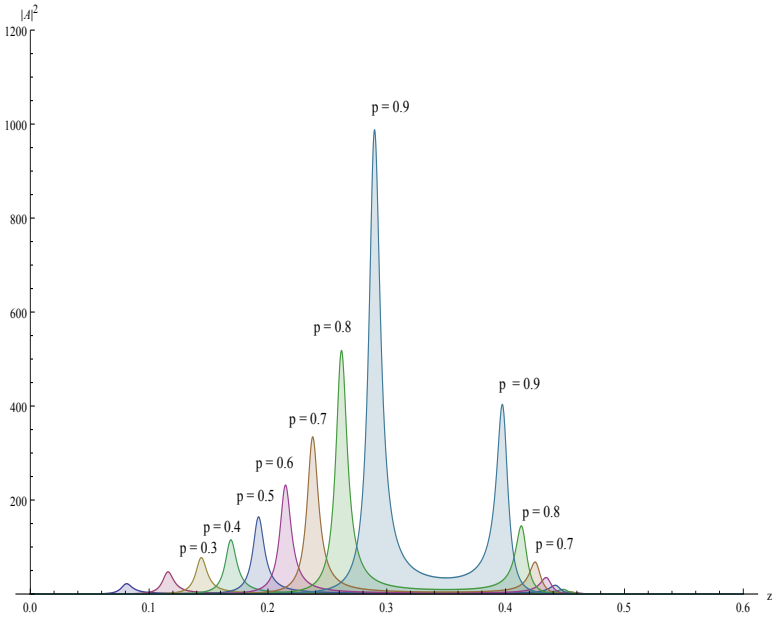

Figure 5.21: Enhancement factor $|A|^2$ versus dimensionless frequency z of spherical metal inclusion with a dielectric core at different metal fraction in the inclusion p; $\epsilon_\infty = 4.5, \epsilon_1 = 6, \epsilon_h = 2.25, \omega_p = 1.45 \times 10^{16}$(frequency of the silver surface plasmons), $\upsilon = 1.68 \times 10^{14}, \gamma = 1.15 \times 10^{-2}$.

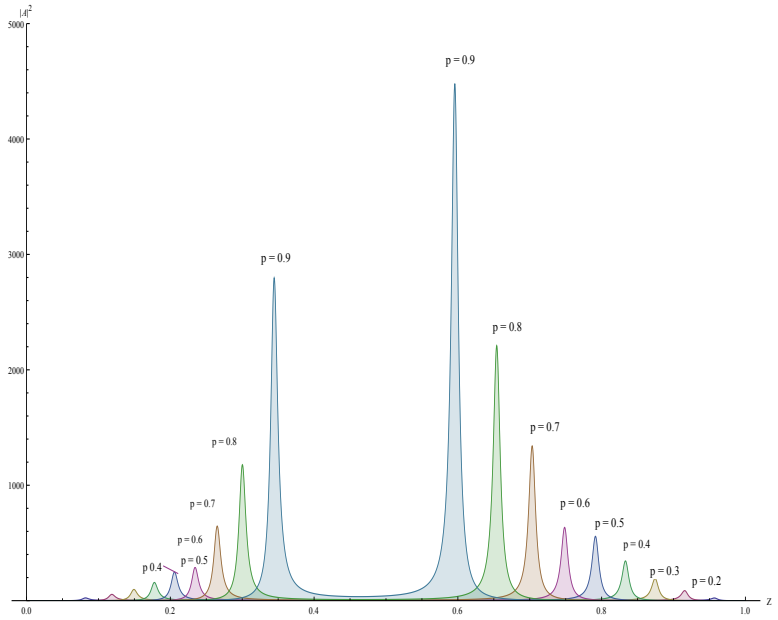

Figure 5.22: Enhancement factor $|A|^2$ versus dimensionless frequency z of spherical metal inclusion with a dielectric core at different metal fraction in the inclusion p; $\epsilon_\infty = 1, \epsilon_1 = 6, \epsilon_h = 2.25, \omega_p = 1.45 \times 10^{16}$(frequency of the silver surface plasmons), $\upsilon = 1.68 \times 10^{14}, \gamma = 1.15 \times 10^{-2}$.

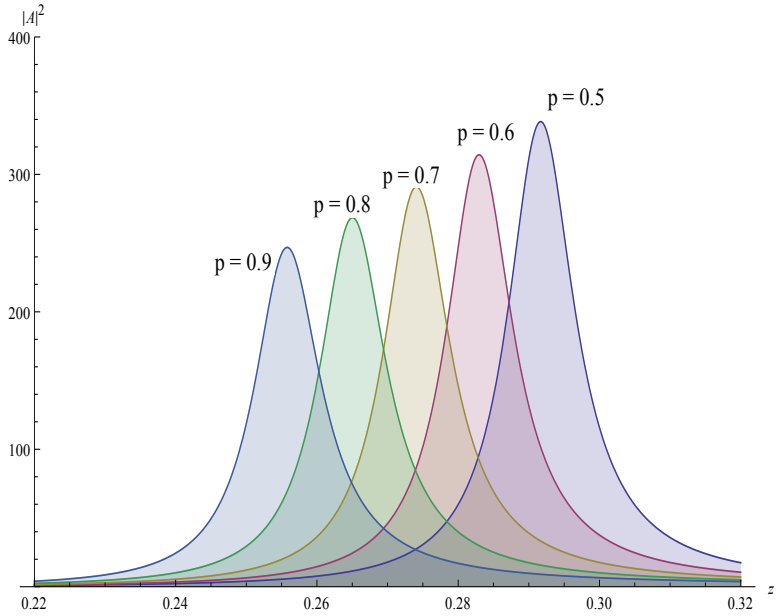

Figure 5.23: Enhancement factor $|A|^2$ versus dimensionless frequency z of spherical metal inclusion covered by dielectric at different metal fraction in the inclusion p; $\epsilon_\infty = 4.5, \epsilon_1 = 6.\epsilon_h = 2.25, \omega_p = 1.45 \times 10^{16}$(frequency of the silver surface plasmons), $\upsilon = 1.68 \times 10^{14}, \gamma = 1.15 \times 10^{-2}$.

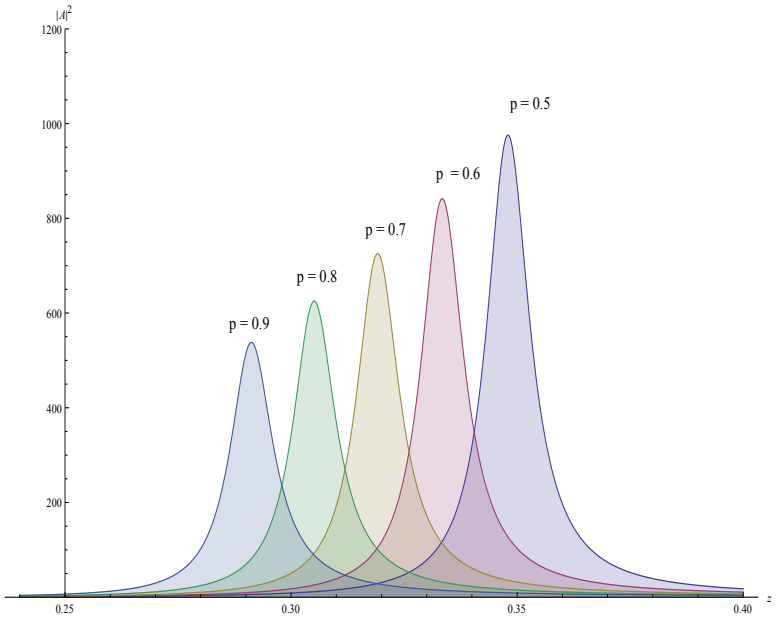

Figure 5.24: Enhancement factor $|A|^2$ versus dimensionless frequency z of spherical metal inclusion covered by dielectric at different metal fraction in the inclusion p; $\epsilon_\infty = 1, \epsilon_1 = 6, \epsilon_h = 2.25, \omega_p = 1.45 \times 10^{16}$(frequency of the silver surface plasmons), $\upsilon = 1.68 \times 10^{14}, \gamma = 1.15 \times 10^{-2}$.

The potential distribution for spherical pure metal inclusion with radius r_2 in a dielectric host matrix is

$$\Phi_{in} = -\mathbf{E}_h A r\cos\theta, r < r_2 \quad (5.5.12)$$

$$\Phi_{out} = -\mathbf{E}_h (r + \frac{B}{r})\cos\theta, r > r_2 \quad (5.5.13)$$

Where Φ_{in} and Φ_{out} are potentials inside the sphere and out side the sphere respectively

By applying electrostatics boundary conditions give by the section (5.4.1) we can get A and B respectively as

$$A = \frac{3\epsilon_h}{\epsilon_2 + 2\epsilon_h} \quad (5.5.14)$$

$$B = \frac{\epsilon_2 - \epsilon_h}{\epsilon_2 + 2\epsilon_h} r_2^3 \quad (5.5.15)$$

Therefore the local field enhancement factor for pure metal cylindrical inclusion becomes :

$$\mid A \mid^2 = \frac{9\epsilon_h^2}{[(\epsilon_2' + 2\epsilon_h)^2 + \epsilon_2''^2]} \quad (5.5.16)$$

Like in the case of pure metal cylindrical inclusion, there is only one maximum value of the local filed enhancement factor of a composite with pure metal spherical inclusion. Fig.(5.25) and Fig.(5.26) are results for $\mid A \mid^2$ versus dimensionless frequency z. From the results we obtained the magnitude of $\mid A \mid^2$ highly varied with the value of ϵ_∞.

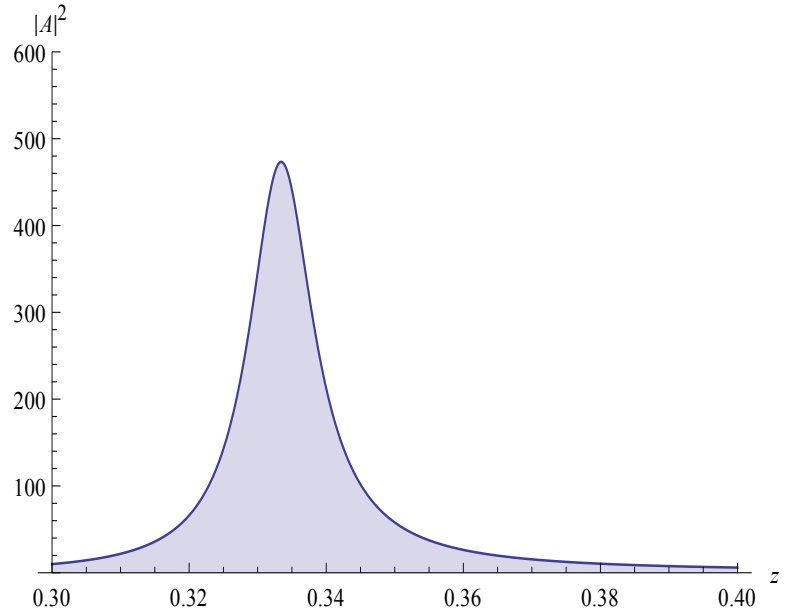

Figure 5.25: Enhancement factor $|A|^2$ versus dimensionless frequency z of pure metal cylindrical inclusion ; $\epsilon_\infty = 4.5, \epsilon_h = 2.25, \omega_p = 1.45 \times 10^{16}$(frequency of the silver surface plasmons), $\upsilon = 1.68 \times 10^{14}, \gamma = 1.15 \times 10^{-2}$.

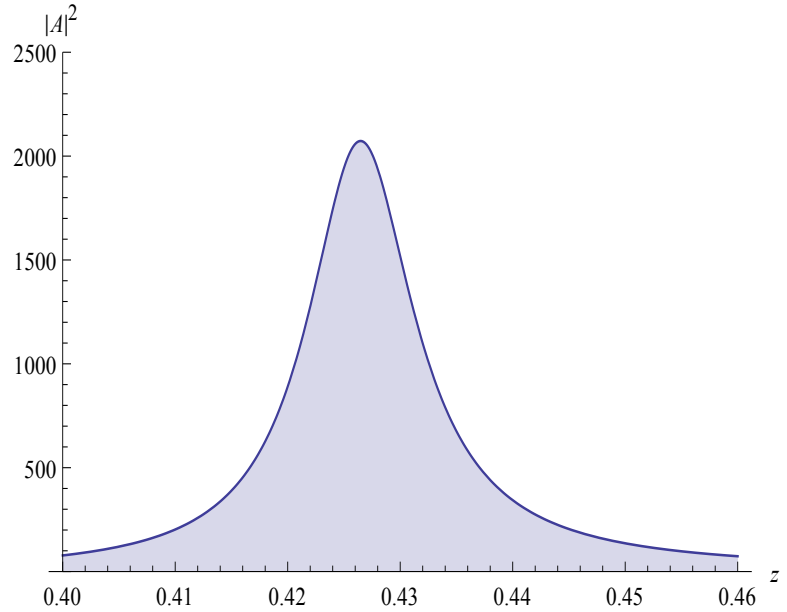

Figure 5.26: Enhancement factor $|A|^2$ versus dimensionless frequency z of pure metal cylindrical inclusion;$\epsilon_\infty = 1, \epsilon_h = 2.25, \omega_p = 1.45 \times 10^{16}$(frequency of the silver surface plasmons), $\upsilon = 1.68 \times 10^{14}, \gamma = 1.15 \times 10^{-2}$.

5.5.3 Effective Polarizability

The effective polarizability of an individual metal covered dielectric spherical nanoinclusion embedded in a dielectric host matrix can be presented as [14]:

$$D = \beta r_2^3 \tag{5.5.17}$$

where,
$\beta = 1 - \frac{3}{2}\frac{\delta}{\Delta}$
$\delta = \epsilon_h[\epsilon_2(3-p) + \epsilon_1 p]$
$\Delta = \epsilon_2^2 + q\epsilon_2 + \epsilon_1\epsilon_h$
$p = 1 - (\frac{r_1}{r_2})^3$

The dielectric function of the core ϵ_1 is real and frequency independent. The dielectric function of metal cover ϵ_2 is chosen to have the Drude form, its real $\epsilon_2^{'}$ and imaginary $\epsilon_2^{''}$ parts are given by Eq.(5.4.20) and Eq.(5.4.21) respectively. Since ϵ_2 and ϵ_h are complex q, Δ, δ and β are also complex:

$$\beta = \beta^{'} + i\beta^{''} \tag{5.5.18}$$
$$q = q^{'} + iq^{''} \tag{5.5.19}$$
$$\Delta = \Delta^{'} + i\Delta^{''} \tag{5.5.20}$$
$$\delta = \delta^{'} + i\delta^{''} \tag{5.5.21}$$

where,
$\beta^{'} = 1 - \frac{3}{2}\frac{\delta^{'}\Delta^{'} + \delta^{''}\Delta^{''}}{\Delta^{'2} + \Delta^{''2}}$
$\beta^{''} = \frac{3}{2}\frac{\delta^{'}\Delta^{''} - \delta^{''}\Delta^{'}}{\Delta^{'2} + \Delta^{''2}}$
$q^{'} = (\frac{3}{2p} - 1)\epsilon_1 + (\frac{3}{p} - 1)\epsilon_h^{'}$
$q^{''} = (\frac{3}{p} - 1)\epsilon_h^{'}$
$\Delta^{'} = (\epsilon^{'2}_2 - \epsilon^{''2}_2 + q^{'}\epsilon_2^{'} - q^{''}\epsilon_2^{''} + \epsilon_1\epsilon_h^{'})$
$\Delta^{''} = (2\epsilon_1^{'}\epsilon_2^{''} + q^{'}\epsilon_2^{''} + q^{''}\epsilon_2^{'} + \epsilon_1\epsilon_h^{''})$
$\delta^{'} = (\frac{3}{p} - 1)[\epsilon_2^{'}\epsilon_h^{'} - \epsilon_2^{''}\epsilon_h^{''}] + \epsilon_1\epsilon_h^{'}$
$\delta^{''} = (\frac{3}{p} - 1)[\epsilon_2^{'}\epsilon_h^{''} + \epsilon_2^{''}\epsilon_h^{'}] + \epsilon_1\epsilon_h^{''}$

For composite with pure spherical metal inclusion the corresponding quantities for $\beta^{'}$ and $\beta^{''}$ of Eq.(5.5.18) are respectively given by

$$\beta_m' = \frac{(\epsilon_2' - \epsilon_h')\Delta_m' + (\epsilon_2'' - \epsilon_h'')\Delta_m''}{|\Delta_m|^2} \tag{5.5.22}$$
$$\beta_m'' = \frac{(\epsilon_2'' - \epsilon_h'')\Delta_m' + (\epsilon_2' - \epsilon_h')\Delta_m''}{|\Delta_m|^2} \tag{5.5.23}$$
$$\tag{5.5.24}$$

where,
$|\Delta_m|^2 = {\Delta'_m}^2 + {\Delta''_m}^2$
$\Delta'_m = \epsilon'_2 + 2\epsilon'_h$
$\Delta''_m = \epsilon''_2 + 2\epsilon''_h$

5.5.4 Refractive Index

Clausius- Mossoti equation for spherical inclusion has the form

$$\frac{\epsilon_{eff} - \epsilon_h}{\epsilon_{eff} + 2\epsilon_h} = \frac{ND}{3} \tag{5.5.25}$$

where ϵ_{eff} is the effective permittivity of the composite, ϵ_h is the permittivity of the host, N is density number of the inclusion, and D effective polarizability of the inclusion.

Maxwell - Garnett formula for spherical inclusion can be written as:

$$n^2 = \epsilon_h(1 + \frac{3f\beta}{1 - f\beta}) \tag{5.5.26}$$

where $\beta = [1 - 3\epsilon_h \frac{[\epsilon_2(3-p)+\epsilon_1 p]}{2p\Delta}]$. Quantities such as ϵ_h and β are complex, so that its important to express n^2 in terms of its real and imaginary parts by following the procedure below:

$$\begin{aligned} n^2 &= (1 + 3f\frac{(\beta' + i\beta'')}{1 - f\beta' + i\beta''}) && (5.5.27)\\ &= (\beta' + i\beta'')(1 + \frac{3f\beta' - 3f^2|\beta|^2 + i3f\beta''}{\Delta_f}) && (5.5.28)\\ &= (\epsilon'_h + 3f\frac{(\beta' - f|\beta|^2)\epsilon'_h - \beta''\epsilon''_h}{\Delta_f})(\epsilon''_h + 3f\frac{(\beta' - f|\beta|^2)\epsilon''_h - \beta''\epsilon'_h}{\Delta_f}) && (5.5.29)\\ &= b_1 + ib_2 && (5.5.30) \end{aligned}$$

where,
$b_1 = (\epsilon'_h + 3f[\frac{(\beta' - f|\beta|^2)\epsilon'_h - \beta''\epsilon''_h}{\Delta_f}])$
$b_2 = (\epsilon''_h + 3f[\frac{(\beta' - f|\beta|^2)\epsilon''_h + \beta''\epsilon'_h}{\Delta_f}])$
$\Delta_f = 1 - f\beta' + f^2|\beta|^2$
Equating the real and the imaginary parts of n^2 with Eq.(5.5.30) gives us the relation

$$\begin{aligned} {n'}^2 - {n''}^2 &= b_1 && (5.5.31)\\ 2n'n'' &= b_2 && (5.5.32) \end{aligned}$$

From Eq.(5.5.31) and Eq.(5.5, 32), we can get the following expressions which we apply for numerical calculations

$$n'^2 = \frac{1}{2}(\sqrt{b_1^2 + b_2^2} + b_1) \quad (5.5.33)$$

$$n''^2 = \frac{1}{2}(\sqrt{b_1^2 + b_2^2} - b_1) \quad (5.5.34)$$

The results on Fig.(5.27a) and Fig.(5.27b) shows that there are two maximum values for the real and the imaginary parts of the refractive index at two different resonant frequencies. Unlike the cylindrical case the magnitude of the first peak is larger than the second on the right. Here again increasing the thickness of the metal in the inclusion cause the increase in the value of the maxima. As p increase the two maxima gets closer to each other and their magnitude increase.

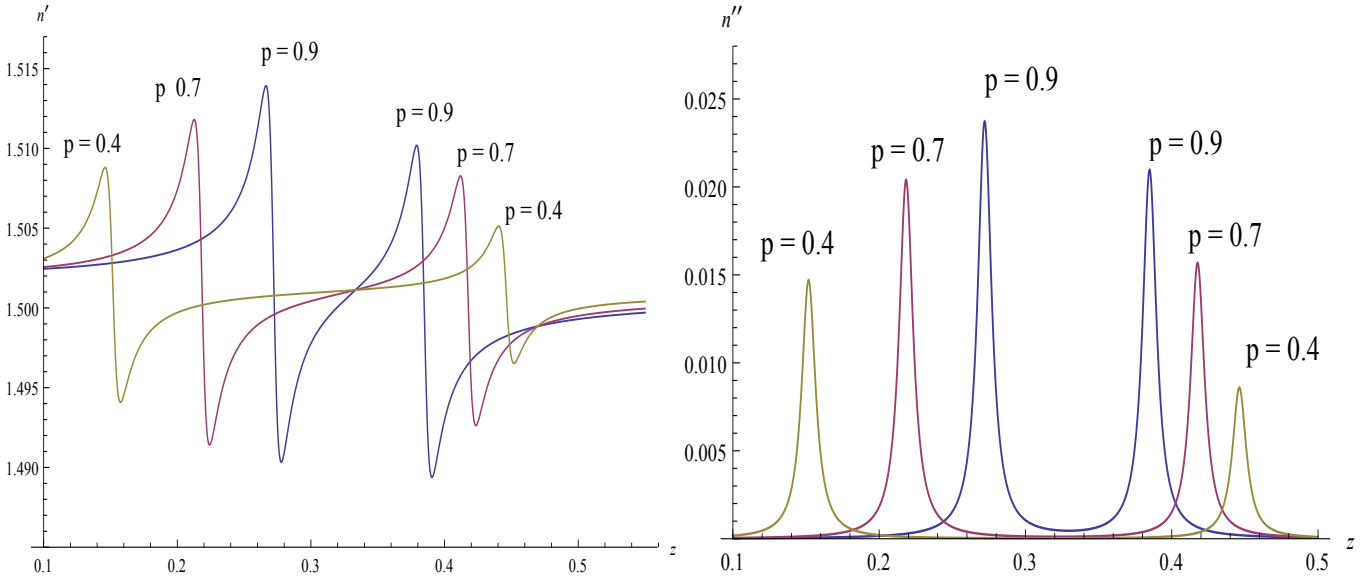

Figure 5.27: Passive composite with tuned spherical nanoinclusions ($\epsilon_h'' = 0$) .a)Real part of refractive index n' versus dimensionless frequency z; b) Imaginary part of refractive index n'' versus z. Numerical values of composite parameters; $\epsilon_1 = 9, \epsilon_h' = 2.25$, metal fraction in the inclusion $p = 0.4, 0.7, 0.9, \epsilon_\infty = 4.5, \omega_p = 1.6 \times 10^{16}(silver), \gamma = 1.15 \times 10^{-2}$, fraction of inclusion in the inclusion $f = 0.001$

For pure metal spherical inclusion in a passive host matrix, there is only one peak value of the real and the imaginary parts of the refractive index. Fig.(5.28a) and Fig.(5.28b) are the numerical values of the real and the imaginary part respectively. When we increase the fraction of the pure metal inclusion i the composite, the magnitude of n' and n'' increases. Hence, large value of n'' implies there is strong absorption of the incident light.

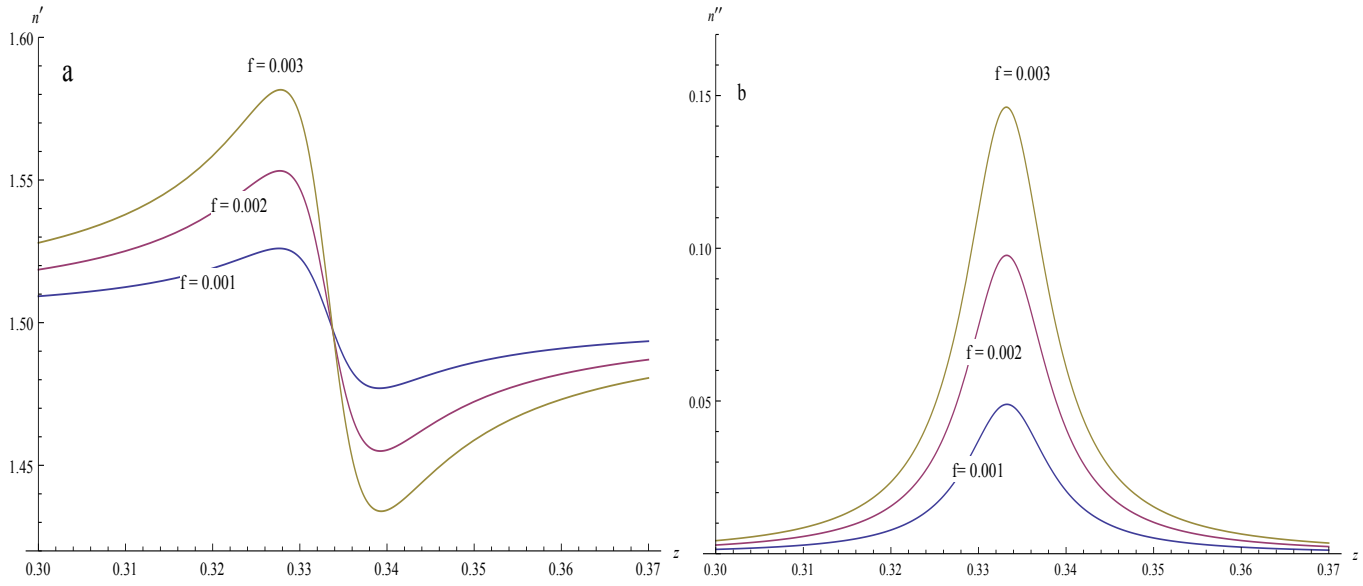

Figure 5.28: Passive composite with pure metal spherical nanoinclusions ($\epsilon_h^{''} = 0$) .a)Real part of refractive index n' versus dimensionless frequency z. b) Imaginary part of refractive index n'' versus z. Numerical values of composite parameters; $\epsilon_1 = 9, \epsilon_h^{'} = 2.25, \epsilon_\infty = 4.5, \omega_p = 1.6 \times 10^{16}(silver), \gamma = 1.15 \times 10^{-2}$, fraction of the inclusion in the composite $f = 0.001, 0.002, 0.003$

Like the case for cylindrical inclusion large value of n'' in a composite of spherical inclusion in passive host matrix prevails strong absorption of the incident light field. Thus, active host matrices is used in order to significantly reduce absorption and allow favorable condition for the propagation of the incident light.

The real and the imaginary part of the refractive index for a tuned inclusion in active host matrix for different p presented on Fig.(5.29 a) and Fig.(5.29 b). The real part of the refractive index has two maximum value at different two resonant frequency , for each metal fraction in the inclusion. The imaginary part in turn shows a tangible change from the case in passive host matrix. There are two minimum values of n'' at two different resonant frequencies, for each p. There is one maximum value for the real part of the refractive index n' of pure metal spherical nanoinclusion in active host matrix (i.e. $\epsilon_h^{''} = -0.115911$), Fig.(5.30a). The imaginary part of

the refractive index, plotted on Fig.(5.30b) prevails that for inclusion fraction $f = 0.0001$ there is one minimum value. But when the f increases to $f = 0.0002$ and $f = 0.0003$ the trend of the curve changed to a fork like structure.

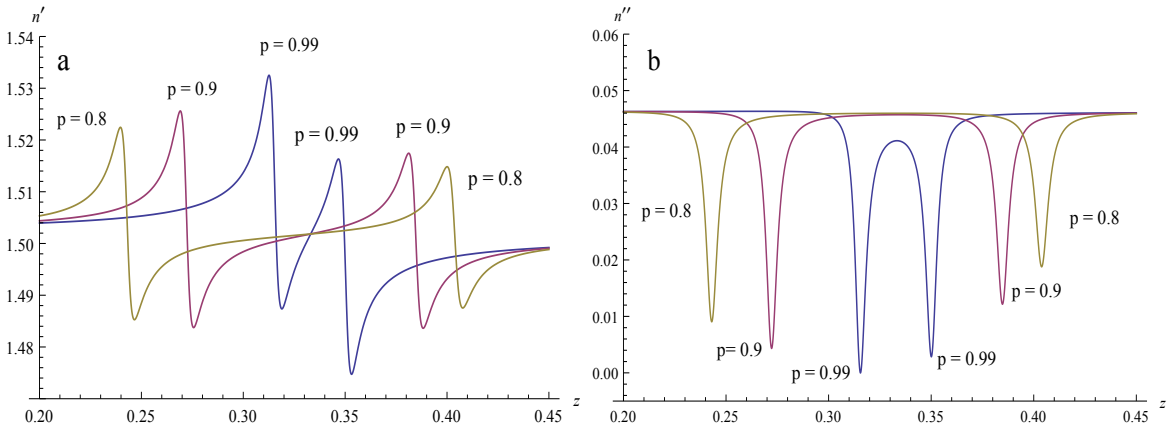

Figure 5.29: Active composite with tuned spherical nanoinclusions ($\epsilon_h^{''} = -0.13866$). *a*)Real part of refractive index n' versus dimensionless frequency z. *b*) Imaginary part of refractive index n'' versus z. Numerical values of composite parameters; $\epsilon_1 = 9, \epsilon_h^{'} = 2.25$, metal fraction in the inclusion $p = 0.99, 0.9, 0.8, \epsilon_\infty = 4.5, \omega_p = 1.6 \times 10^{16}(silver), \gamma = 1.15 \times 10^{-2}$, fraction of the inclusion in the composite $f = 0.001$

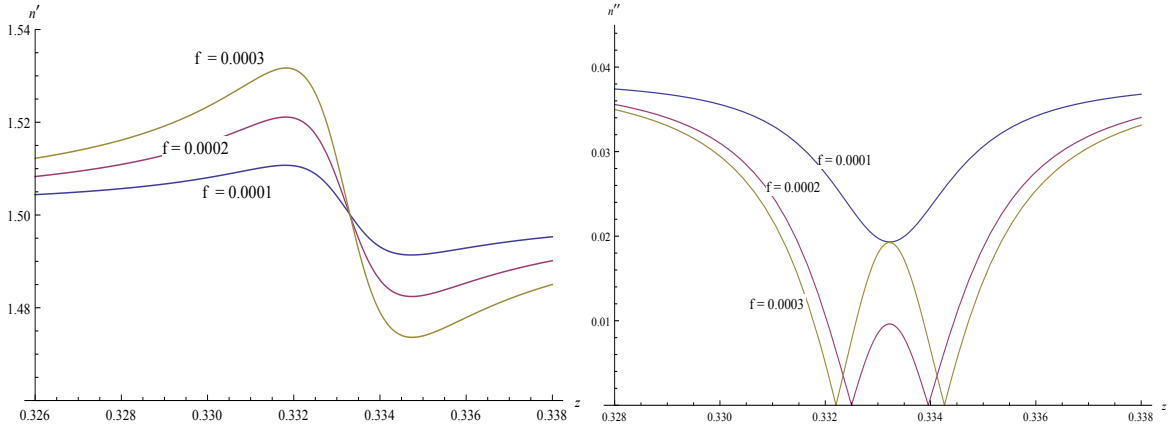

Figure 5.30: Active composite with pure metal spherical nanoinclusions ($\epsilon_h^{''} = -0.115911$). *a*)Real part of refractive index n' versus dimensionless frequency z. *b*) Imaginary part of refractive index n'' versus z. Numerical values of composite parameters; $\epsilon_1 = 9, \epsilon_h^{'} = 2.25, \epsilon_\infty = 4.5, \omega_p = 1.6 \times 10^{16}(silver), \gamma = 1.15 \times 10^{-2}$, fraction of the inclusion in the composite $f = 0.0001, 0.0002, 0.0003$

5.5.5 Slow, Superluminal and Backward Lights

As discussed on the earlier sections of this thesis work, the concepts slow and fast light refers to the value of the group velocity of a light pulse that propagates through a dispersive optical material in comparison to the speed of light in vacuum.

Fig.(5.31) and Fig.(5.32) are plots for $\mathbf{v}_g/c$ versus z for a composite of tuned spherical inclusion in passive host matrix with metal fraction in the inclusion $p = 0.9$ and $p = 0.4$ respectively. We have got that, there are two maximum values of $\mathbf{v}_g/c$ at two different resonant frequency, for each metal fraction used. For $p = 0.9$, we got $\mathbf{v}_g = 2.5c$ at the first resonant frequency and $\mathbf{v}_g = 10c$ at the second resonant frequency. As we make the metal cover thin the magnitude of the normalized group velocity significantly lower : for instance for $p = 0.4$ at the first resonant frequency we found slow light of $\mathbf{v}_g = 0.9c$ and at the second resonant frequency superluminal light of group velocity $\mathbf{v}_g = 1.2c$. So by comparing each results we have found for the two different metal fraction in the inclusion, we can see the magnitude of the peak values vary with respect to the metal fraction in the inclusion.

For pure metal spherical inclusion in passive host matrix, like the case of cylinder, there are three branches of $\mathbf{v}_g/c$ for different fraction of the inclusion in the composite. Fig.(5.33) and Fig.(5.34) shows, far from the left of first asymptote line and far from the right of the second asymptotic line we obtain slow light with value around $\mathbf{v}_g = 0.5c$. But as the dimensionless frequency z get closer to the first asymptote from the left and to the second from the right the normalized group velocity $\mathbf{v}_g/c$ tends to infinity. Between the two asymptotic line we can determine slow backward light goes deeper as we increase the fraction of the inclusion.

Fig.(5.35) and Fig.(5.36) are the results we have found for group index and group velocity for a composite of spherical tuned inclusion in active host matrix with metal fraction $p = 0.99$ and $p = 0.8$ respectively. To all of the three metal fraction in the inclusion there are two minimum values of the group index. The trend of the plot for $\mathbf{v}_g/c$ versus z is also identical for the two p values. There are five branches of $\mathbf{v}_g/c$. When the frequency goes closer to the first and the third asymptote from the left, and to the second and the forth from the right the value of the normalized group velocity tends to infinity.

The result we have obtained for a composite of pure metal spherical inclusion in active host matrix depict that their is one negative minimum value of the group index, Fig.(5.37) and Fig.(5.38). Based on the curve that shows $\mathbf{v}_g/c$ versus z, the curve type for inclusion fraction $f = 0.0001$and $f = 0.0003$ has the same structure. As the frequency approaches to the first

singularity point from the left and from the right two the second singularity point, the value $\mathbf{v}_g/c \to +\infty$. Between the two singularity point we got slow backward light, which varies with the inclusion fraction within the active host matrix.

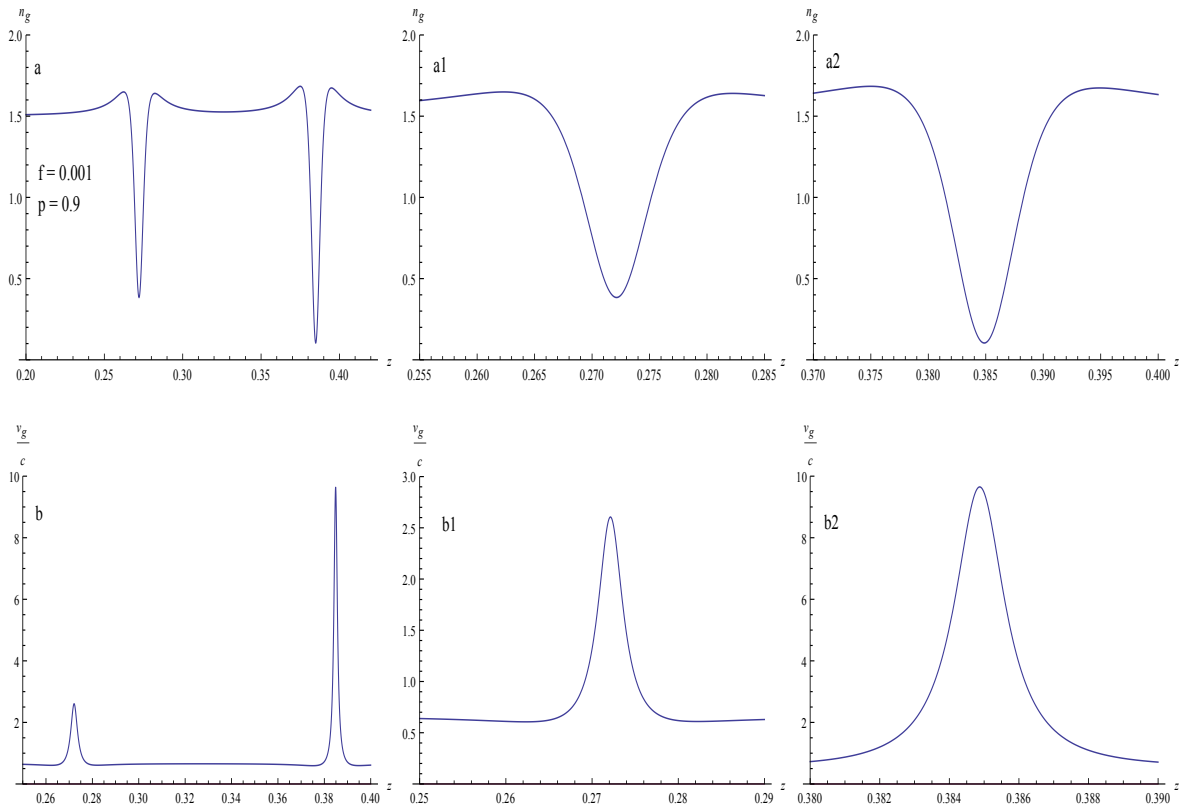

Figure 5.31: Passive composite with tuned spherical nanoinclusions ($\epsilon_h^{''} = 0$) . *a*) is group index n_g versus dimensionless frequency z. *a*1) is enlarged left tip of n_g. *a*2) is enlarged right tip of n_g. *b*) is normalized group velocity $\mathbf{v}_g/c$ versus dimensionless frequency z. *b*1) is enlarged left tip of v_g/c . *b*2) is enlarged right tip of $\mathbf{v}_g/c$. Numerical values of composite parameters; $\epsilon_1 = 9, \epsilon_h^{'} = 2.25$, metal fraction in the inclusion $p = 0.9, \epsilon_\infty = 4.5, \omega_p = 1.6 \times 10^{16}(silver), \gamma = 1.15 \times 10^{-2}$, fraction of inclusion in the composite $f = 0.001$

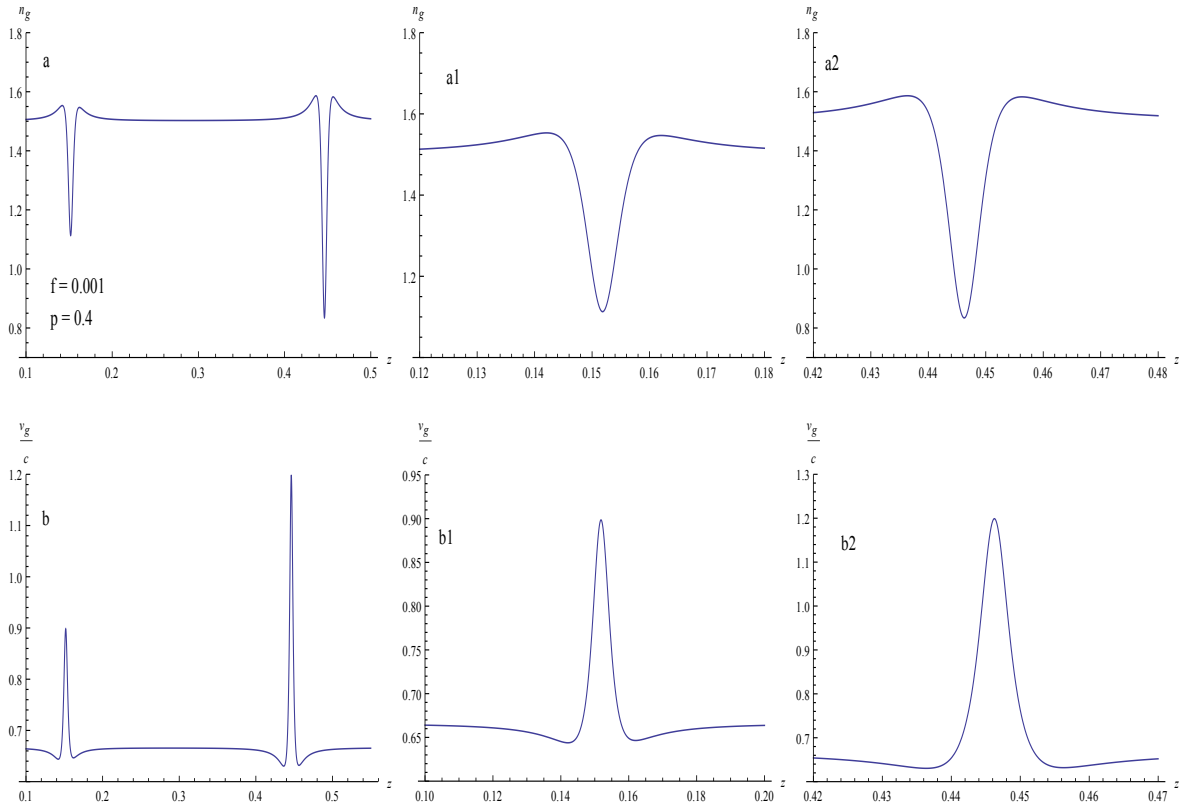

Figure 5.32: Passive composite with tuned spherical nanoinclusions ($\epsilon_h^{''} = 0$) . a) is group index n_g versus dimensionless frequency z. $a1$) is enlarged left tip of n_g. $a2$) is enlarged right tip of n_g. b) is normalized group velocity $\mathbf{v}_g/c$ versus z. $b1$) is enlarged left tip of $\mathbf{v}_g/c$. $b2$) is enlarged right tip of v_g/c. Numerical values of composite parameters; $\epsilon_1 = 9, \epsilon_h^{'} = 2.25$, metal fraction in the inclusion $p = 0.4, \epsilon_\infty = 4.5, \omega_p = 1.6 \times 10^{16}(silver), \gamma = 1.15 \times 10^{-2}$, fraction of the inclusion in the composite $f = 0.001$

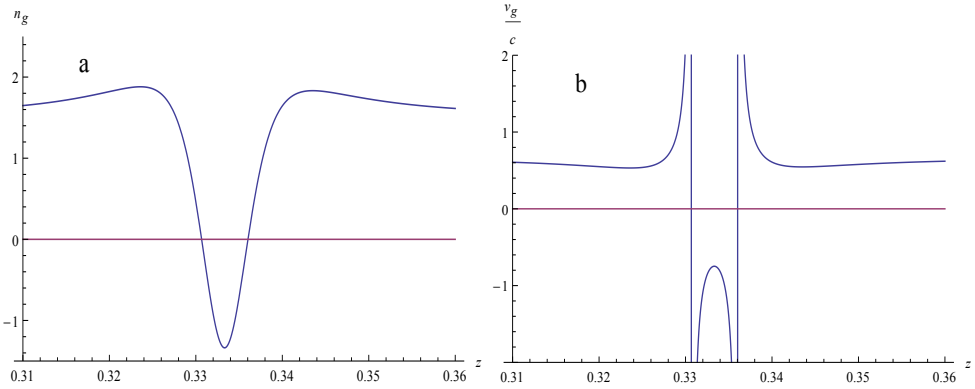

Figure 5.33: Passive composite with spherical pure metal inclusions ($\epsilon_h^{''} = 0$) . *a*) is group index n_g versus dimensionless frequency z. *b*) is normalized group velocity $\mathbf{v}_g/c$ versus z. Numerical values of composite parameters; $\epsilon_1 = 9, \epsilon_h^{'} = 2.25, \epsilon_\infty = 4.5, \omega_p = 1.6 \times 10^{16}(silver), \gamma = 1.15 \times 10^{-2}$, fraction of the inclusion in the composite $f = 0.001$

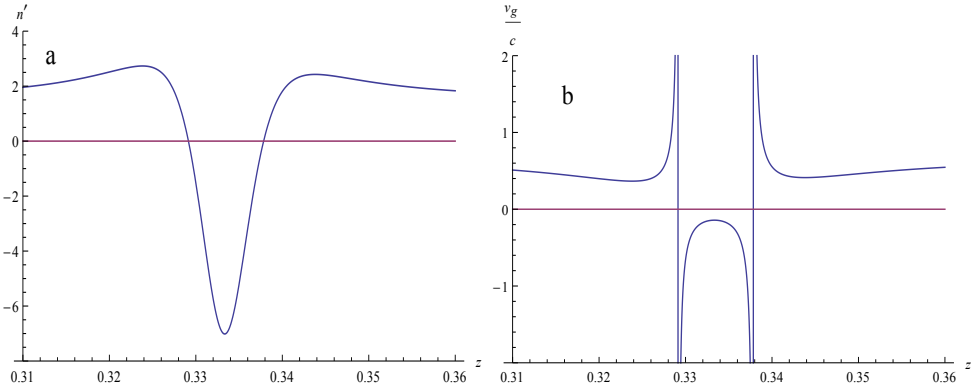

Figure 5.34: Passive composite with spherical pure metal inclusions ($\epsilon_h^{''} = 0$) . *a*) is group index n_g versus dimensionless frequency z. *b*) is normalized group velocity $\mathbf{v}_g/c$ versus z. Numerical values of composite parameters; $\epsilon_1 = 9, \epsilon_h^{'} = 2.25, \epsilon_\infty = 4.5, \omega_p = 1.6 \times 10^{16}(silver), \gamma = 1.15 \times 10^{-2}$, fraction of the inclusion in the composite $f = 0.003$

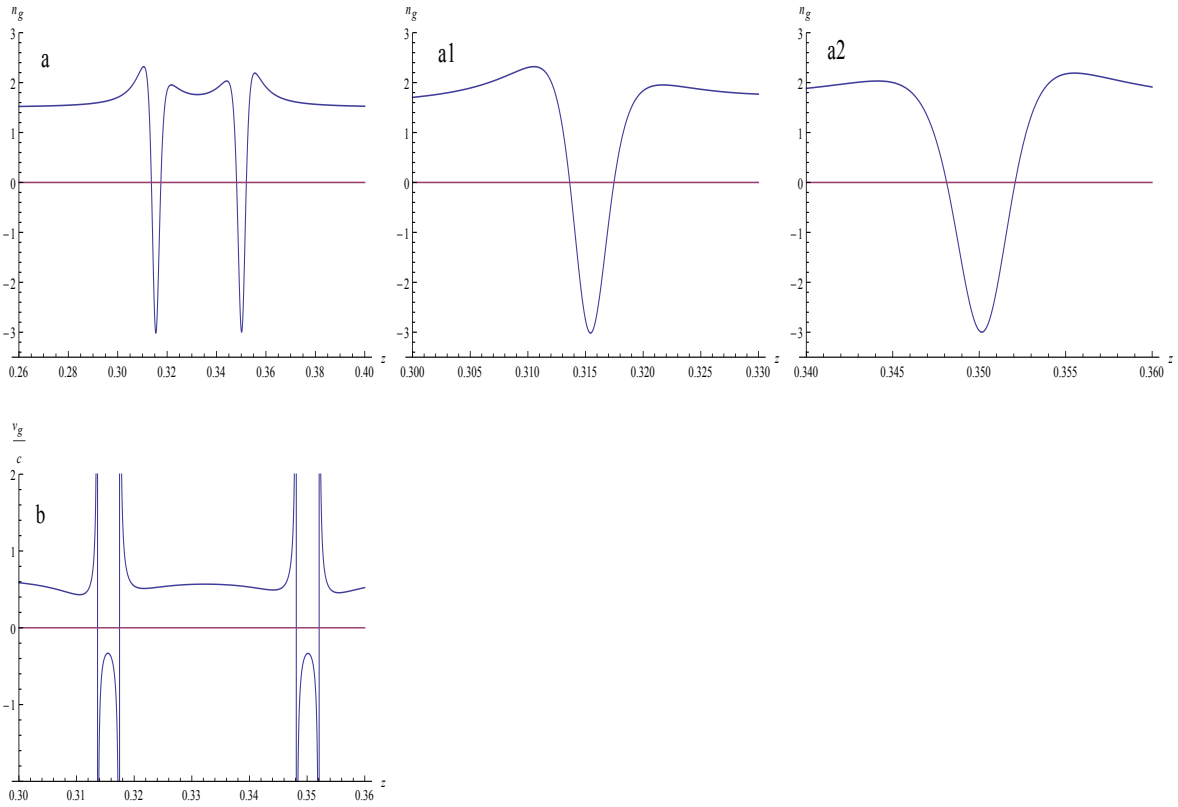

Figure 5.35: Active composite with tuned spherical nanoinclusions ($\epsilon_h^{''} = -0.13866$). a) is group index n_g versus dimensionless frequency z. $a1$) is enlarged left tip of n_g. $a2$) is enlarged right tip of n_g. b) is normalized group velocity $\mathbf{v}_g/c$ versus z . $b1$) is enlarged left tip of v_g/c. $b2$) is enlarged right tip of $\mathbf{v}_g/c$. Numerical values of composite parameters; $\epsilon_1 = 9, \epsilon_h^{'} = 2.25$, metal fraction in the inclusion $p = 0.99, \epsilon_\infty = 4.5, \omega_p = 1.6 \times 10^{16}(silver), \gamma = 1.15 \times 10^{-2}$, fraction of the inclusion in the composite $f = 0.001$

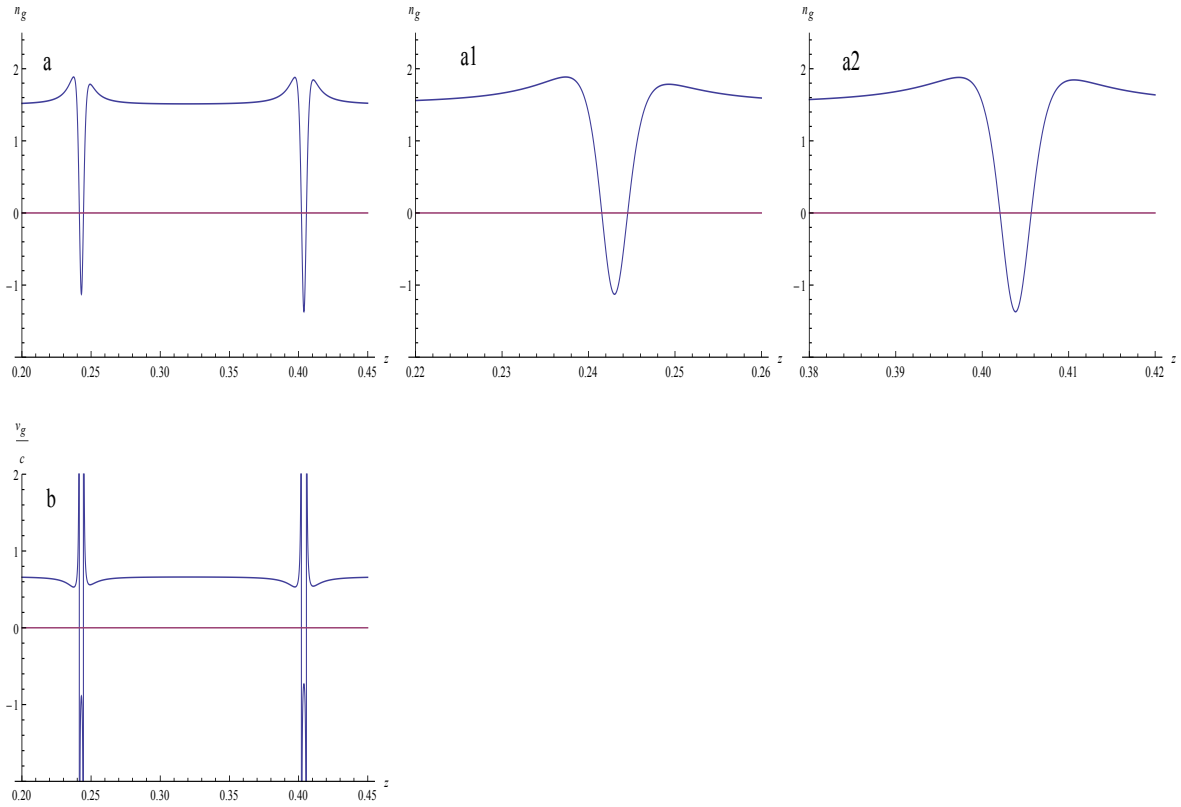

Figure 5.36: Active composite with tuned spherical nanoinclusions ($\epsilon_h^{''} = -0.13866$) . a) is group index n_g versus dimensionless frequency z. $a1$) is enlarged left tip of n_g. $a2$) is enlarged right tip of n_g.b) is normalized group velocity $\mathbf{v}_g/c$ versus z . $b1$) is enlarged left tip of $\mathbf{v}_g/c$. $b2$) is enlarged right tip of v_g/c. Numerical values of composite parameters; $\epsilon_1 = 9, \epsilon_h^{'} = 2.25$, metal fraction in the inclusion $p = 0.8, \epsilon_\infty = 4.5, \omega_p = 1.6 \times 10^{16}(silver), \gamma = 1.15 \times 10^{-2}$, fraction of the inclusion in the composite $f = 0.001$

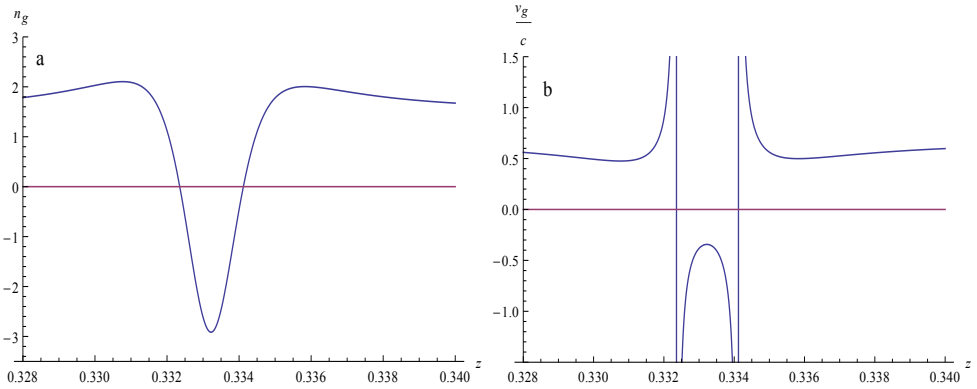

Figure 5.37: Active composite with spherical pure metal inclusions ($\epsilon_h^{''} = -0.115911$) . *a*) is group index n_g versus dimensionless frequency z. *b*) is normalized group velocity $\mathbf{v}_g/c$ versus z. Numerical values of composite parameters; $\epsilon_1 = 9, \epsilon_h^{'} = 2.25, \epsilon_\infty = 4.5, \omega_p = 1.6 \times 10^{16}(silver), \gamma = 1.15 \times 10^{-2}$, fraction of the inclusion in the composite $f = 0.0001$

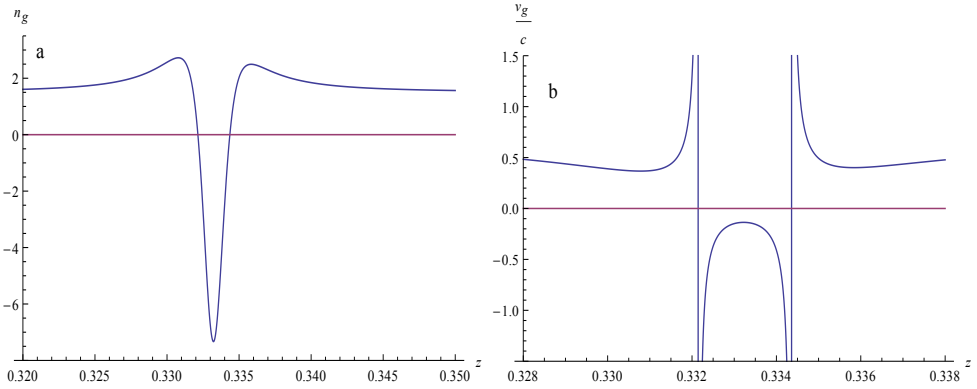

Figure 5.38: Active composite with spherical pure metal inclusions ($\epsilon_h^{''} = -0.115911$) . *a*) is group index n_g versus dimensionless frequency z. *b*) is normalized group velocity $\mathbf{v}_g/c$ versus z. Numerical values of composite parameters; $\epsilon_1 = 9, \epsilon_h^{'} = 2.25, p = 1, \epsilon_\infty = 4.5, \omega_p = 1.6 \times 10^{16}(silver), \gamma = 1.15 \times 10^{-2}$, fraction of the inclusion in the composite $f = 0.0003$

Chapter 6

Conclusion

Based on the results of our study, composites of metal coated dielectric cylindrical/spherical nanoinclusion in passive host matrix significantly enhance an externally applied electric field at their core. By keeping ϵ_h and ϵ_1 constant, the magnitude of the local field enhancement factor can be controlled by three parameters: the shape of the inclusion, thickness of metal in the inclusions and the value of ϵ_∞. According to the obtained results, the local field enhancement factor is comparatively higher in metal coated dielectric spherical inclusions than in cylindrical metal coated dielectric spherical inclusions. In both geometries ,raising the fraction of metal in the inclusion increase the enhancement factor and the second maxima of the enhancement factor becomes more important for metal fraction $p > 0.6$. Unlike the two stated factors, lowering ϵ_∞ increases the magnitude of the enhancement factor.

So, regarding the enhancement of an applied external electric field, we can conclude that composites with metal coated dielectric cylindrical/spherical nanoinclusion strongly enhance an externally applied electric field for thick metal cover. And these composites can be recommended as a promising material for nonlinear optical phenomenas such as optical bistability .

The speed of light can be controlled in composite of tuned and pure metal cylindrical/spherical inclusions in passive and active host matrices. We have obtained that, light pulse can propagates with slow, superluminal and even with negative group velocity in the stated composites. In both tuned and pure metal inclusion in passive host matrix, the main challenge in the propagation distance of light pulse is strong absorption. By introducing a negative part in to the imaginary part of the permittivity, the problem of strong attenuation of an electromagnetic wave by the composite can be considerably reduced. From manufacturing point of view and less absorption coefficient of light pulse within a composite of pure metal cylindrical/spherical in active host matrix, we can conclude that it is a promising material for optical applications.

Bibliography

[1] http://en.wikipedia.org/wiki/Speed- of-light

[2] Grant R. Fowler, Introduction to modern Optics, 2^{nd} Edition, NEW YORK (1975)

[3] P W Milonni, Fast Light, Slow Light and Left Handed Light, Los Alamos, New Mexico (2005)

[4] Bahaa E. A. Saleh, Malvin Carl Teich, Fundamentals of Photonics, John Wiley and Son, Inc (1991)

[5] David Jackson, Classical Electrodynamics, 3^{rd} Edition, John Wiley and Son, Inc, USA (1999)

[6] Leon Brillouin, Wave Propagation and Group Velocity, ACADAMIC PRESS, NEW YORK and London (1960)

[7] M S Bigelow, N N Lepeshkin and R W Boyd, J.Phys: Condensed Matter 16(2004)R1321 - R1340

[8] L.V.Hau et al, Nature 397, 594(1999)

[9] M. M. Kash et al, Phys.Rev.Lett.82, 5229(1999)

[10] A. M. Akulshin, S. Barreiro, and A. Lezema, Phys.Lett.85, 4277(1999)

[11] K. Kim et al, Phys.Rev.A68, 013816(2003)

[12] Wang L J, Kuzmich A and Dogariu A 2000 Nature 406 277

[13] A. M. Seinberg, P. G. Kwait, R. Y. Chiao, Phys.Rev.Lett.71, 708(1993)

[14] V. N Mal'nev and Sisay, Physica B 426 (2013) 52-57

[15] http://scienceworld.wolfram.com/physics/MaxwellEquations.html

[16] Charles Kittle, Introduction to Solid State Physics, John Wilay and Sons Inc, USA(2005)

[17] Germain Charter,Introduction to Optics, Springer, (2005)

[18] Robert W. Boyd, Nonlinear Optics, 3rd edition, (2007)

[19] Robert D. Guenther, Modern Optics, John Wiley and Sons, Inc (1990)

[20] Wenshin Cai,Valdimir Shalaev, Optical Metamaterials Fundamentals and Applications, Springers, New York (2010)

[21] Julius Adams Stratton, Electromagnetic Theory, First edition, NEW YORK and LONDON, (1941)

[22] L. F. Chen, C. K. Ong, C. P. Neo, V. V. Verden and V. K. Verden, Microwave Electronics Measurement and Material Characterization, John Wilay and Sons ltd, (2004)

[23] http://en.wikipedia.org/wiki/Composite - material

[24] Greame W. Milton, The Theory of Composite,Cambridge university Press, NEW YORK, (2004)

[25] T. Pan, J. P. Huang, Z. Y. Li, physica B 301(2001)190-195.

[26] K.M.Lenng, Phys.Rev.A33 (1986)2461.

[27] D. S. bergman, O. Levy, D. Stroud, phys.Rev.B 49 (1994)129.

[28] Lie. Gao, X. P. Yu, Physics letters A 335(2005)457-463, December 2004.

[29] CHEN Guo-Qing, WU Ya-Min, CHIN.PHYS.LETT, Vol.24, No.6(2007)1724

[30] Micheal Quenten, Optical Properties of Nanosystems, WILEY-VCH Verlay Gmbtt and Co kGaA, (2011)

[31] Stefano Giordano, Journal of Electrostatics 58(2003) 59-76

[32] C. F. Bohren and D. R. Huffman, Absorption and Scattering of light by small particles(Wilay New York, 1983)

[33] V. N Mal'nev and Sisay, Physica B 407 (2012) 4837-4842

[34] David J .Griffith, Introduction to Electrodynamics, 3^{rd} edition, Prentice Hall.Inc, (1999)

[35] C. G. B. Garrett and D. McCumber, Phys.Rev.A 1, 305(1970)

[36] S. Chu and S. Wong, Phys.Rev.Letters 48, 738 (1982)

Declaration

This thesis is my original work, has not been presented for a degree in any other University and that all the sources of material used for the thesis have been dully acknowledged.

Name: Yilak Alemu Abbo

Signature:– – – – – – – – – – –

Place and time of submission: Addis Ababa University, June 2014

This thesis has been submitted for examination with my approval as University advisor.

Name: Prof. Vadim N. Mal'nev

Signature:– – – – – – – – ––